

DI Kathrin Schittelkopf

Silyl-Terminated Polyurethanes - Adhesion and Surface Phenomena

DISSERTATION

zur Erlangung des akademischen Grades
Doktorⁱⁿ der Technischen Wissenschaften



Technische Universität Graz

Betreuer:

Univ.-Prof. Dipl.-Chem. Dr.rer.nat. Uhlig Frank
Institut für Anorganische Chemie
Technische Universität Graz

in Kooperation mit
Dr. Simone Klapdohr
BASF Construction Chemicals GmbH

Graz, August 2011

Eidesstattliche Erklärung

Ich erkläre an Eides statt, dass ich die vorliegende Arbeit selbstständig verfasst, andere als die angegebenen Quellen/Hilfsmittel nicht benutzt, und die den benutzten Quellen wörtlich und inhaltlich entnommene Stellen als solche kenntlich gemacht habe.

Graz, am

.....

(Unterschrift)

Statutory declaration

I declare that I have authored this thesis independently, that I have not used other than the declared sources / resources, and that I have explicitly marked all material which has been quoted either literally or by content from the used sources.

.....

date

.....

(signature)

Danksagung

Mein besonderer Dank gilt Frank Uhlig, der mir die Möglichkeit gab dieses interessante Thema zu bearbeiten und erfolgreich zu beenden.

Außerdem gilt mein Dank Simone Klapdohr und Burkhard Walther von der Firma BASF, die das Zustandekommen dieser Dissertation überhaupt ermöglichten und durch ständige Diskussionsbereitschaft einen entscheidenden Beitrag zu dieser Arbeit lieferten. Andrea Schneider möchte ich meinen Dank für die sehr gute Zusammenarbeit während meiner Forschungsaufenthalte in Trostberg aussprechen.

Bei Roland Fischer möchte ich mich für die fachliche Betreuung der Dissertation bedanken. Petra Wilfling möchte ich für die außergewöhnlich gute Zusammenarbeit und ausnahmslose Unterstützung während der Dissertation danken. Ein herzliches Dankeschön geht auch an Astrid Falk, Monika Filzwieser und Johanna Flock, die mir immer wieder tatkräftig zur Seite gestanden sind.

Grundsätzlich gilt mein Dank allen Mitarbeitern der Arbeitsgruppe Uhlig und des Instituts für Anorganische Chemie an der TU Graz für Hilfestellungen jeglicher Art und das gute Arbeitsklima. Besonders möchte ich hierbei Georg Witek, Sarah Meyer, Michaela Flock, Johann Pichler, Kiristina Schrempf, Sandra Wiesenhofer, Eva Lackner und Thomas Schalk hervorheben. Zusätzlich möchte ich allen Projekt- und Bachelorstudenten danken, mit denen ich im Lauf der letzten drei Jahre zusammengearbeitet habe.

Dem Zentrum für Elektronenmikroskopie (FELMI-ZFE) möchte ich für die gute Zusammenarbeit danken. Durch die tatkräftige Unterstützung von Stefan Mitsche und Harald Plank wurden zahlreiche Oberflächencharakterisierungen erfolgreich durchgeführt.

Schlussendlich möchte ich mich besonders bei allen Freunden und meiner Familie bedanken, die mir während der Entstehung dieser Arbeit mit Rat und Tat zur Seite waren.

Kurzfassung

Silyl-terminierte Polyurethane (STPU) werden weltweit als Ausgangsstoffe für Dichtstoffsysteme verwendet. Durch die Mischung aus einem organischen Polyurethan- und einem anorganischem Alkoxysilane-Anteil werden die Vorteile handelsüblicher PU und Silikon Techniken vereint. Dieses organisch-anorganische Hybrid Harz System und die Einflüsse auf das Aushärte- bzw. Haftverhalten wurden untersucht.

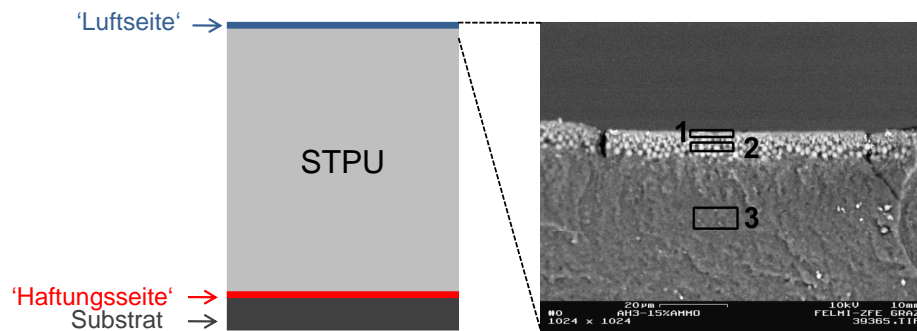


Figure 1: Links: Schematische Darstellung des Dichtstoffsystems, rechts: BSE Querschnittsbild der 'Luftseite' mit abnehmendem Siliciumanteil von (1) zu (2) und (3).

In der Anwendung dieser Dichtstoffsysteme stellen vor allem Oberflächenverhalten wie Klebrigkeit und Elastizität der Dichtstoffmasse große Probleme dar. Untersuchungen haben gezeigt, dass diese Effekte sehr stark mit der Art und Menge der verwendeten Alkoxysilane als Endcapper und Haftvermittler im Zusammenhang stehen. Verschiedene Oberflächenanalysen wie REM, IR-ATR, AFM, XPS und Festkörper-NMR-Spektroskopie wurden verwendet und zeigen, dass eine starke Siliciumanreicherung an der 'Luftseite' (siehe Abbildung 1) detektiert werden kann. Dies wiederum steht im Zusammenhang mit Klebrigkeit und Trübung der Proben. Haftvermittler wie N-(2-Aminoethyl)-3-aminopropylmethyldimethoxysilan (DAMO-D) oder N-(2-Aminoethyl)-3-aminopropyltrimethoxysilan (DAMO-T), die sehr polare Alkylreste besitzen, wandern zu der hydrophilen Luftseite der Probe und zeigen sich bei der Anwendung weniger klebrig, dafür aber trüber als Formulierungen mit Haftvermittlern wie 3-Aminopropyltrimethoxysilan

(AMMO) oder N-(n-Butyl)-3-aminopropyltrimethoxysilan (1189). In diesem Zusammenhang ist vor allem IR-ATR eine sehr geeignete, schnelle und günstige Methode um Siloxanstrukturen an der Oberfläche zu detektieren. Im Gegensatz dazu, wurde an der Haftungsseite keine Anreicherung der Haftvermittler gefunden. Je mehr Haftvermittler in der Formulierung eingearbeitet wird, umso mehr Silikonstrukturen werden an der Luftoberfläche detektiert. Die Haftung der Dichtstoffsysteme zu unterschiedlichen Materialien wird auch durch Alkoxysilane, die als Haftvermittler eingesetzt werden, beeinflusst. Aufgrund der Komplexität dieses Themas kann keine eindeutige Zuordnung der Haftungsmechanismen geliefert werden. In den Untersuchungen wurde eine Kombination von physikalischen und chemischen Effekten, die zur Haftung beitragen, festgestellt. Silyl-terminierte Polyurethane, die ohne zusätzliche Haftvermittler als Dichtstoffe getestet wurden, zeigen nur sehr schwache Haftungseigenschaften zu Aluminium, Kupfer, Stahl und Polyethylen. Durch die Zugabe unterschiedlicher Haftvermittler kann die Haftung zu Metallen stark verbessert werden. Im Fall von Polyethylen wird jedoch keine Verbesserung erzielt. Durch chemische Interaktion der Haftvermittler mit den Substraten und Aufrauung dieser, werden gute Haftungsergebnisse erreicht.

Abstract

Silyl-terminated polyurethanes (STPU) are the basis for numerous sealants used worldwide. A mixed organic (polyurethane proportion) and inorganic (alkoxysilane proportion) hybrid resin system combines the advantages of conventional polyurethane- and silicone techniques. The exact working principle of this system and the influences of the components on the curing process have been investigated.

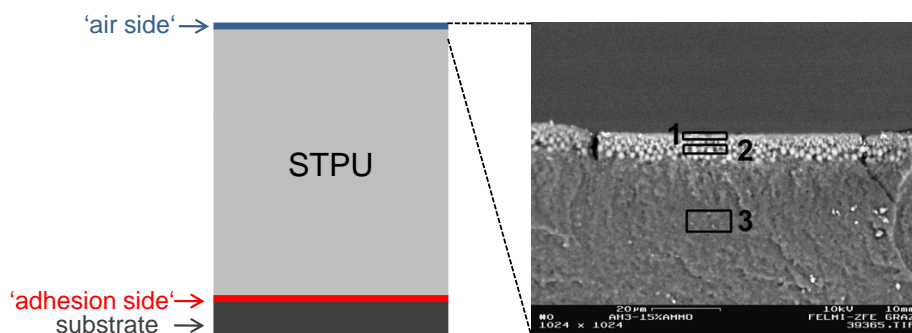


Figure 2: Left side: schematic description of STPU on substrate, right side: SEM BSE image of the cross section of the 'air side' with decreasing amount of Si from (1) to (2) and (3).

Most of all, the surface characteristics like tack behavior or elasticity create problems and investigations show that these effects are linked with the amount and type of alkoxysilane added as end-cappers and adhesion promoters. A combination of various surface techniques such as SEM, IR-ATR, AFM, XPS, solid state NMR and contact angle measurements were employed to analyze these surface properties. SEM, IR-ATR, AFM and XPS analyses showed that there is an accumulation of siloxane structures at the surface exposed to the air ('air side'), which has a strong influence on tack characteristics and turbidity of the samples. N-(2-Aminoethyl)-3-aminopropyltrimethoxysilane (DAMO-T) and N-(2-aminoethyl)-3-aminopropylmethyldimethoxysilane (DAMO-D) show the strongest silicon accumulation at the 'air side' in all investigations. Alkoxysilanes with strong polar alkyl chains like DAMO-D or DAMO-T move to the hydrophilic 'air side' surface and tend to be less sticky but also more turbid than others. IR-ATR especially, can be employed as a cheap and powerful tool

to detect siloxane structures at the 'air side' of the cured STPU. At the 'adhesion side' this silicon accumulation cannot be detected. The more adhesion promoter is added the more siloxane structures can be seen at the 'air side'.

Adhesion of the inorganic-organic hybrid materials to different substrates is also influenced by the alkoxysilanes applied as adhesion promoters. Due to the complexity of this topic no definitive adhesion mechanism can be reported; rather, a combination of physical and chemical effects was detected. In all investigations the pure silyl-terminated polyurethanes with no additional adhesion promoter lead to weak interaction between polymer and substrates of the type aluminum, copper, steel and polyethylene. By adding alkoxysilanes as adhesion promoters, adhesion abilities of the sealants increase significantly to aluminum, copper and steel. However, no adhesion improvement could be detected for plastic substrates. Chemical bonding between the metal surface and the sealant seems to be given. Additional roughness of the substrate leads to slightly better adhesion.

List of Abbreviations

1146	Co-oligomeric diamino/alkylfunctional silane
1189	N-(n-Butyl)-3-aminopropyltrimethoxysilane
AES	Auger electron spectroscopy
ADXPS	Angular-dependent X-ray photoelectron spectroscopy
AFM	Atomic force microscopy
A-link 15	N-ethyl-3-trimethoxysilyl-2-methylpropanamine
AMMO	3-Aminopropyltrimethoxysilane
AMEO	3-Aminopropyltriethoxysilane
ATR	Attenuated total reflection
BND	Bismuth neodecanoate
BTSE	1,2-Bis(triethoxysilyl)ethane
BYK-333	Polyether modified polydimethylsiloxane
CoatOsil 1211	Organomodified polydimethylsiloxane
CA	Contact angle
DAMO-T	N-(2-Aminoethyl)-3-aminopropyltrimethoxysilane
DAMO-D	N-(2-Aminoethyl)-3-aminopropylmethyldimethoxysilane
DBTL	Dibutyltin dilaurate
DBU	1,8-Diazabicycloundec-7-ene
DEPT	Distortionless enhancement by polarization transfer
DMPA	Dimethylol propionic acid
GLYMO	3-Glycidyoxypropyltrimethoxysilane
INEPT	Insensitive nuclei enhanced by polarization transfer
IR	Infrared
IR-RA	Infrared reflection-absorption
ITPU	Isocyanate-terminated polyurethane

Jeffcat ZF-10	2-((2-(2-(Dimethylamino)ethoxy)ethyl)(methyl)amino)ethanol
Jeffcat Z-110	2-((2-(2-(Dimethylamino)ethyl)(methyl)amino)ethanol
Lpol	Linseed polyol
MEMO	3-Methacryloxypropyltrimethoxysilane
MTES	Methyltriethoxysilane
n	Molar amount
NMR	Nuclear magnetic resonance
OCA	Optical contact angle analysis
PE	Polyethylene
PTMS	Propyltrimethoxysilane
PU	Polyurethane
PVC	Polyvinyl chloride
rt	Room temperature
SEM	Scanning electron microscopy
SIMS	Secondary ion mass spectroscopy
STPU	Silyl-terminated polyurethane
TBP	Titanium dibutoxide(bis-2,4-pentanedionate)
TGA	Thermogravimetric analysis
TOF-SIMS	Time-of-flight secondary ion mass spectrometry
tr	Reaction time
VTMO	Vinyltrimethoxysilane
XPS	X-ray photoelectron spectroscopy

Contents

1	Introduction	12
1.1	Definition of the Project	13
2	Literature Overview and Theory	15
2.1	Synthesis of Silyl-terminated Polyurethanes	15
2.1.0.1	Polyurethane Formation	17
2.1.0.2	End-capping	17
2.1.0.3	Hydrolysis	18
2.2	Adhesion	21
2.2.1	Adhesion Theories	21
2.2.1.1	Mechanical Coupling Theory	21
2.2.1.2	Adhesion by Physical Adsorption	22
2.2.1.3	Thermodynamic Mechanism of Adhesion	23
2.2.1.4	Chemical Bonding Theory and the Application of Silane Coupling Agents	24
2.2.2	Direct Adhesion Measurements and Pre-treatments	27
2.2.2.1	Peel Test	28
2.2.2.2	Lap Shear Test	29
2.2.2.3	Scratch Test	30
2.2.2.4	Pull-off Test	30
2.2.2.5	DIN Standards	31
2.3	Surface Characteristics	32
2.3.1	Topography and Surface Energy	32
2.3.2	Silanol Detection	33
3	Results and Discussion	35
3.1	Surface Analyses	35

<i>CONTENTS</i>	10
3.1.1 Sample Composition	36
3.1.2 Increasing Amount of Alkoxysilane	38
3.1.2.1 SEM Measurements	38
3.1.2.2 IR Measurements	41
3.1.3 Influence of Different Alkoxysilanes	43
3.1.3.1 SEM Measurements	43
3.1.3.2 IR Measurements	47
3.1.3.3 AFM Measurements	49
3.1.3.4 XPS Measurements	52
3.1.3.5 NMR Measurements	52
3.1.4 Summary	58
3.2 Tack Tests	61
3.2.1 Sample Composition	61
3.2.2 Increasing Amount of Alkoxysilane	63
3.2.3 Influence of Different Alkoxysilanes	65
3.2.4 Influence of Catalysts	67
3.2.5 Summary	68
3.3 Adhesion Tests	70
3.3.1 Sample Composition	70
3.3.2 Analyses of the Substrates	74
3.3.2.1 SEM Measurements	74
3.3.3 Influence of Substrate Roughness	75
3.3.4 Influence of Different Alkoxysilanes	77
3.3.5 Influence of Different Amines	79
3.3.6 Summary	82
4 Experimental	83
4.1 Chemicals	83
4.2 Synthesis of the Cured Prepolymers	84
4.2.1 Preparation of Isocyanate-Terminated Polyurethanes	85
4.2.1.1 Isocyanate-Terminated Polyurethane 1a	85
4.2.2 Preparation of Silyl-Terminated Polyurethanes	86
4.2.2.1 Silyl-Terminated Polyurethane 2a	86
4.2.3 Curing of Silyl-Terminated Polyurethanes	87
4.2.4 Pull-off Tests	89

<i>CONTENTS</i>	11
4.2.5 Tack Tests	90
4.3 Analytics and Preparations	92
4.3.1 NCO Determination by Titration	92
4.3.2 Silver Coating	92
4.3.3 NMR Spectroscopy	93
4.3.4 IR Spectroscopy	93
4.3.5 SEM	93
4.3.6 AFM	94
4.3.7 XPS	94
4.3.8 Contact Angle	94
List of Figures	98
List of Tables	100
Literature	101

Chapter 1

Introduction

Sealants, as they are used in many fields, require a series of different properties for optimal function. Customers are looking for high-performance construction sealants useful for a broad range of applications. In modern construction, water-based and solvent-free systems are dominating due to their low toxicity with regard to the environment.¹⁻³ These types of sealants avoid strong curing shrinkage, which typically appears in solvent-based systems, and, additionally, the liberation of volatile compounds is reduced. Furthermore, one-component type adhesives and sealants are very popular due to the ease of handling them, as it is not necessary to mix the components before using them.¹

Polyurethanes have grown commercially as sealants as they have excellent adhesion to a wide range of materials, perfect abrasion resistance, good flexibility and hardness. These properties make them useful for products such as coatings, adhesives and sealants.² Hence, there has been an industrial emphasis on producing one-component, solvent-free urethane sealants based on isocyanate-terminated polyurethanes. However, curing times for these are slow and toxicity is high. A new type of sealant for versatile applications has been developed and will be focused on in this thesis;¹ So-called Silyl-terminated polyurethanes (STPU) combine the advantages of polyurethane and silicone sealants.

- A significant benefit is the fact that final products are isocyanate-free as the isocyanate groups are end-capped with silane molecules. As a consequence the high toxicity as well as gas formation during the hardening process due to the isocyanates is eliminated. Furthermore, the absence of highly reactive isocyanate groups provides the possibility of a wide range of applications as fillers, additives, stabilizing and hardening agents.
- The inorganic hybrid provides high stability due to silicone bond formation. This results in enhanced UV resistance, chemical resistance, weatherability and colour fast-

ness.

- The alkoxy silane group is used as a linking unit and leads to good adhesion abilities and stability of the sealants. This effect is achieved without addition of primers on such different substrates as glass, metals or organic polymers.
- Combination of the polyurethane backbone and the silicone end-capping unit leads to good mechanical abilities with respect to elasticity and modulus of elasticity. High flexibility and mechanical toughness are possible.³

All these advantages of STPU lead to a wide range of application abilities and provide an interesting field of research.

1.1 Definition of the Project

The aim of this project was to obtain new scientific findings leading to improvements of the existing hybrid resin systems used for industrial applications.

Therefore, a silyl-terminated polyurethane test polymer close to the real system was developed in order to investigate several phenomena not yet clarified, mainly adhesion and surface characteristics of the sealants produced, since synthesis is already well investigated in literature.¹⁻⁹

The test polymer was synthesized, formulated, cured and analyzed with respect to adhesion abilities, surface characteristics, stability and appearance. A short overview is given in figure 1.1. Several correlations between polymer consistence and properties of the sealants used in everyday life were developed.

- Adhesion promoter/end-capping unit
 - Application of novel alkoxyaminosilane precursors
 - Correlation between length of the alkyl spacer and alignment of the resin units at the surface
 - Analysis of the crosslinking reaction of the silane units by spectroscopic methods like ²⁹Si NMR and IR
 - Influence of amount and type of alkoxyaminosilane with respect to mechanical and optical characteristics
- Adhesion abilities

- Interface adhesion for application of sealants utilisable without primers
- Adhesion of the sealant on different substrates
- Surface stickiness
 - Surface characterization techniques such as SEM, AFM, contact angle measurements, IR-ATR and XPS
- Storage of the sealant
 - Storage stability of the inorganic-organic resin system
 - Influence of water trapping agents, fillers, et cetera.

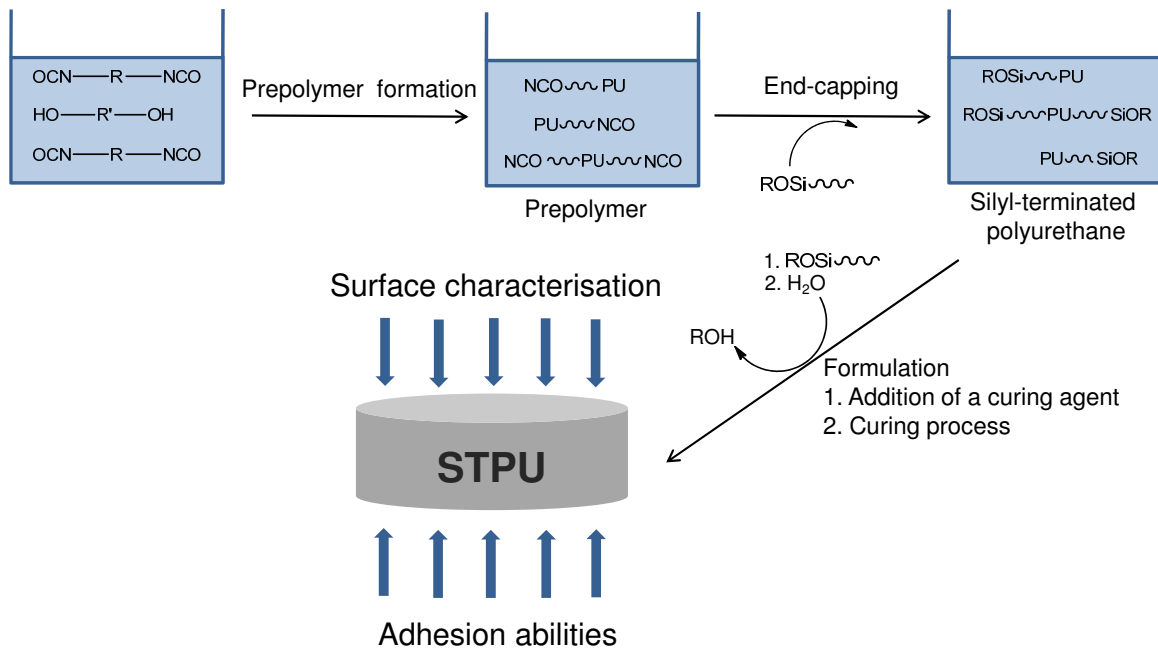


Figure 1.1: Schematic overview of the project.

Chapter 2

Literature Overview and Theory

Silyl-terminated polyurethanes have great industrial power. They are very important as a consequence of their low toxicity compared to solvent-based products. Hence, many industrial patents which deal with the synthesis, properties and stability of this hybrid system exist. Research is still up-to-date as several patents were also published in 2010 and 2011.¹⁰⁻¹³ So far much work has been done to improve this inorganic-organic resin system. The next subchapters overview the results accomplished by several research groups in the last few decades with a focus on the synthesis, adhesion abilities, and surface characteristics of the sealants.

2.1 Synthesis of Silyl-terminated Polyurethanes

In 2004 O'Connor et al.³ were the first to review the synthesis methods and development of silyl-terminated polyurethanes for construction sealants. The use of organofunctional silanes as crosslinking units for polyurethanes was first reported in the early 1970s by a patent by 3 M.¹⁴ Brode and Conte¹⁵ followed shortly and synthesized STPU polymers with different aliphatic and mercapto silanes. In the early 1980s Berger et al.¹⁶ improved this new technology by using secondary amino bis-silanes which improved significantly the properties of the sealants with respect to flexibility and curing times. From then on several publications for industrial applications appeared in the literature as the new developed sealants upgraded the traditional polyurethane chemistry. As the polyurethane synthesis was well-established, standard polyurethane chemistry was used to synthesize the prepolymer.

In the first step a conventional polyurethane prepolymer is formed by reaction of a polyol with an excess amount of a diisocyanate. The free isocyanate groups are then end-capped with compounds containing reactive alkoxy silane groups. After application the alkoxy silane

end groups undergo hydrolysis and condensation reactions in the presence of moisture giving the cured prepolymers desired. The reaction steps are explained in detail in the following subchapters.

Several strategies to synthesize organic-inorganic hybrid polyurethanes have been developed and published in journals in the last ten years. In 2006 Xu et al.⁹ reported the synthesis and shape memory effects of Si-O-Si cross-linked hybrid polyurethanes. The first step is the synthesis of a silane end-capper by Michael addition of aminosilane and acrylate. In the second step a diisocyanate and polyol compound are reacted to give the polyurethane backbone having free isocyanate groups. In the third step the isocyanate-terminated polyurethane reacts with the silane end-capper and results in the inorganic-organic hybrid material. The same synthesis strategy was applied by Nomura et al. in 2007¹ and is displayed in figure 2.1.

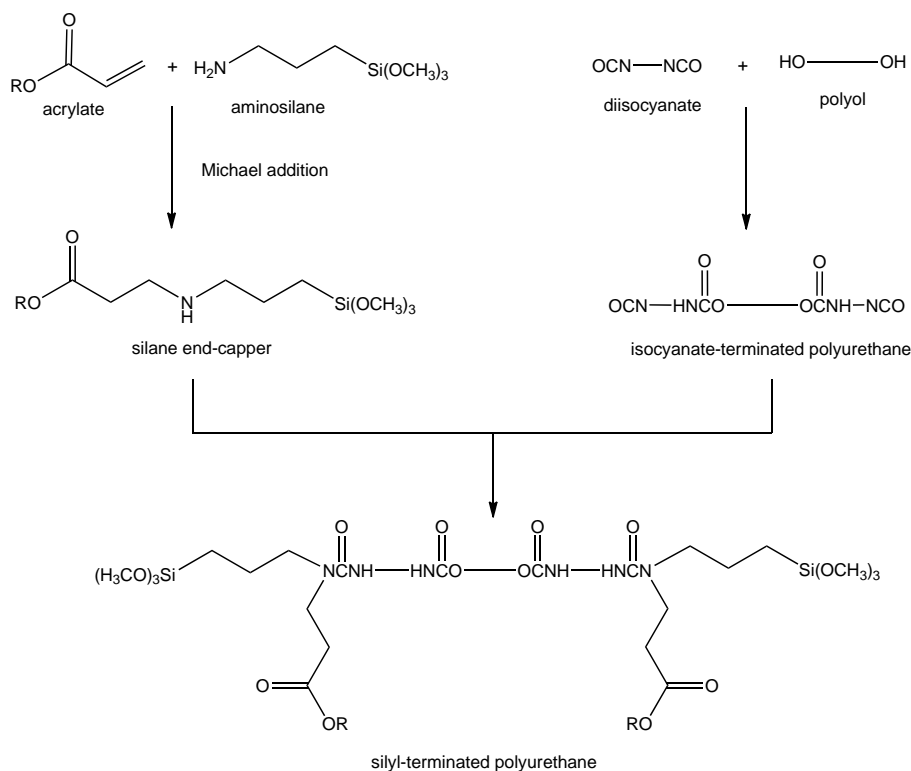


Figure 2.1: Synthesis pathway for STPUs according to Nomura¹ and Xu.⁹

Subramani et al.⁵⁻⁷ used a slightly different route to prepare the STPU desired. A polyol is reacted with a dimethylol propionic acid (DMPA) and a diisocyanate in the first step. The free isocyanate groups of the polyurethane are then end-capped with an aminoalkoxysilane. Furthermore, acetone is added in order to reduce the viscosity of the polymer and triethy-

lamine to neutralize the COOH groups. Sardon et al.² used the same reaction pathway by using acetone as solvent of the reaction. After functionalization of the polyurethane with an aminoalkoxysilane the emulsification process is started by the addition of water, and acetone is removed by distillation. The reaction scheme of this synthetic route is shown in figure 2.2.

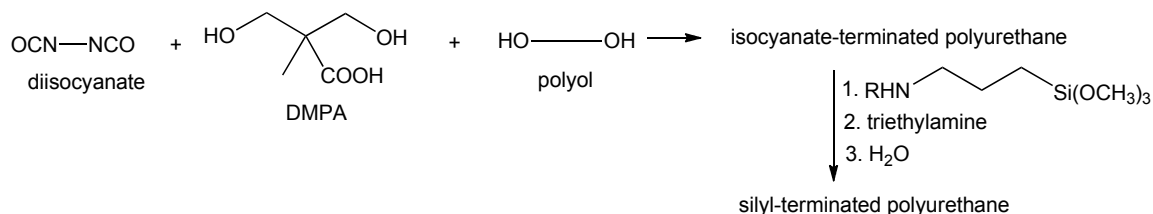


Figure 2.2: Synthesis pathway for STPUs according to Sardon² and Subramani.⁵⁻⁷

Other strategies that slightly deviate from the pathway described above have also been developed by varying the kind of silane used as the inorganic part. Triethoxysilane and linseed polyol (Lpol) as inorganic and organic precursors were used by Akram et al.⁴ This so called Si/Lpol is further treated with a diisocyanate to give organic-inorganic hybrid polyurethane composites. Vega-Baudrit et al.⁸ investigated the properties of thermoplastic polyurethanes by agglomeration of nanosilica particles within a polyurethane matrix. The thermoplastic polyurethane is prepared by the standard prepolymer method and mixed with the nanosilica in 2-butanone.

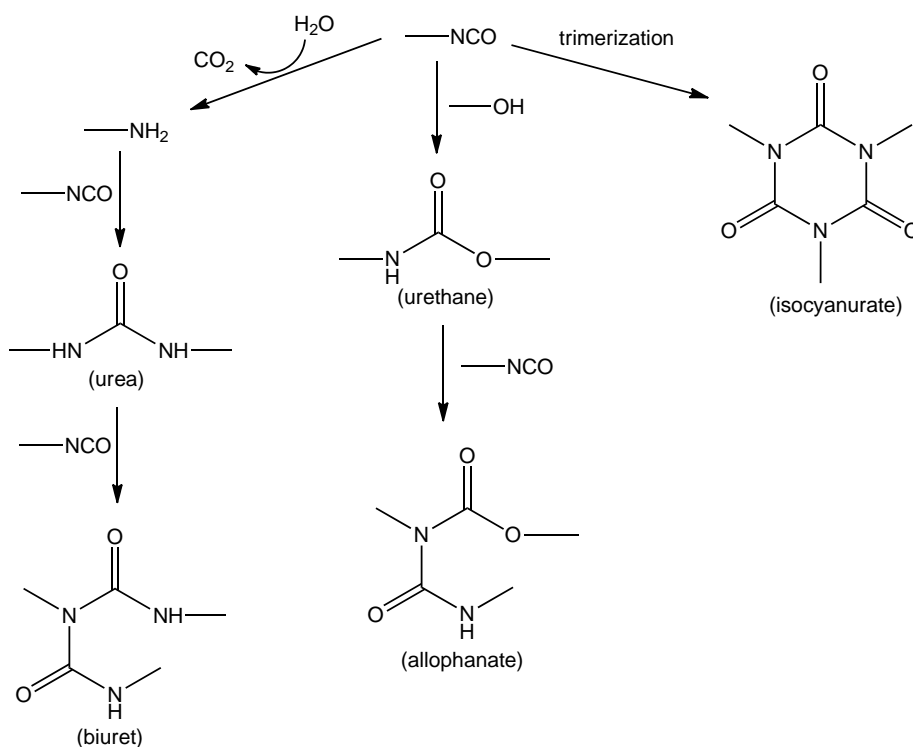
2.1.0.1 Polyurethane Formation

The network formation process of diol-diisocyanate systems catalyzed by dibutyltin dilaurate was investigated by Dusek et al.¹⁷ in 1990. The most important reactions that occur are summarized in figure 2.3.

They claim that the molar ratio OH/NCO has an impact on the importance of the side reactions. Side reactions cannot be inhibited as long as isocyanate is in excess. However, at lower temperatures ($\leq 60^\circ\text{C}$) the formation of biuret and allophanate is very slow. As a consequence, reaction temperatures of about 50°C to 60°C are appropriate.

2.1.0.2 End-capping

The end-capping reaction is done with di- or tri-functional amino silanes of the type R'NH-spacer-Si(OR'')₃ or R'NH-spacer-SiR''(OR'')₂ (R'=Alkyl, H; R''=Me, Et).³ The amino groups are reacted with the free isocyanates to give stable urea groups. A tri-functional

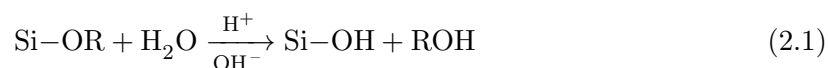
Figure 2.3: Isocyanate side reactions according to Dusek.¹⁷

silane having three methoxy or ethoxy groups induces higher cross linking and faster cure. Methoxysilanes as end-cappers also lead to faster cure rates than those of ethoxysilanes. These compounds can also be used as adhesion promoters, as is described in chapter 2.2.1.4.

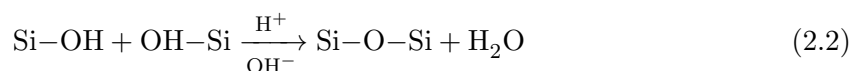
2.1.0.3 Hydrolysis

In 1992 Osterholz and Pohl¹⁸ gave a review of the proceedings and kinetics of hydrolysis and condensation of organofunctional alkoxy silanes. The commercial use of alkoxy silanes as coupling agents or cross linkers has increased steadily since the 1950s. In the first step the alkoxy silanes are hydrolyzed to silanols. The following condensation reaction can be divided into two kinds giving siloxane bonds: water-producing and alcohol-producing condensation.¹⁹

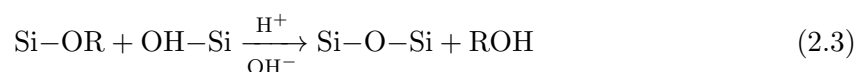
Hydrolysis:



Water-producing condensation:



Alcohol-producing condensation:



The reaction occurs in basic or acidic media which has an influence on the rates and chemistry of the sol-gel process, as Surivet et al.²⁰ reported. Hydrolysis is very slow at neutral pH. Change of one pH unit into the acidic or basic field induces a tenfold increase of the hydrolysis rate. The lowest condensation rate can be observed at pH 4. In summary, acidic catalysis accelerates the hydrolysis reaction and slows down the condensation reaction whereas basic catalysis favors the condensation of the silanol groups. In the case of the silyl-terminated polyurethanes acid-catalyzed reaction leads to lightly cross-linked polymers whereas bases induce densely cross-linked compounds as products.¹⁸

Hydrolysis and condensation of alkoxy silanes are important processes applied in commercially available products like sealants, adhesives etc. and consequently great effort has been made to characterize the mechanisms. The main tools for analysis included ²⁹Si NMR spectroscopy^{18,20-25} and ATR-IR spectroscopy.²⁶

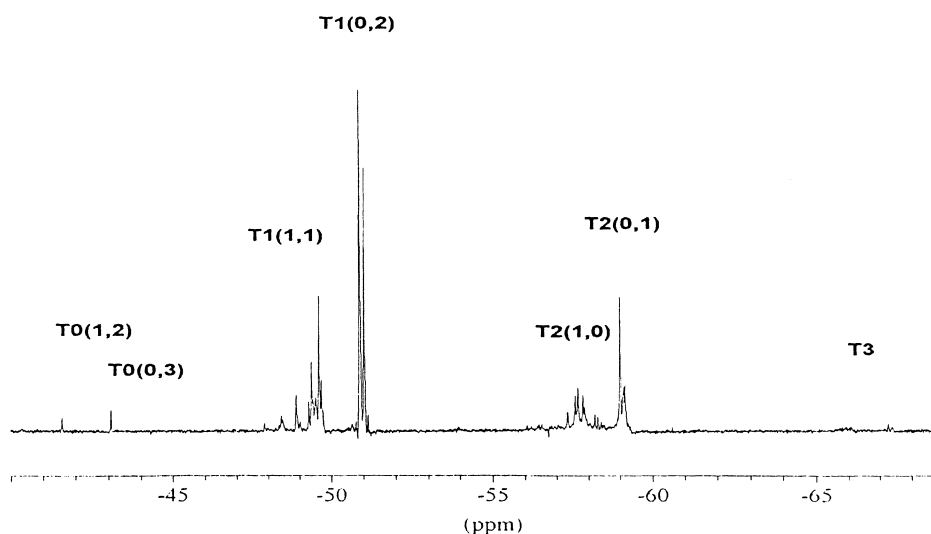


Figure 2.4: ²⁹Si NMR spectrum of mixture IV ($w = 1$, pH=1) obtained at 59.59 MHz and 296 K using DEPT sequence recorded by Brunet²²

Brunet²² reported that the monitoring of the hydrolysis and condensation reaction by ²⁹Si NMR spectroscopy is limited due to the weak sensitivity of ²⁹Si (natural abundance 4.7% and small negative γ). Additionally, the efficiency of recording decoupled spectra is reduced by the negative Nuclear Overhauser Effect, and relaxation of the ²⁹Si nucleus is slow. These

problems can be minimized by using methods such as INEPT (Insensitive Nuclei Enhanced by Polarization Transfer) or DEPT (Distortionless Enhancement by Polarization Transfer). In 1998 Brunet studied polymerization reactions of methyltriethoxysilane (MTES) in mixtures of ethanol and acidic water by ^{29}Si NMR polarization transfer (DEPT) methods. The experimental parameters of the DEPT sequence were optimized and finally led to good sensitivity and quantitative results. The mixtures were prepared by addition of H_2O and HCl to MTES. The molar ratio $w = \text{H}_2\text{O}/\text{Si}$ was chosen ($w = 1$, $w = 2$ and $w = 6$) and the pH was fixed at 1.0 or 2.4, respectively. Consequently, fast hydrolysis and slow condensation conditions were given. An NMR spectrum recorded by Brunet is shown in figure 2.4. Brunet interpreted the products ($\text{T}^n(i,j)$, n =number of siloxane bonds attached to silicon, i = number of OH groups and j =number of OR groups) obtained of different mixtures and characterized hydrolysis and condensation activities in acid conditions. This labeling of the hydrolysis products will be used in following discussions. In 1999 Rankin et al.²³ investigated the base-catalyzed polymerization of dimethyldiethoxysilane in 1999 and suggested important differences regarding polymerization under acidic conditions.

Further analyses were done on typical silane coupling agents used as end-cappers or adhesion promoters. As shown in section 2.1.0.2 and 2.2.1.4, they possess functional groups like amines, epoxides, methacrylates etc. In 2001 Beari²¹ et al. hydrolyzed alkyltrialkoxysilanes like 3-aminopropyltriethoxysilane (AMEO), 3-glycidyloxypropyltrimethoxysilane (GLYMO) and 3-methacryloxypropyltrimethoxysilane (MEMO) in aqueous solution and analyzed the products with time-dependent ^1H and ^{29}Si spectroscopy by reducing relaxation delays through addition of chromium(III)acetylacetonate.

Salon et al.²⁴ investigated even more functional trialkoxysilanes which are commercially available. The reaction was carried out in a mixture of ethanol- d_6 and deuterated water. In following investigations²⁵ of the same work group, acidic conditions were selected in order to enhance silanol formation and slow down self-condensation. Poor signal-to-noise ratios were solved by using a 10-mm BB probe. Relaxation delays between 20 and 100 s with proton decoupling only were applied during acquisition time in order to avoid negative Nuclear Overhauser Effects. Investigations showed that strong acidic or basic catalysis leads to high hydrolysis rates.

Hydrolysis and condensation mechanisms involved in alkoxysilane-terminated polyurethanes were reported by Surivet et al.²⁰ in 1992. Polyurethanes were end-capped with AMEO and hydrolysis was monitored in CDCl_3 with 3 mol of H_2O . According to them, no reaction occurs without any catalyst. In acidic conditions ^{29}Si NMR spectra that show siloxane formation were obtained.

2.2 Adhesion

Adhesion is defined as the interatomic and intermolecular interaction at the interface of two surfaces. Due to the complexity of this topic, the ultimate goal of finding one single mechanism to understand adhesion phenomena has not been accomplished.^{27–31} From the 1960s on, adhesion science has become a proper discipline and a lot of work has been done to solve adhesion phenomena problems. At the beginning, automotive and aerospace industry especially were investigating this topic, and other industries such as building, engineering and biomedical branches joined them. In this period the “theories of adhesion” as they are still known today were expounded. With the years more sophisticated techniques were applied giving new knowledge of surface properties³² and consequently of adhesion mechanisms. Unfortunately, adhesion phenomena have not yet been fully clarified.

2.2.1 Adhesion Theories

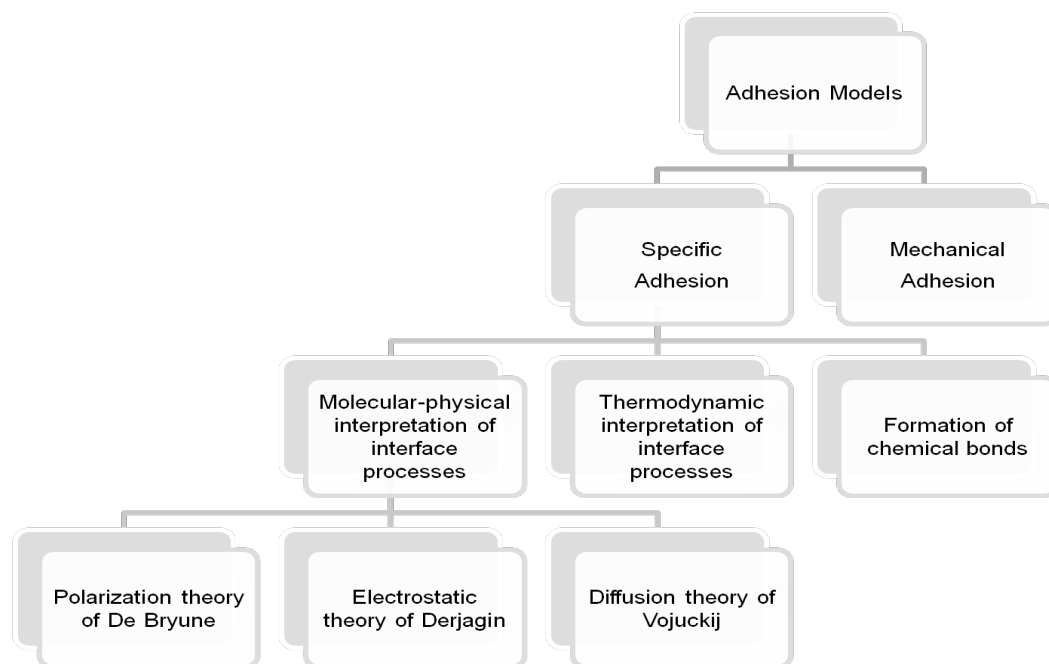
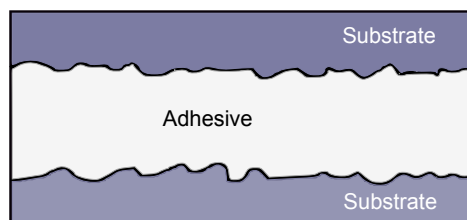
To understand adhesion mechanisms, several interactions between substrate and adhesive must be considered because of cohesive and adhesive forces that are at play. While cohesion refers to the tendency of molecules of the polymer to stick together, adhesion refers to attractive forces between polymer and surface.³³

The “theories of adhesion” which overview and summarize all interactions in polymer-substrate systems were reviewed in 2006 by John Comyn.³⁴ According to Comyn adhesion can be described by six theories. Recent literature²⁷ has a focus on the four main adhesion mechanisms: mechanical coupling, molecular bonding, thermodynamic adhesion and physical adsorption. The principles of these four theories are shown in the next subchapters.

2.2.1.1 Mechanical Coupling Theory

The mechanical coupling or interlocking adhesion theory describes the polymer as keying into the surface of the substrate. This occurs if a substrate has an irregular surface and the sealant may enter the interspaces before hardening. This concept is shown in figure 2.6. This kind of mechanical bonding of adhesives to wood was demonstrated by Smith et al. in 2002 with the help of SEM measurements.³⁶ According to this research group the adhesive penetrates large pore openings to depths of hundreds of micrometers.

Recent debates question the accuracy of this theory. On the one side it is believed that mechanical coupling increases adhesion abilities, on the other side research groups propose that rough surfaces simply increase the surface area to form chemical bonds.³⁷

Figure 2.5: Scheme of adhesion models.³⁵Figure 2.6: Mechanical interlocking of an adhesive between two substrates.²⁷

2.2.1.2 Adhesion by Physical Adsorption

Physical effects such as Van der Waals forces, polarization, electrostatic states and diffusion form the basis for adsorption in molecular-physical adsorption theory.

In the early 1930s De Bruyne³⁸ developed the polarization theory and started the molecular-physical interpretation of the adhesion phenomena. This theory acts on the assumption that adhesion only occurs between adhesive and substrate of the same polarity. Both parts must have polar functional groups producing dipole forces. Consequently many adhesives containing functional groups like hydroxyl (-OH), carbonyl (-CO), carboxyl (-COOH), amino (NH₂), nitrile (-CN), acid amide (-CONH₂) and ester (-COOR) at the side chains were

developed.

20 years later Derjagin³⁹ proposed the electrostatic theory, saying that by contact of a metal with a polymer the thermodynamic potential difference between them leads to charge carrier diffusion. This results in the formation of an electric bilayer in the contact zone, which is responsible for the polymer-metal adhesion. Another model developed by Vojuzkij⁴⁰ is also based on diffusion effects. The interface layer is built through diffusion of the molecules at the contact area according to Brownian motion. This effect is strongly temperature-dependent.⁴¹

2.2.1.3 Thermodynamic Mechanism of Adhesion

The idea of the thermodynamic theory is that an equilibrium process exists at the polymer substrate interface. Molecular interaction is not required to obtain good adhesion. Adhesion is seen as a wetting process in which the surface free energy plays an important role. Basic principles of this theory were obtained by Zismann, Fowkes and Good in 1963.⁴² According to their theory liquids show good adhesion on surfaces, if the energetic state of the phase interface is more favorable than of the inner part of the polymer. In this case full wetting is possible as all particles of the liquid adhere to the surface. In contrast no wetting takes place if the energetic state of the interior is benefited and a sphere is formed by the adhesive. The contact to the surface is consequently very low. Generally, good adhesion is correlated with good wetting in this theory. The experimental determination of surface and interface energy is possible by contact angle (Θ) measurements according to the Young equation 2.4.⁴¹

$$\gamma_{lv} \cos \Theta = \gamma_{sv} - \gamma_{sl} \quad (2.4)$$

γ_{lv} is defined as the surface tension of the liquid in equilibrium with the saturated vapour phase of the liquid. γ_{sv} displays surface tension of the solid in equilibrium with the saturated vapour phase of the liquid. γ_{sl} stands for the interface tension between liquid and solid.

The two values for γ_{lv} and Θ can be measured. By extrapolation of γ_{lv} to $\Theta = 0$ (complete wetting) the critical surface tension γ_c can be calculated according to equation 2.5. The factor b is an absolute term.

$$\cos \Theta = 1 + b(\gamma_{lv} - \gamma_c) \quad (2.5)$$

Analyzing the contact angle is only feasible with homogeneous, plane samples. In reality such samples are rarely the case and consequently the determination of the contact angle and adhesion abilities of a polymer is difficult. As a rough rule of thumb, good absorption

of substances on surfaces is obtained if the surface energy of the polymer is smaller or as big as the critical surface energy of the solid.

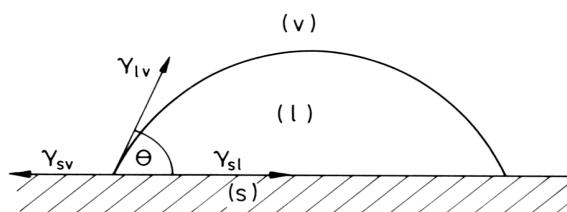


Figure 2.7: Contact angle for determination of wetting according to Young.^{41,42}

2.2.1.4 Chemical Bonding Theory and the Application of Silane Coupling Agents

The chemical interaction of polymer and substrate includes the formation of covalent, ionic or hydrogen bonds.³⁴ To promote the first, the use of silane coupling agents is very common. Silane coupling agents are considered to react with the adhesive and substrate to form covalent bonds across the interface. These mainly three processes are shown in figure 2.8, published by Wacker Silicones in their online media library.⁴³ Like the end-cappers described in chapter 2.1, the silane coupling agents have the general structure Y_3SiRX where X is the organofunctional and Y the hydrolysable group.

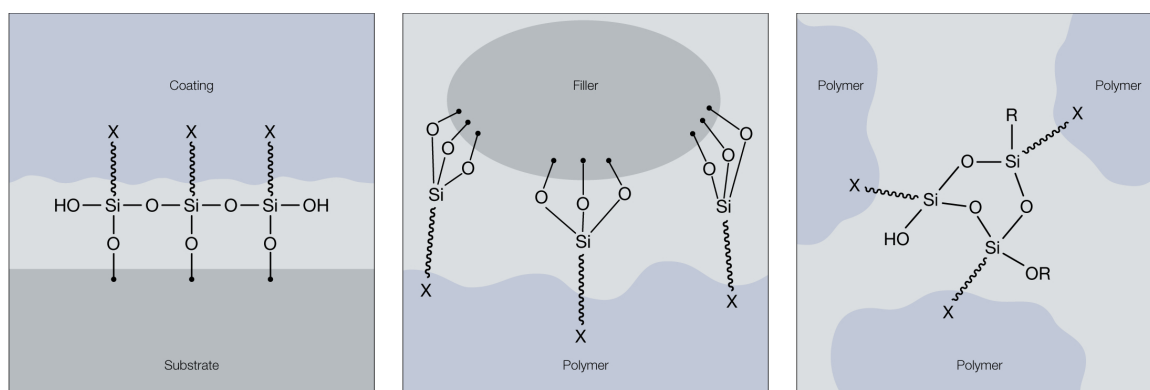


Figure 2.8: Reaction of the silane coupling agent with substrate (left), filler (middle) and polymer (right).⁴³

Plueddemann⁴⁴ claims that the coupling mechanism depends on a stable link between the organofunctional group X and the hydrolysable groups Y. Vinylsilanes were the first silane

coupling agents applied in industry, and many other types followed. Besides silanes other coupling agents based on titanium and zirconium of the type R-OTiY or R-OZrY have also been used.³⁴ Some commercially available silanes are summarized in figure 2.9.

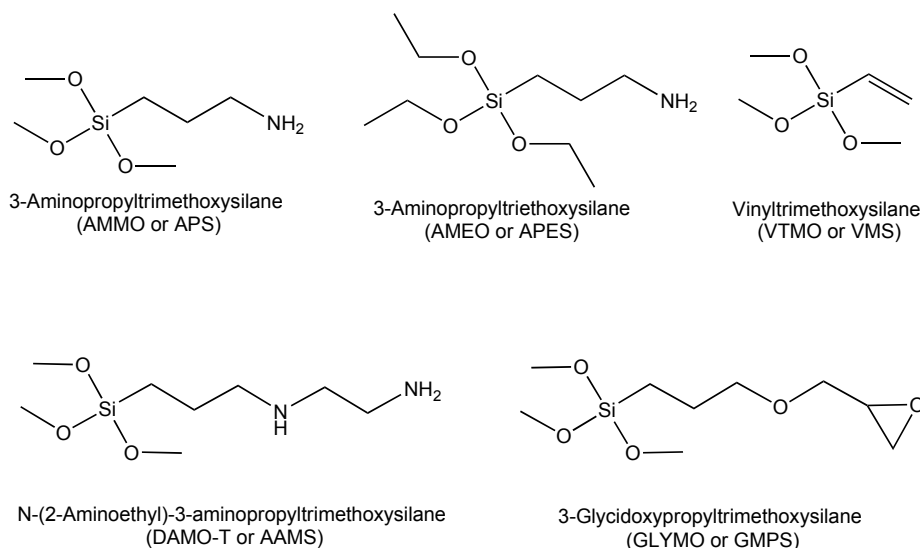


Figure 2.9: Popular silane coupling agents.

The reactive organofunctional group X like vinyl, amine or epoxide is reactive towards the adhesive polymer backbone. In the case of amine containing silanes such as AMMO or DAMO-T the free amine group can link to the epoxide adhesives or liquid resins containing free isocyanate groups. GLYMO, which contains epoxide groups, would react with the amine groups in adhesives whereas the double bond of VTMO, for instance, would copolymerize with styrene or unsaturated polyesters in liquid resins.³⁴ The hydrolysable group Y is considered to interact with the substrate to form stable S-O-Si bonds (S=substrate, e.g. glass, polyethylene, metals). Silanol groups of the hydrolyzed silane coupling agent will first form hydrogen bonds with the hydroxyl bonds of the mineral surface and then condense to oxane bonds. This process is not yet fully understood as the covalent bond formation is hard to prove. The possible reaction scheme of the silane reaction towards substrate and adhesive is shown in figure 2.10.

The question of whether silane coupling agents form oxane bonds of the type M-O-Si (M=metals, e.g. Si, Ti, Al, Fe) was precisely discussed by Plueddemann in 1982.⁴⁴ According to Plueddemann it is well established that silane coupling agents form M-O-Si bonds with mineral surfaces and the investigations summarized in this book were used as working hypothesis in further attempts to study silane-mineral-composites. Unfortunately, the ob-

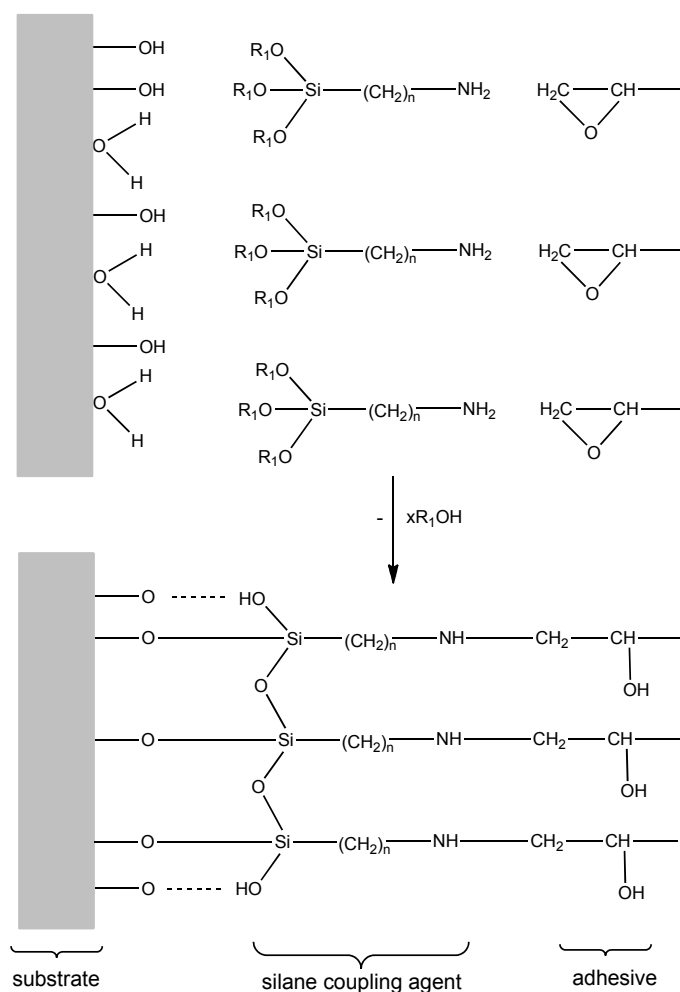


Figure 2.10: Possible reaction of the silane coupling agent with substrate and adhesive.³³

servations do not give any evidence or scientific proof for the formation of oxane bonds of the type M-O-Si. Furthermore, the development of surface sensitive instruments such as infrared reflection-absorption (IR-RA), X-ray photoelectron spectroscopy (XPS), angular-dependent X-ray photoelectron spectroscopy (ADXPS), secondary ion mass spectroscopy (SIMS) or time-of-flight secondary ion mass spectrometry (TOF-SIMS) has contributed significantly to the investigation of the chemical bonding mechanism. Further techniques such as scanning electron microscopy (SEM), Auger electron spectroscopy (AES), optical contact angle analysis (OCA) and atomic force microscopy (AFM) give additional information. The reaction of aluminum with silane coupling agents has been investigated very precisely.

In 2007 Fir et al.⁴⁵ studied the corrosion and interfacial bonding of urea/poly(dimethylsiloxane)sol/gel hydrophobic coatings on aluminum alloys. The

actual structure of the urea/poly(dimethylsiloxane)sol/gel coating was obtained and the silane-metal interface bonding Al-O-Si was analyzed by IR-RA yielding a broad band in the region $800 - 900 \text{ cm}^{-1}$. Unfortunately this band cannot be correlated a 100 % to the formation of the silane-metal interface bonding, as the authors point out.

ADXPS was used by Leung et al.⁴⁶ to characterize interfaces formed by γ -glycidoxypropyltrimethoxysilane (GLYMO) deposited onto aluminum panel surfaces; earlier studies⁴⁷ with XPS only gave limited insight into the adhesion bonding. When the sample was biased negatively, an extra peak in the Al 2p spectrum showed up that was interpreted as an effect of the direct Si-O-Al bonding. Later in 1997 the same research group⁴⁸ used static SIMS to characterize the same silane-metal system. They assign the $m/z = +71$ peak as the AlOSi^+ ion, which provides circumstantial support for the direct Al-O-Si interfacial bonding.

In 2001 Bexell et al.⁴⁹ improved the technique of Fang et al. and used ToF-SIMS and AES to analyze the interface between 1,2-bis(triethoxysilyl)ethane and three different metal substrates (aluminum, zinc and an aluminum-zinc alloy). Furthermore, ion etching using Ga^+ ions was executed to expose the interfacial region of interest. This led to the TOF-SIMS detection of an ion fragment that is indisputably assigned to AlOSi^+ at $m/z=70.9536$. They report that this ion fragment gives evidence for a chemical interaction between BTSE silane and the metal substrates. Additionally, SIMS depth profiling shows that there is an interfacial layer between the silane and the metal substrates.

Many other research groups also found significant hints in support of the chemical bonding theory. For instance, addition of silanes as adhesion promoters at the interface of maleic anhydride-grafted polypropylene improves adhesion performance.⁵⁰ Hutchinson et al.⁵¹ studied sealants and foam used in building construction, coming to the conclusion that mechanical interlocking only plays a marginal role in the adhesive strength of the system. The primary mechanism they identified is chemical bonding between polymer and substrate.

2.2.2 Direct Adhesion Measurements and Pre-treatments

In general, adhesion tests can be divided into qualitative and quantitative, mechanical or contactless, and destructive or non-destructive methods.⁴² Direct measurement methods such as pull off tests, peel tests, lap and shear test, and scratch tests are destructive methods that measure the force required to break, tear or delaminate surfaces at the interface. These methods do not provide physical interpretation of the different mechanisms but are required to produce consistent results. A combination with surface characterization methods is helpful to investigate polymer adhesion.²⁷ Theoretical calculated adhesion σ_H according to equation

2.6 cannot be compared to adhesion values determined through experiments. F_i is defined as force per unit area while A_w stands for the real surface area formed at the rupture.^{41,42} As a consequence, Mittal defined the two terms “practical adhesion” and “fundamental adhesion”.⁵²

$$\sigma_H = \frac{F_i}{A_w} \quad (2.6)$$

To obtain good adhesion to different substrates, several prearrangements have to be performed.³⁰ The surface preparation by cleaning is especially important. Different surface pre-treatments, listed below, lead to better adhesion of the polymers on the substrates.^{53,54}

1. surface preparations

- cleaning and degreasing (organic solvents and alkaline cleaning baths)

2. surface pretreatments

- mechanical (sanding, brushing, abrasive blasting)
- chemical (non-oxidizing acids such as HCl or diluted H_2SO_4 , oxidizing acids such as HNO_3 or H_3PO_4)
- electrochemical
- plasma

For instance Teo et al⁵⁵ analyzed the interfacial bonding when chemical pre-treatments (H_2SO_4 , H_2 plasma or heat) are applied to oxidized aluminum surfaces. Analyses of the samples show that pre-treatment does have a positive effect on the Al-O-Si bonding.

2.2.2.1 Peel Test

Peel tests provide a relative test method of determining adhesion strength. Adhesive tape is placed and pressed on the surface of the sample having an ink/paint layer, for instance. A pressure is applied and with a defined force the tape is detached quickly. The percentage of ink remaining on the substrate is interpreted.²⁷ More common is the so called T-peel test in which the peel resistance of two adhesive bonds is determined.⁵⁶ Two bonded parts consisting of flexible material are used and arranged as shown in figure 2.11. The force is applied to the unbonded ends of the specimen. The T-peel test is suited for use with metal adherents, but other flexible adherents (e.g. fibre-reinforced plastics) may also be applied. For instance Vega-Baudrit et al.⁸ performed T-peel tests of PVC/polyurethane adhesive joints containing

nanosilica in 2007. This publication reports that the immediate peel strength values of the PVC/polyurethane adhesive joints increase in those adhesive joints containing nanosilica.

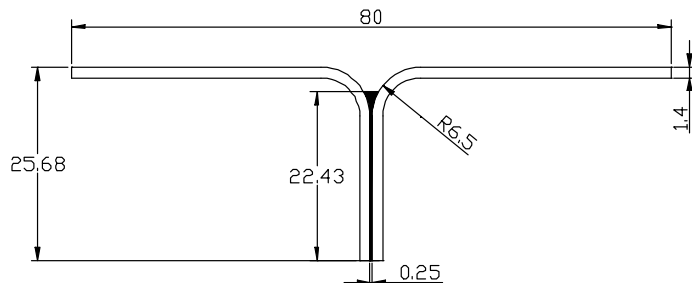


Figure 2.11: T-peel test geometry dimensions (mm) with sample in the middle (black).⁵⁶

2.2.2.2 Lap Shear Test

Lap shear tests are similar to peel tests. The adhesion is tested, giving quantitative results, by applying an in-plane shear stress to the assemblies. Rabilloud et al.⁵⁷ published the set up shown in figure 2.12 as recommended in ASTM D 1002, Federal Specification MMM-A 132 and Federal Test Method Standard No. 175. The adhesive layer is applied between two aluminium coupons giving an overlap bonding area of defined dimensions. The assembly is then fixed and cured under standard conditions. The lap shear strength is measured with a tensile machine at a certain pull rate expressed in MPa.

Nomura et al.¹ used this method to investigate the adhesion of novel silane end-cappers synthesized by the Michael addition reaction of commercially available primary aminosilanes with acrylates. The substrates for the tensile shear bond strength measurements were PMMA, polycarbonate, nylon and aluminum. According to their results the tensile shear bond strength of the silylated polyurethane-based adhesive decreased with decreasing trimethoxysilane end-capping ratio. Furthermore, a 100% trialkoxysilane end-capping ratio (equimolar amount of the reactive amino groups of the silane endcapper to the isocyanate groups) gave the best results in terms of a good balance of adherence and strength.

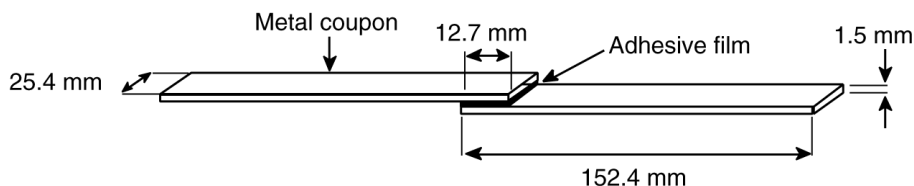


Figure 2.12: Lap shear test setup dimensions with sample (black).⁵⁷

2.2.2.3 Scratch Test

The scratch test is closely related to the nanoindentation test.²⁷ Both test methods are used to determine adhesion by dragging a fine tip across the sample surface. In the normal configuration of the test a diamond stylus is drawn across the coated surface under an increasing load until some well defined failure occurs, which is often termed the critical load (L_c). L_c is defined as the smallest load at which a recognizable failure occurs and can be correlated with the adhesion abilities of the polymer investigated.^{58,59} This method is a useful tool for analyzing thin films and coatings. The set-up is shown in figure 2.13.

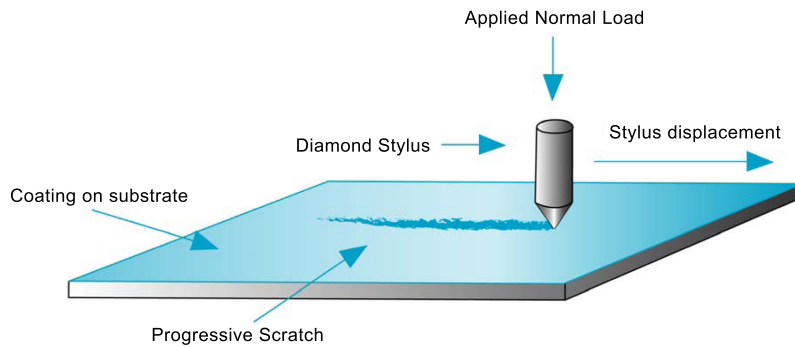


Figure 2.13: Schematic of scratch test.⁶⁰

Subramani et al.⁵ synthesized polyurethane/urea compositions terminated by hydrolysable trialkoxysilane groups with different NCO/OH ratios and characterized the films by nanoindentation. The mechanical properties such as changes in depth, modulus and hardness with an applied load of the films were summarized. The work group concluded that samples prepared at 1.6 and 1.4 NCO/OH ratios showed the best physical and mechanical properties.

2.2.2.4 Pull-off Test

Pull-off tests, which are commonly known as stud or butt tests, are mainly used to measure adhesion between a substrate and an ink or paint coating. The adhesion strength σ_z is defined as quotient of the force F (necessary to separate the polymer-metal interface) and the pull stud area.

$$\sigma_z = \frac{4F}{\pi d^2} \quad (2.7)$$

For the test a pull-off stud is glued to a coated substrate (see (a) in figure 2.14) and a pre-cut around the stud is made. The sample is then clamped in the tensile machine (see (b) in 2.14) and the force is applied at a 90° angle. The load is increased until fracture occurs.⁶¹ The choice of the glue is very important as the fracture must occur in the sample

under investigation. Therefore the cohesion and adhesion properties of the glue used must be better than those of the coating to be analyzed. Solvent-free cyano-acrylate, two-component-epoxide or peroxide-catalyzed polyester glues are used most commonly. This test provides a superior adhesion measurement method for polymer-metal interfaces.⁶²

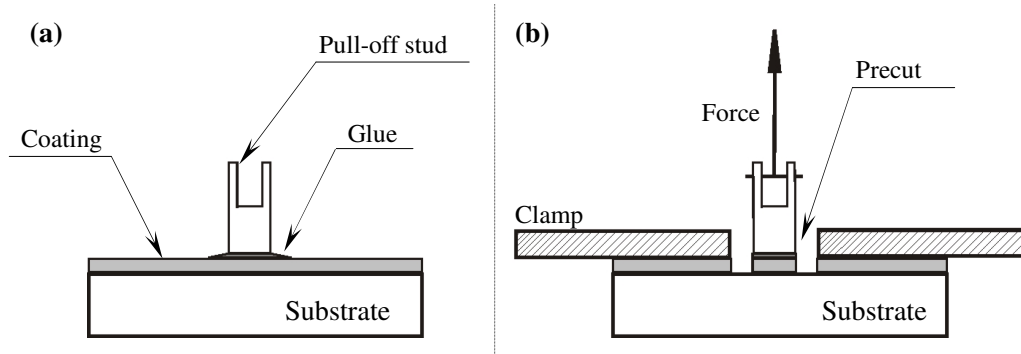


Figure 2.14: Pull-off test set up with (a) sample preparation and (b) pull off procedure.⁶¹

In 2006 the adhesion between foams and sealants were investigated using tack and peel tests.⁵¹ The results were compared with measurements of the surface energies of the foams and the surface tensions of the sealants. Unfortunately the reproducibility of the peel test data was low and only adhesion trends could be obtained. The set-up of the tack test is shown in section 2.3.1.

2.2.2.5 DIN Standards

For the tests listed above a series of DIN standards exist. The tests as far as adhesion is concerned often deal with adhesives and mortars used for flags. The most important ones with respect to this thesis are:

- Peel Test
 - DIN EN 1372 (“Prüfverfahren für Klebstoffe für Boden- und Wandbeläge, 1999”)
- Lap Shear Test
 - DIN EN 12003 (“Mörtel und Klebstoffe für Fliesen und Platten - Bestimmung der Scherfestigkeiten von Reaktionsharz-Klebstoffen, 1997”)
- Pull off Test
 - DIN EN 1346 (“Mörtel und Klebstoffe für Fliesen und Platten - Bestimmung der offenen Zeit, 2007”)

- DIN EN 15870 (“Klebstoffe - Bestimmung der Zugfestigkeit von Stumpfklebungen, 2009”)
- DIN EN ISO 4624 (“Beschichtungsstoffe - Abreißversuch zur Bestimmung der Haftfestigkeit, 2003”)
- ÖNORM EN 1323 (“Mörtel und Klebstoffe für Fliesen und Platten - Betonplatten für Prüfungen, 2007”)
- EN ISO 10365 (“Klebstoffe - Bezeichnung der wichtigsten Bruchbilder, 1992”)
- DIN EN 12004 (“Mörtel und Klebstoffe für Fliesen und Platten - Anforderungen, Konformitätsbewertung, Klassifizierung und Bezeichnung”)

2.3 Surface Characteristics

As well as the adhesion abilities of the sealants, the properties of the surface exposed to air are of great interest for industrial applications. Mainly surface properties such as stickiness, roughness, chemical composition, turbidity etc. arouse curiosity. Furthermore, consideration of adhesion mechanisms requires information about the physical and chemical properties of the adhering surfaces.²⁷ Hence, several studies have looked at surface properties with the help of surface techniques. As described in chapter 2.2.1.4, analyzing tools like ToF-SIMS, XPS, IR-ATR, AFM or SEM can be applied. Additionally, methods like zeta-potential,² solid state NMR or contact angle measurements⁶³ are suitable to analyze surface phenomena of the samples. Very often a combination of various surface techniques is applied. Stickiness studies of polymers have not been presented yet.

2.3.1 Topography and Surface Energy

To study the topographical composition of polyurethane surfaces, Zhu et al.⁶⁴ applied XPS analysis to polystyrene-polyurethane (PS/PU) composites. In their work, uncrosslinking and crosslinking PS/PU nanocomposites were prepared to demonstrate that nanoparticles of PU encapsulate the styrene monomers effectively. Additionally, TEM pictures were taken to underline the results obtained by XPS.

Majumdar et al.⁶³ characterized siloxane-urethane coatings by AFM, surface energy and contact angle measurements. The results were compared to those of pure polyurethane and silicone rubber. Static contact angles and consequently energy surfaces of all siloxane-urethane coatings having different mixing times of the isocyanate crosslinker did not vary significantly. The values obtained were very close to those of pure rubber silicone. However,

the surface energy of the PU was reported to be lower than of the coatings synthesized. By AFM microstructured surfaces were detected. Hutchinson et al.⁵¹ also investigated surface energies of foams and surface tension of sealants as described in section 4.2.4. They developed a tack test with which tack-free times of the sealants were analyzed. The tack test is based on the principle of the pull off set-up but low contact pressure and short contact times are applied. With this application tack-free times between 3 and 24 hours can be detected for different sealants. The set-up is shown in figure 4.8.

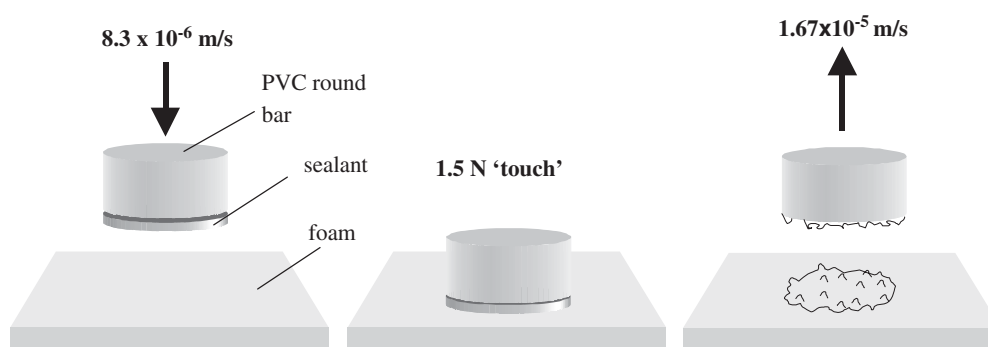


Figure 2.15: Schematic of tack test according to Hutchinson.⁵¹

2.3.2 Silanol Detection

Molecular properties of silicas are strongly related to the nature of their surface sides. Unsaturated surface valencies are satisfied by surface hydroxyl functionalities which can exist as vicinal (hydrogen-bonded silanols), geminal (two silanol groups at the same silicon atom) and isolated (no hydrogen bonds possible) groups. These are shown in figure 2.16, discussed by Dijkstra et al. in 2002.⁶⁵ According to the literature, the silanol surfaces are best studied by a combination of vibrational⁶⁶ and solid-state NMR spectroscopy.^{67,68} Furthermore, inverse reaction chromatography,^{69,70} Karl Fischer titration^{71,72} or ζ -potential measurements² can be employed.

In 2010 Sardon et al.² studied the effect of the curing agent in waterborne hybrid polyurethanes functionalized with (3-aminopropyl)triethoxysilane (AMEO) on particle morphology by TEM and investigated surface properties by ζ -potential measurements. Additionally, curing grades were analyzed by FTIR, ^1H and solid state ^{29}Si NMR, which confirm the quantitative incorporation of the alkoxy silane into the polyurethane chains. Furthermore, the presence of silanols at the surface can be demonstrated by ζ -potential analyses and their condensation can be shown by TEM, FTIR and SEM. The group found out that surface

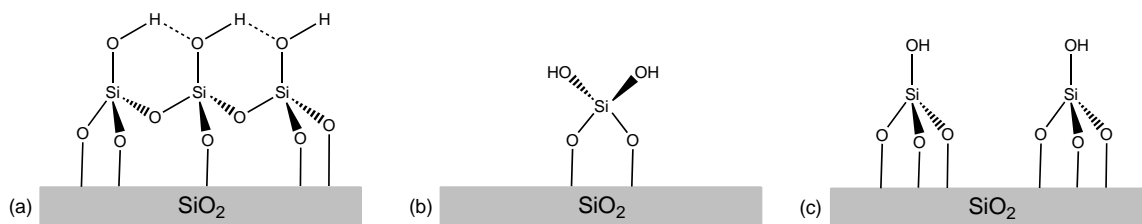


Figure 2.16: Silanol groups existing on silica surfaces according to Dijkstra: (a) vicinal, (b) geminal and (c) isolated silanols.⁶⁵

silica domains can be detected by TEM at AMEO concentrations higher than 9.7 wt%; the highest number of silanol groups was also obtained at this alkoxy silane concentration. The silanol content was determined by comparison measurements with colloidal silica and a pure polyurethane dispersion.

Chapter 3

Results and Discussion

Silyl-terminated polyurethanes are the basis of numerous sealants used worldwide. A mixed organic (polyurethane proportion) and inorganic (alkoxysilane proportion) hybrid resin system combines the advantages of conventional polyurethane and silicone techniques. The exact working principle of this system and the influences of the components on the formulation process are still under investigation and will be the subject of this chapter.

Most of all, the surface characteristics of the sealants, like tack behavior or elasticity pose problems and investigations will show that these effects are linked with the amount and type of alkoxysilane added as end-capper and adhesion promoter.

The adhesion of the STPUS to different substrates is also influenced by alkoxysilanes. Relatively open is the question of whether chemical or physical interactions between the silane group and the substrate of interest are responsible for adhesion strength. To describe adhesion of silyl terminated polyurethanes to different surfaces it is necessary to understand the processes involved and the nature of interaction between the silane group and the surface. Consequently, surface and adhesion phenomena of silyl-terminated polyurethanes applied as sealants will be discussed in this chapter.

3.1 Surface Analyses

Surface analyses suitable for silyl-terminated polyurethanes were already described in detail in chapter 2.3. For this investigation, a combination of various surface techniques such as SEM, IR-ATR, AFM, XPS, solid state NMR and contact angle measurements were used to determine surface properties like stickiness, roughness, chemical composition and turbidity of the samples of interest. The aim of these measurements was to analyze the influence of different end-cappers or adhesion promoters on the curing process.

For SEM analysis, SE- and BSE-images of the ‘air side’ (surface exposed to the air during the hardening process), the ‘adhesion side’ (surface connected to the hardening board) and cross-section-images were recorded as displayed in figure 3.1. Additionally, EDX-spectra were measured. IR spectra of the ‘air’ and ‘adhesion side’ were recorded, whereas AFM images, XPS spectroscopy and contact angle analyses were made only of the ‘air side’ of various cured prepolymers. Solid state NMR spectroscopy of the polymer were carried out by analyzing a sample removed about 2 to 5 mm of depth of the ‘air side’.

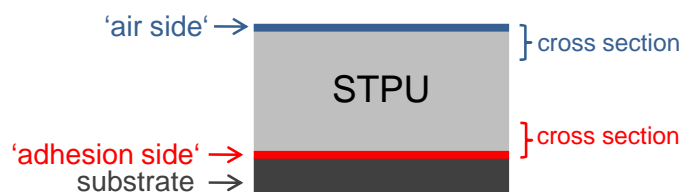


Figure 3.1: Investigated areas of the samples.

3.1.1 Sample Composition

To investigate surface phenomena, various STPU prepolymers were prepared. In order to simplify surface analyses fillers which are used to formulate the prepolymers to sealants were omitted. Synthesis and proceedings are described in section 4.2. Special sample composition for SEM, IR, AFM, XPS, NMR, CA and TGA analyses are summarized in this section. All analyses of one test series were done at the same conditions after the same curing times.

For SEM investigations, prepolymers were prepared according to the following tables. In one test series the same alkoxy silane was used as end-capper and adhesion promoter (see table 3.1). In the second experiment series AMMO-encapped polyurethanes were mixed with various adhesion agents (see table 3.2). In table 3.3 cured prepolymers with the same silicon concentrations are listed. Another test series investigated the curing characteristics under reduced moisture conditions (see table 3.4). Sample 2a_3DAMOT_dc was cured at 50°C in a drying cabinet.

The samples for IR-ATR measurements were prepared according to table 3.3, 3.4 and 3.5. The effect of increasing adhesion promoter concentration as well as that of various alkoxy silanes was studied.

AFM and XPS investigations were done (table 3.4 and 3.5) to study samples formulated with different adhesion promoters under varying curing conditions. Additionally, one sample prepared with 15wt% of AMMO was analyzed by AFM.

Solid state NMR, contact angle and TGA analyses were done of samples listed in table 3.4.

Table 3.1: Sample preparation for SEM measurements, end-capper=adhesion promoter (test series 1).

ITPU	end-capper	adhesion agent	substrate	name
IPDI-Acclaim_2 (1b)	AMMO (2b)	0 wt%	PVC	2b_0_PVC
IPDI-Acclaim_2 (1b)	AMMO (2b)	15 wt% AMMO	PVC	2b_15AMMO_PVC
IPDI-Desmophen_1.5 (1c)	AMMO (2c)	0 wt%	Al	2c_0_Al
IPDI-Desmophen_1.5 (1c)	AMMO (2c)	10 wt% AMMO	Al	2c_10AMMO_Al
IPDI-Desmophen_1.5 (1c)	AMMO (2c)	0 wt%	PE	2c_0_PE
IPDI-Desmophen_1.5 (1c)	AMMO (2c)	10 wt% AMMO	PE	2c_10AMMO_PE
IPDI-Desmophen_1.5 (1c)	AMEO (2c')	10 wt% AMEO	Al	2c'_10AMEO_Al
IPDI-Desmophen_1.5 (1c)	1189 (2c'')	10 wt% 1189	Al	2c''_101189_Al
IPDI-Desmophen_1.5 (1c)	Alink-15 (2c''')	10 wt% A-link 15	Al	2c'''_10Alink15_Al

Table 3.2: Sample preparation for SEM measurements, end-capper \neq adhesion promoter (test series 2).

ITPU	end-capper	adhesion agent	substrate	name
IPDI-Acclaim_2 (1b)	AMMO (2b)	10 wt% 1189	Al	2b_101189_Al
IPDI-Acclaim_2 (1b)	AMMO (2b)	10 wt% A-link 15	Al	2b_10Alink15_Al
IPDI-Acclaim_2 (1b)	AMMO (2b)	10 wt% 1146	Al	2b_101146_Al
IPDI-Acclaim_2 (1b)	AMMO (2b)	10 wt% DAMO-T	Al	2b_10DAMO-T_Al

Table 3.3: Sample preparation for SEM and IR-ATR measurements, end-capper \neq adhesion promoter, n(Si)=4.99 mmol (test series 3).

ITPU	end-capper	adhesion agent	substrate	name
IPDI-Acclaim_1.5 (1a)	AMMO (2a)	3.00 wt% AMMO	Al	2a_3AMMO_Al
IPDI-Acclaim_1.5 (1a)	AMMO (2a)	4.26 wt% 1189	Al	2a_4.261189_Al
IPDI-Acclaim_1.5 (1a)	AMMO (2a)	3.74 wt% A-link 15	Al	2a_3.74Alink15_Al
IPDI-Acclaim_1.5(1a)	AMMO (2a)	3.76 wt% DAMO-T	Al	2a_3.76DAMOT_Al
IPDI-Acclaim_1.5(1a)	AMMO (2a)	3.50 wt% DAMO-D	Al	2a_3.50DAMOD_Al

Table 3.4: Sample preparation for SEM, IR and AFM measurements, different alkoxy silanes (test series 4).

ITPU	end-capper	adhesion agent	substrate	name
IPDI-Acclaim.1.5 (1a)	AMMO (2a)	-	Al	2a_Al
IPDI-Acclaim.1.5 (1a)	AMMO (2a)	3 wt% AMMO	Al	2a_3AMMO_Al
IPDI-Acclaim.1.5 (1a)	AMMO (2a)	3 wt% DAMO-T	Al	2a_3DAMO-T_Al
IPDI-Acclaim.1.5 (1a)	AMMO (2a)	3 wt% DAMO-T	Al	2a_3DAMOT_dc

Table 3.5: Sample preparation for SEM and IR measurements, increasing amount of AMMO (test series 5).

ITPU	end-capper	adhesion agent	substrate	name
IPDI-Acclaim.1.5 (1a)	AMMO (2a)	3 wt% AMMO	Al	2a_3AMMO_Al
IPDI-Acclaim.1.5 (1a)	AMMO (2a)	5 wt% AMMO	Al	2a_5AMMO_Al
IPDI-Acclaim.1.5 (1a)	AMMO (2a)	7 wt% AMMO	Al	2a_7AMMO_Al
IPDI-Acclaim.1.5 (1a)	AMMO (2a)	10 wt% AMMO	Al	2a_10AMMO_Al
IPDI-Acclaim.1.5(1a)	AMMO (2a)	15 wt% AMMO	Al	2a_15AMMO_Al

3.1.2 Increasing Amount of Alkoxy silane

Practical experience shows that different amounts of adhesion promoters do have a large impact on stickiness and adhesion abilities of the polymers. Molecular activities were investigated using surface analysis methods including SEM and IR-ATR.

3.1.2.1 SEM Measurements

Scanning electron microscopy (SEM) investigations were performed in order to analyze the impact of an increasing amount of alkoxy silane. Six AMMO-end-capped samples with varying concentrations of AMMO as adhesion promoter (2b_0_PVC, 2b_15AMMO_PVC, 2c_0_Al, 2c_10AMMO_Al, 2c_0_PE, 2c_10AMMO_PE) as shown in table 3.1, were investigated. The amount of AMMO varied between 0 and 15 wt%. Additionally, different substrates were selected (PVC, Al and PE).

The samples prepared without additional adhesion agents, like 2c_0_Al and 2c_0_PE, give SEM images of homogeneous surfaces containing mainly carbon, oxygen and traces of silicon and chloride. This is true for both the ‘air side’ surface and ‘adhesion side’ surface.

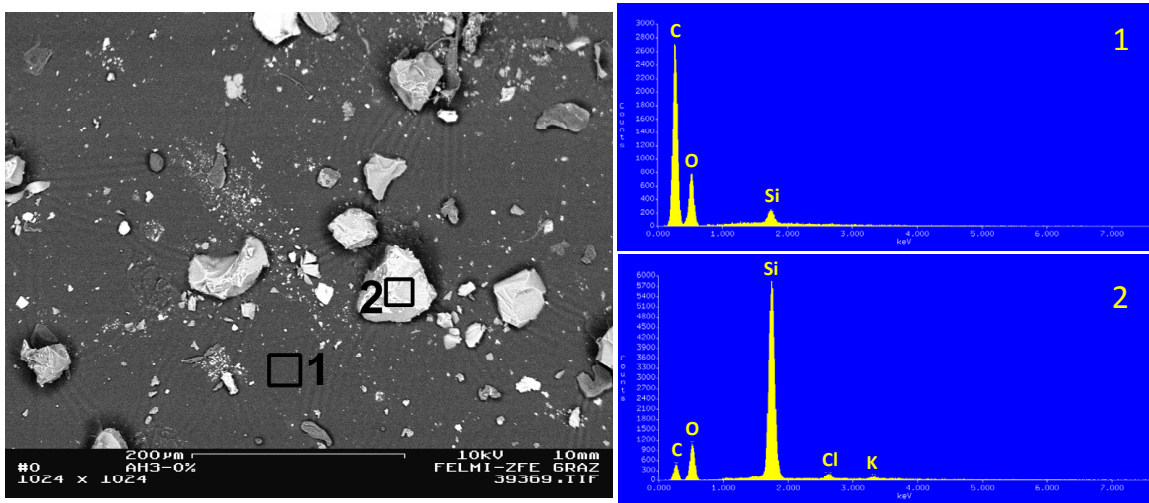


Figure 3.2: ‘Air side’ of sample 2b_0_PVC showing silicon-containing crystallites (BSE image).

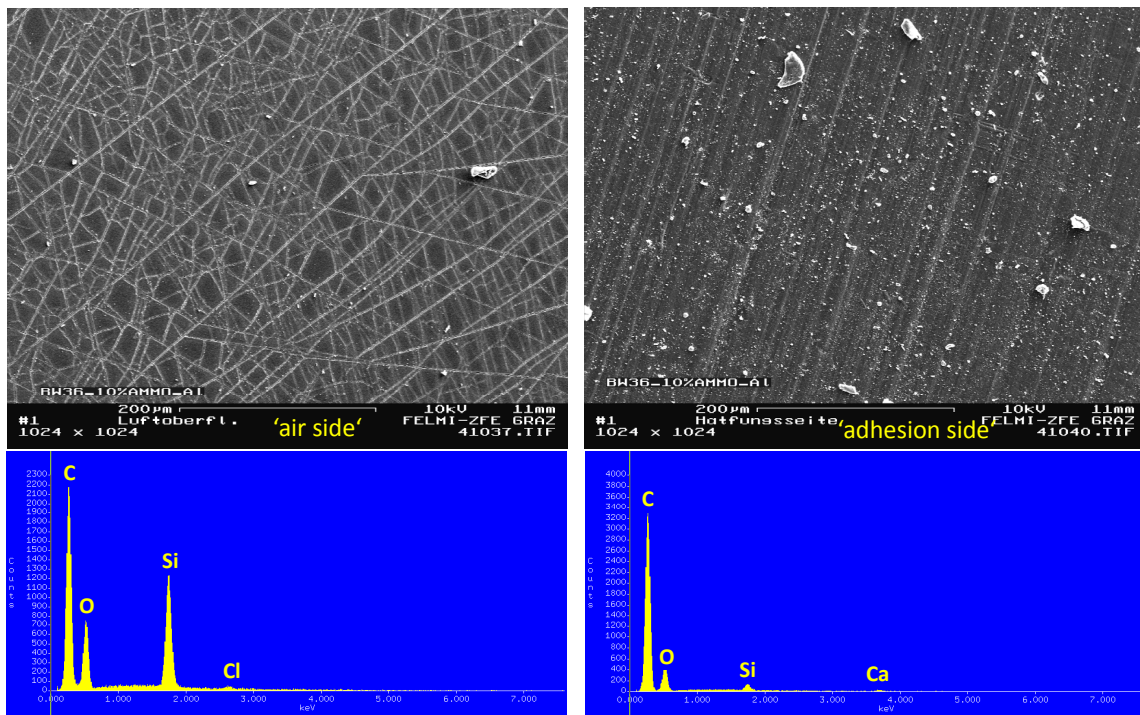


Figure 3.3: Accumulation of silicon on the ‘air and adhesion side’ of sample 2c_10AMMO_AI (SE image) and EDX spectra of the BSE image (‘air side’: left column, ‘adhesion side’: right column).

By increasing the amount of added alkoxy silane either by varying the NCO/OH ratio, as in sample 2b_0_PVC (NCO/OH=2, no adhesion promoter, substrate=PVC) or through addition of AMMO as adhesion promoter (2b_15AMMO_PVC, 2c_10AMMO_Al, 2c_10AMMO_PE) clear accumulation of silicon can be seen at the ‘air side’.

In the case of 2b_0_PVC the ‘air side’ shows eye-catching crystallites (2) with a high proportion of silicon. These are displayed in figure 3.2. The backbone (1) consists of the polyurethane-polymer. Silicon can also be detected in this region, however 10 times less than the amount of the crystallites (2). The BSE image of the ‘adhesion side’ shows fewer silicon-accumulated crystallites.

Further increase of the amount of added adhesion promoter AMMO leads to clear changes of the sample characteristics. The silicon crystallites are replaced by a homogeneous brittle film. This is true for the ‘air’ and ‘adhesion side’ of the cured polymers, shown in figure 3.3.

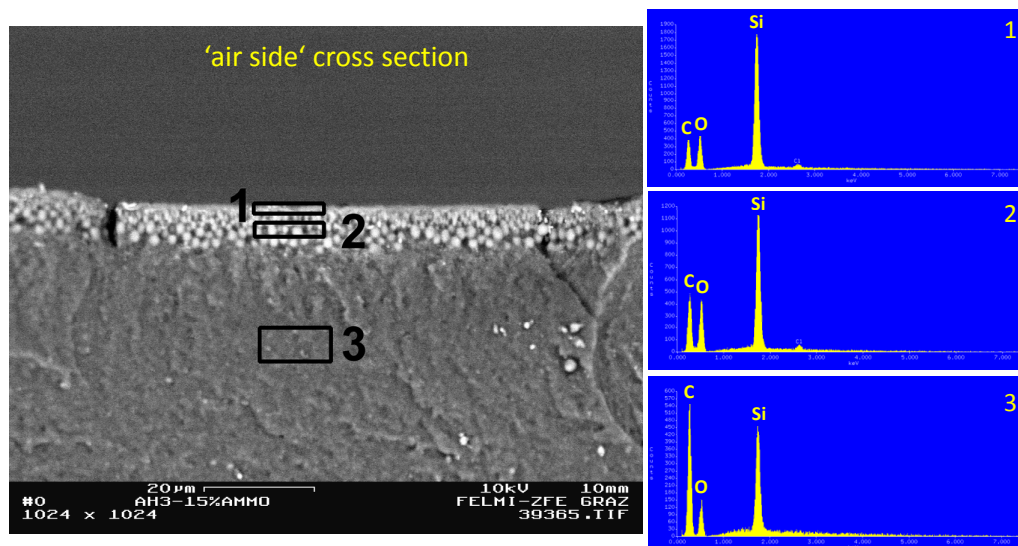


Figure 3.4: Decrease of the silicon content at the ‘air side’ of sample 2b_15AMMO_PVC (BSE cross section image).

Very eye-catching is the accumulated silicone layer formed at the ‘air side’ of the sample. This effect can also clearly be seen in the SEM cross section measurements of sample 2b_15AMMO_PVC in figure 3.4. Going from the surface to the inner part of the sample a decreasing content of silicon and oxygen relative to carbon is observed. This phenomenon cannot be detected on the cross section BSE picture of the ‘adhesion side’; the silicon concentration stays constant at the ‘adhesion side’ of the sample. The adhesion surface consists of a polyurethane-silicon-backbone containing some domains in which silicon and oxygen are

more accumulated relative to carbon. Increasing the amount of AMMO leads to a greater accumulation of silicon on the ‘air side’ surface, but not on the ‘adhesion side’. Furthermore, no influence of the substrates aluminum, PVC and PE on the appearance of the ‘adhesion side’ of the samples could be detected. This accumulation effect can be clearly followed by increasing the amount of AMMO in intervals from 5wt% to 15wt%. Samples 2a_3AMMO_Al, 2a_5AMMO_Al, 2a_7AMMO_Al, 2a_10AMMO_Al, 2a_15AMMO_Al were investigated by EDX analyses. The area of the κ X-ray line of silicon and carbon were determined. Increase of the silicon concentration and decrease of the carbon concentration with rising amount of AMMO can be seen in figure 3.5. Because of silicone formation at the ‘air side’, the polyurethane backbone concentration and consequently carbon accumulation decreases.

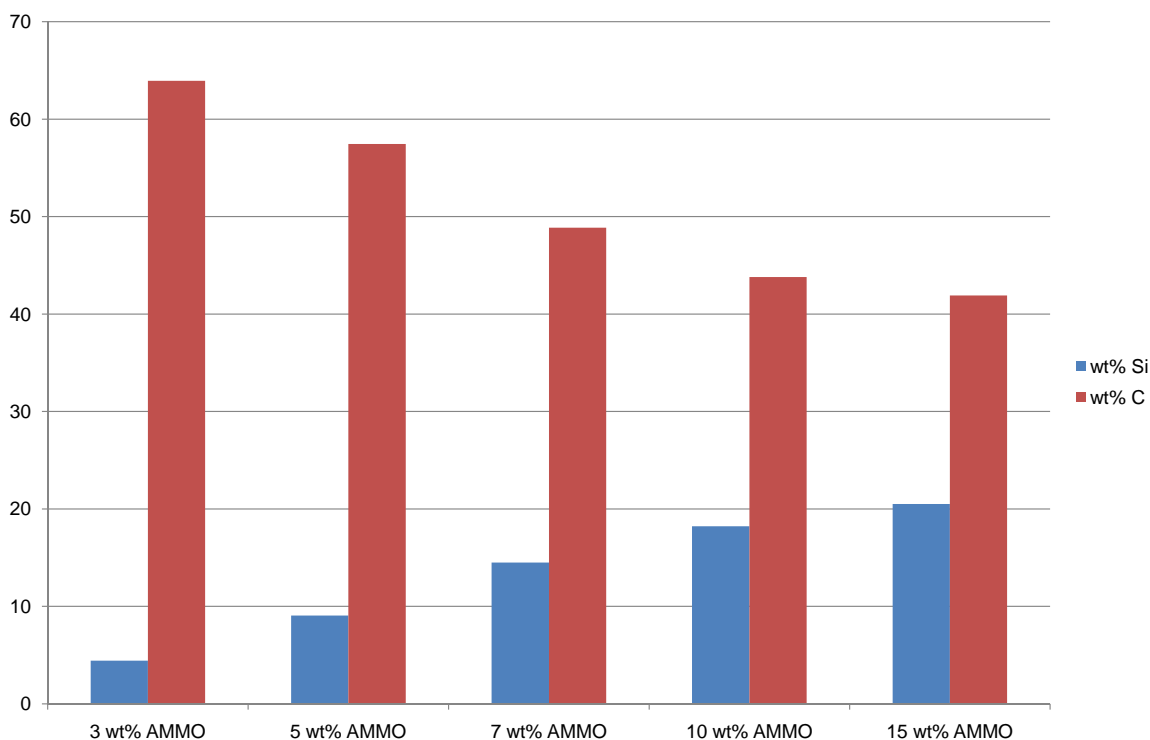


Figure 3.5: Silicon (blue) and carbon (red) concentration versus increasing amount of AMMO.

3.1.2.2 IR Measurements

Besides SEM, Infrared-Attenuated Total Reflection (IR-ATR) measurements are an easy and cheap analytical tool for investigating the surfaces of polymers. The aim of the analyses

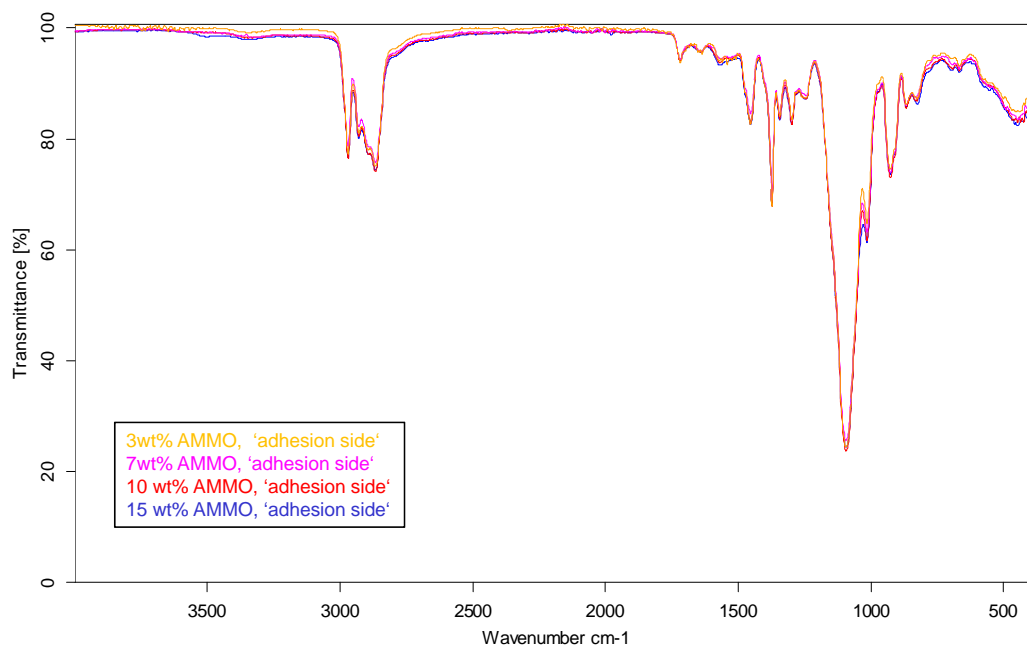


Figure 3.6: IR spectra of the ‘adhesion side’ of samples 2a.3AMMO_Al, 2a.7AMMO_Al, 2a.10AMMO_Al, 2a.15AMMO_Al having increasing amount of AMMO as adhesion promoter.

reported here was to obtain correlations between SEM and IR-ATR results. Consequently, the focus was on the influence of the adhesion promoter concentration and the chemical composition of the alkoxy silane on the polymer characteristics. As shown in figure 3.1, the ‘air side’ and ‘adhesion side’ of the cured prepolymers (2a.3AMMO_Al, 2a.5AMMO_Al, 2a.7AMMO_Al, 2a.10AMMO_Al, 2a.15AMMO_Al) were investigated by IR-ATR.

The ‘adhesion side’ spectra of all five investigated samples are the same (2970, 2932, 2867, 1719, 1452, 1372, 1343, 1297, 1242, 1093, 1012, 924, 866, 825, 423 cm^{-1} , see figure 3.6) whereas the ‘air side’ spectra show significant differences as displayed in figure 3.7. Additional bands at 1560, 1195, 763, 690 cm^{-1} appear with increasing amount of added adhesion agent. Furthermore, the band at 1012 cm^{-1} increases strongly. The strong band in the region of 1012 cm^{-1} can be attributed to siloxane (Si-O-Si) bonds, whereas the bands at 1195 and 763 cm^{-1} appear due to Si-O stretching vibrations.^{6,8,73} For coupling agents of the type $(\text{RO})_3\text{SiCH}_2\text{CH}_2\text{CH}_2\text{NH}_2$ the infrared spectrum is dominated by bands of the $(\text{RO})_3\text{Si}$ -part, with additional weak bands of the NH_2 functionality at 1560 cm^{-1} and in the region of 3370 to 3290 cm^{-1} .⁷³

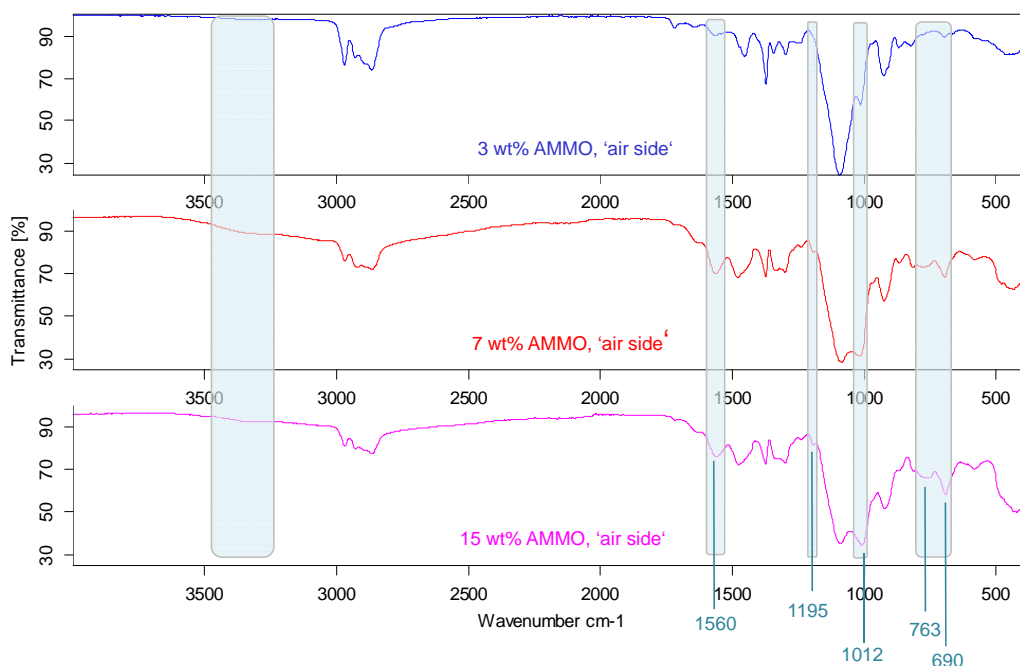


Figure 3.7: IR spectra of the ‘air side’ of samples 2a_3AMMO_Al, 2a_7AMMO_Al, 2a_15AMMO_Al with increasing amount of AMMO as adhesion promoter.

Hence, strong silicone accumulation at the ‘air side’ can be detected by IR-ATR measurements. For sample 2a_3AMMO_Al, the IR spectra of ‘air’ and ‘adhesion side’ do not show any differences; the silicone accumulation at the air surface is not detected. With increasing amount of AMMO added, the strong siloxane formation can be seen in the spectra. This effect becomes observable at concentrations of 5 wt% of AMMO. Consequently, the IR-ATR measurements correlate with the SEM analyses and can be used as a cheap analytical tool to detect strong silicone accumulations at surfaces of STPU surfaces.

3.1.3 Influence of Different Alkoxysilanes

Besides the alkoxysilane concentration, the identity of different adhesion promoters also significantly impacts the performance of the cured prepolymers. Various alkoxysilanes that have been used as additives were summarized in chapter 2.2.1.4.

3.1.3.1 SEM Measurements

SEM images were taken of samples synthesized with different adhesion promoters to see differences in the surface appearance with respect to the silicon accumulation. The results

of these analyses are summarized in the section ‘Qualitative Comparison’. In order to obtain direct correlations between adhesion promoter and silicon concentration at the surface, quantitative comparisons were made, described in the second subsection.

Qualitative Comparison

To compare the qualitative influence of the alkoxyxilanes, different STPUs synthesized with several end-cappers and adhesion promoters were analyzed.

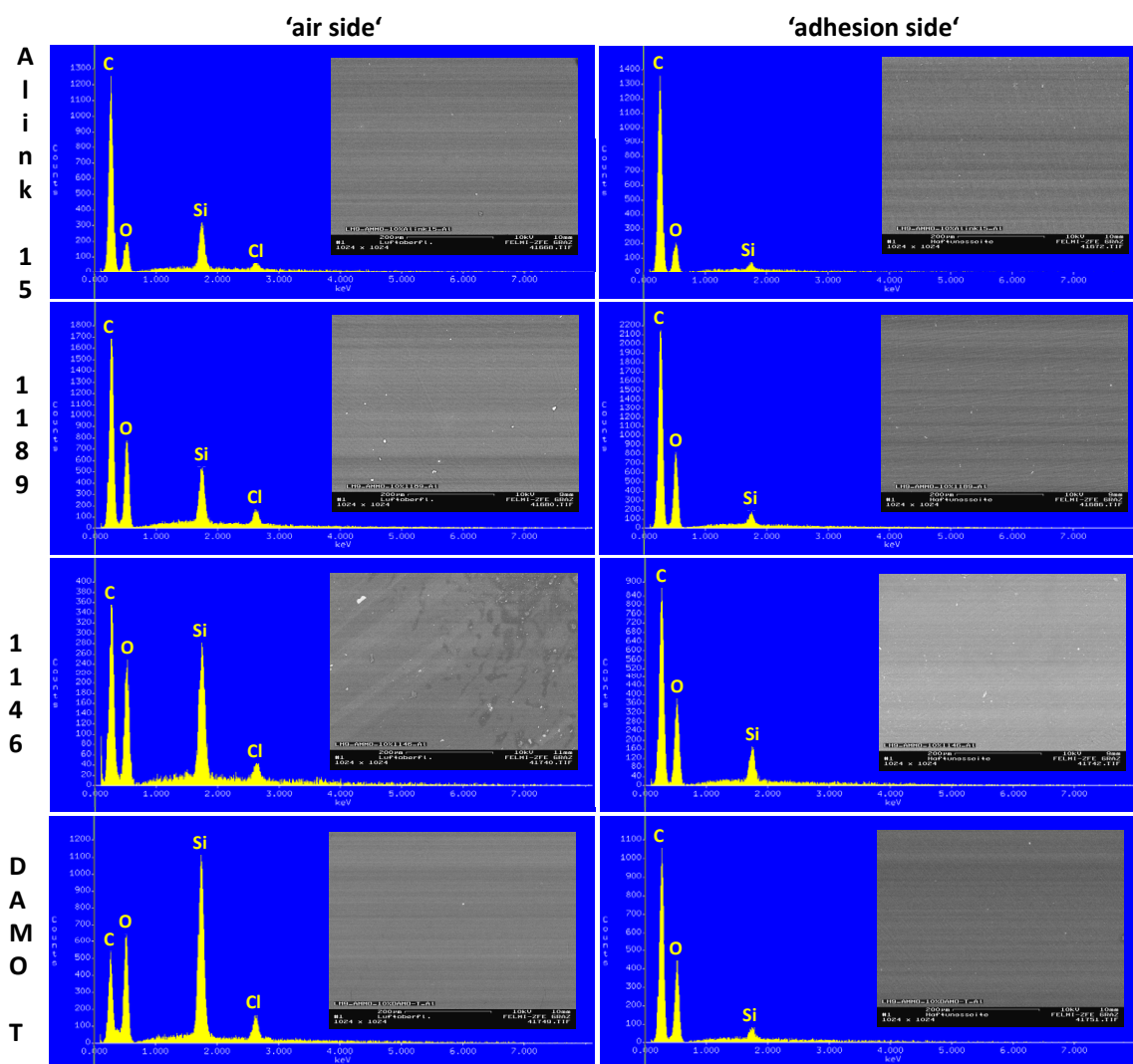


Figure 3.8: Accumulation of silicon on the ‘air and adhesion side’ of sample 2b_10Alink15_Al, 2b_101189_Al, 2b_101146_Al, 2b_10DAMO-T_Al and EDX spectra of the BSE image (‘air side’: left column, ‘adhesion side’: right column).

Polymers having the same alkoxy silane as end-capper and adhesion promoter (2c_10AMMO_Al, 2c'_10AMEO_Al, 2c''_101189_Al, 2c'''_10Alink15_Al) and AMMO-endcapped hybrid resins mixed with differing alkoxy silanes (2b_101189_Al, 2b_10Alink15_Al, 2b_101146_Al, 2b_10DAMO-T_Al) were prepared (table 3.1 and 3.2). 10 wt% of each adhesion agent was added.

The 'air side' of each sample can be identified as a homogeneous surface, with different degrees of impurity. Sample 2c''_101189_Al especially appears contaminated at the 'air' and 'adhesion side' as the result of sample storage and pretreatment. All samples show a clear accumulation of silicon at the surface exposed to air during the curing process. This effect is shown in figure 3.8 for all samples of AMMO-endcapped polyurethanes mixed with 10wt% Alink-15, 1189, 1146 and DAMO-T as additives, respectively. Quantitative conclusions cannot be drawn due to the different molecular weights of the adhesion promoters. In the case of DAMO-T (2b_10DAMO-T_Al) and AMEO (2c'_10AMEO_Al) as adhesion promoter the silicon accumulation seems the strongest. Poor-moisture atmosphere such as that in a drying cabinet lead to reduced silicon accumulation at the 'air side' surface. Siloxane formation is slower due to lack of humidity.

Direct correlations between adhesion promoter and silicon concentration at the surface are discussed in the next section.

Quantitative Comparison

As seen in section 'Qualitative Comparison', silicon accumulation at the sample surface due to addition of alkoxy silanes is clear. The probabilities of chemically different silanes to accumulate at the 'air side' are investigated in this section. Several prepolymers having the same molar silicon amount were synthesized (see table 3.3). Aim of these measurements was to detect correlations between silicon accumulation at the 'air side' and type of adhesion promoter applied.

Application of different alkoxy silanes leads to different surface characteristics of the cured prepolymers. Conspicuous behavior with respect to tack characteristics will be summarized in section 3.2. Additionally, some alkoxy silanes applied as adhesion promoters produce turbid samples. This is the case for the addition of small amounts of DAMO-T or DAMO-D (3 wt%) or for the addition of more than 7 wt% of other alkoxy silanes like AMMO, AMEO, 1198 or Alink-15. These influences obviously go hand in hand with the curing behavior of the various samples. In figure 3.9 the results of SEM and EDX measurements of samples 2a_3AMMO_Al, 2a_4.261189_Al, 2a_3.74Alink15_Al, 2a_3.76DAMOT_Al and 2a_3.50DAMOD_Al of test series 3 in table 3.3 are displayed. As the samples contain the same silicon amount of 4.99 mmol

the results can be correlated directly.

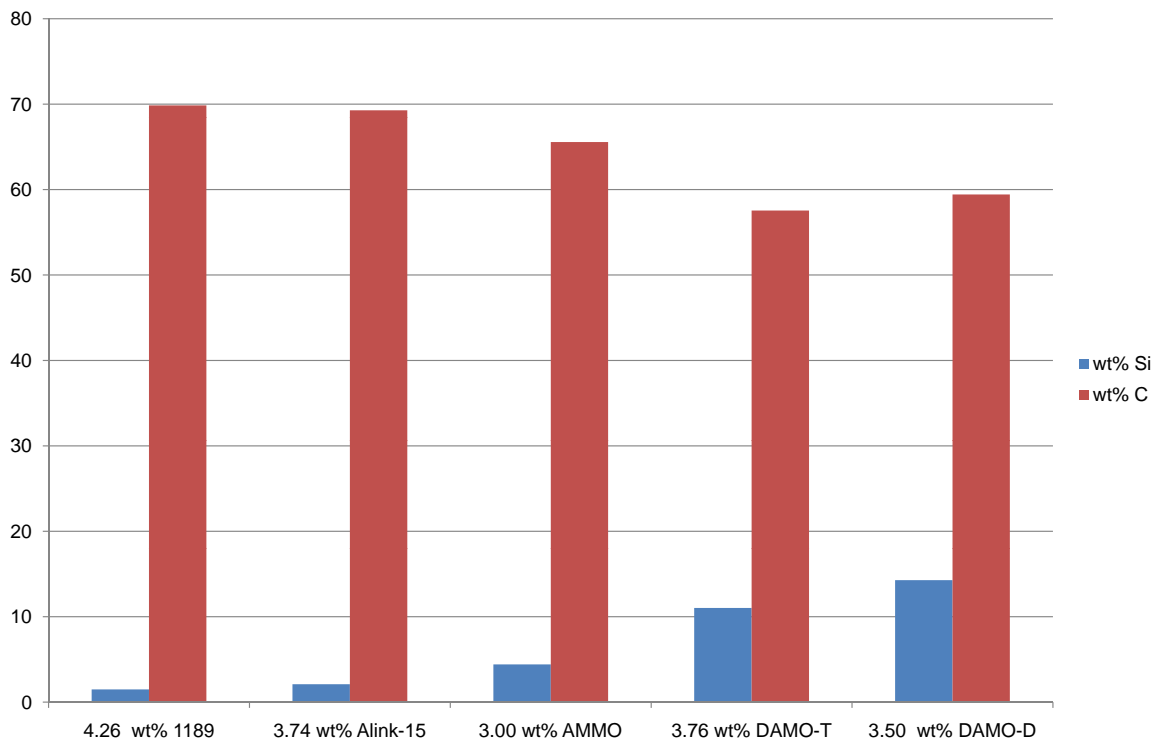


Figure 3.9: Silicon (blue) and carbon (red) concentration versus alkoxysilanes 1189, Alink-15, AMMO, DAMO-D and DAMO-T.

The silicon accumulation increases going from 1189 to DAMO-D. In contrast, the carbon concentration decreases. In the case of 2a.3.50DAMOD_Al the carbon concentration does not follow this trend exactly which can be explained by having a closer look at the sample surface. Prepolymers formulated with DAMO-D tend to have two different areas: Silicone-accumulated areas and polyurethane-accumulated. In all samples silicone accumulation can be detected, but DAMO-T and DAMO-D show the strongest effects in all investigations. This effect can also be seen by comparing sample 2a.3DAMOT_Al with 2a.3DAMOT_Al_dc of table 3.4. The two samples have the same composition. Sample 2a.3DAMOT_Al was cured under standard conditions in the laboratory whereas sample 2a.3DAMOT_Al_dc was cured in a moisture-poor atmosphere in a drying cabinet at 50°C. The EDX spectra of the two samples show impressively the stronger silicone accumulation in sample 2a.3DAMOT_Al (see (1a) in figure 3.10). Moisture enriched atmosphere and big amounts of added alkoxysilane cause strong silicon concentrations at the ‘air side’ surface.

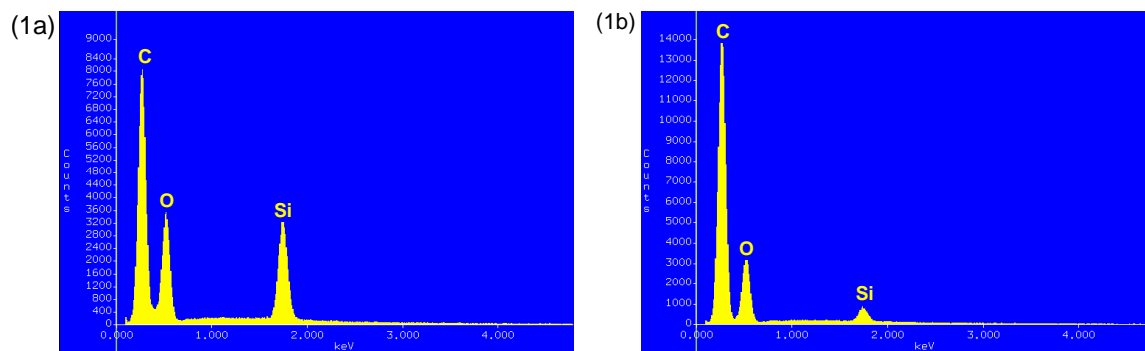


Figure 3.10: EDX spectra of sample 2a.3.76DAMOT_Al (1a) and 2a.3DAMOT_Al.dc (1b).

Obviously, the two amine groups of DAMO-T and DAMO-D initiate strong silicone network formation at the surface as they wander to the ‘air side’ of the STPU. This effect is related to the polar alkyl chains. In the case of monofunctional amines like AMMO, 1189 or Alink-15 the silicone accumulation at the surface is smaller. Hydrolysis behavior of AMMO, 1189, Alink-15 and DAMO-T were investigated by liquid ^1H and ^{29}Si NMR spectroscopy and can be seen in section 3.1.3.5.

3.1.3.2 IR Measurements

IR-ATR analyses of samples 2a.3AMMO_Al, 2a.4.261189_Al, 2a.3.74Alink15_Al, 2a.3.76DAMOT_Al and 2a.3.50DAMOD_Al, summarized in table 3.3, were performed with focus on the ‘air’ and ‘adhesion side’ of the polymers. As all samples had the same silicon amount of 4.99 mmol the results of the obtained IR-ATR spectra can be correlated with the applied adhesion promoters AMMO, 1189, Alink-15, DAMO-T and DAMO-D.

In the case of samples 2a.3AMMO_Al, 2a.4.261189_Al and 2a.3.74Alink15_Al no differences of the IR spectra of ‘adhesion’ and ‘air side’ could be detected. The two surfaces seem to be chemically identical. In the case of 2a.3.76DAMOT_Al and 2a.3.50DAMOD_Al the spectra of the two surfaces of interest differ obviously. As described in section 3.1.2.2 strong silicone accumulation at the ‘air side’ can be detected, which was the case for samples 2a.3.76DAMOT_Al and 2a.3.50DAMOD_Al. The corresponding IR spectra of sample 2a.3.76DAMOT_Al are displayed in figure 3.11.

Adhesion promoters like DAMO-T and DAMO-D lead to a stronger accumulation of silicone at the ‘air side’ of the polymers, which can also be proved by SEM analyses as in section 3.1.3.1 ‘Quantitative Comparison’.

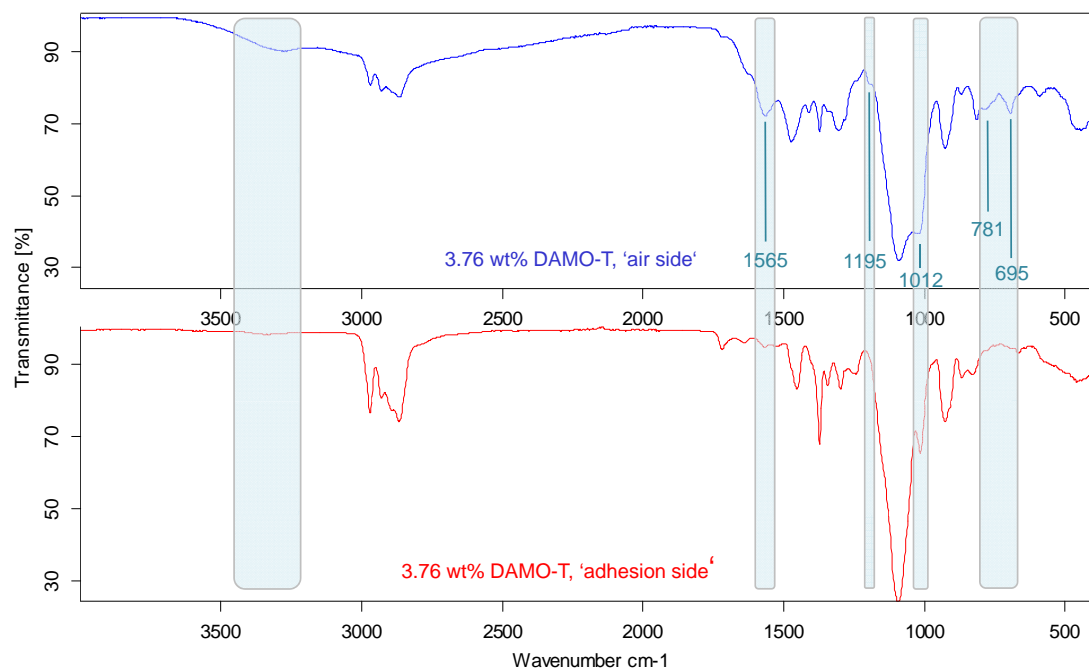


Figure 3.11: IR spectra of the 'air side' and 'adhesion side' of sample 2a_3.76DAMOT_Al.

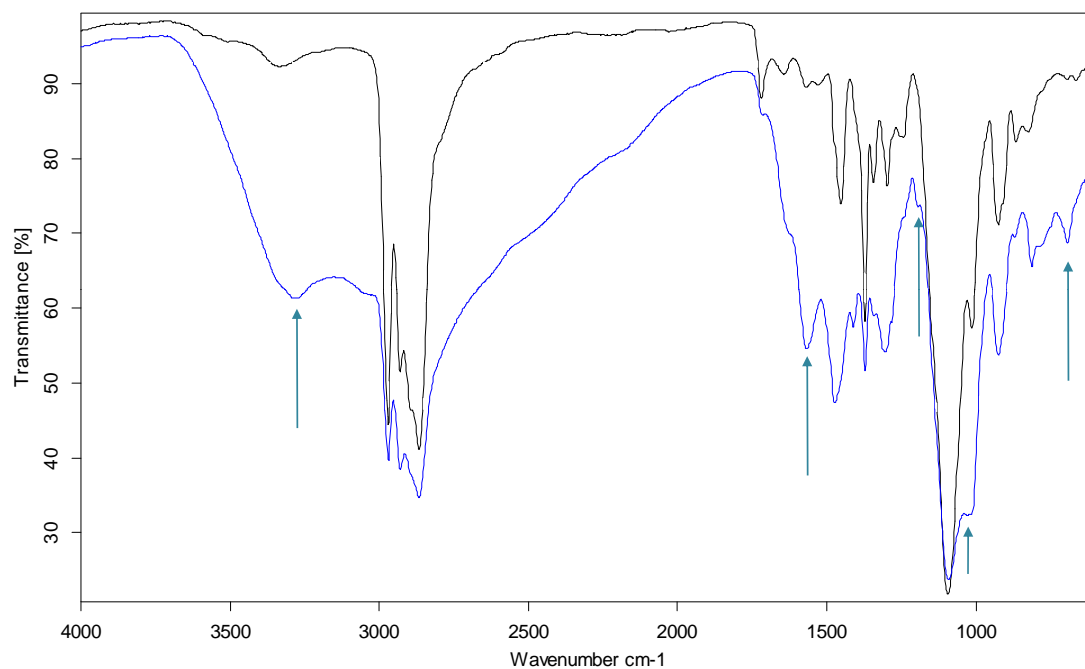


Figure 3.12: IR spectra of the 'air side' of samples 2a_3DAMOT_Al (blue) and 2a_3DAMOT_dc (black).

Short curing times or poor moisture atmosphere such as that in a drying cabinet lead to reduced silicone accumulation at the ‘air side’ surface. This can be seen by comparing the IR spectra of sample 2a_3DAMOT_Al and 2a_3DAMOT_dc of test series 4 in figure 3.12. The differing bands are marked with an arrow. In sample 2a_3DAMOT_Al (blue line) the presence of silicone structures can be seen. In the slower cured sample 2a_3DAMOT_dc (black line) no bands referring to silicone can be detected.

3.1.3.3 AFM Measurements

Surface analyses like Atomic Force Microscopy (AFM) give an insight into the topographic and qualitative characteristic of surfaces. Height and phase images were recorded from the same area and can be compared directly. Additionally, 3D views and cross section investigations will be presented in this section. To detect topographic differences, samples 2a_Al, 2a_3AMMO_Al, 2a_3DAMO-T_Al, 2a_3DAMOT_dc (table 3.4) and sample 2a_15AMMO_Al (table 3.5) were analyzed.

Due to strong stickiness of the samples, AFM measurements were difficult and sample 2a_Al (without adhesion promoter) could not be investigated as the AFM needle became stuck in the polymer matrix. Sample 2a_3AMMO_Al (3wt% AMMO) could be measured but gave slightly blurred pictures due to this effect. IR-ATR and SEM analyses had already shown that sample 2a_3DAMO-T_Al (3wt%DAMO-T) has different surface characteristics than the other three samples, an effect which can also be seen in the AFM images in figure 3.13.

The formulation containing 3wt% of DAMO-T (2a_3DAMO-T_Al) shows well defined structures of ~ 15 nm width and ~ 5 nm height (1a). A close look at the phase image (2a) demonstrates that the structures have different chemical composition than the darker displayed backbone. As the SEM analyses showed high accumulation of silicon on the surface, the structures will correspond to silicone network formations. The chemically equivalent sample 2a_3DAMOT_dc, which also contained 3 wt% DAMO-T but was cured in the drying oven under moisture-poor conditions, causes a completely different surface appearance according to AFM. In this case the surface does not show surface structures (1b). The contrary effect can be seen. Holes with a diameter of ~ 30 -50 nm and a depth of ~ 5 -7 nm are formed. The impression of a layered system is given, as seen on the phase picture (2b). Through changing the curing conditions, a network formation like that in (1a) cannot be detected. Sample 2a_3DAMOT_dc was removed from the drying cabinet and stored at standard conditions in the laboratory; after one month the surface showed the same holes at the surface as in (1b). Similar effects can be seen in sample 2a_3AMMO_Al (3wt% AMMO). Holes are formed with a depth of about ~ 3 -6 nm (1c). Unfortunately, the images are blurred as described above.

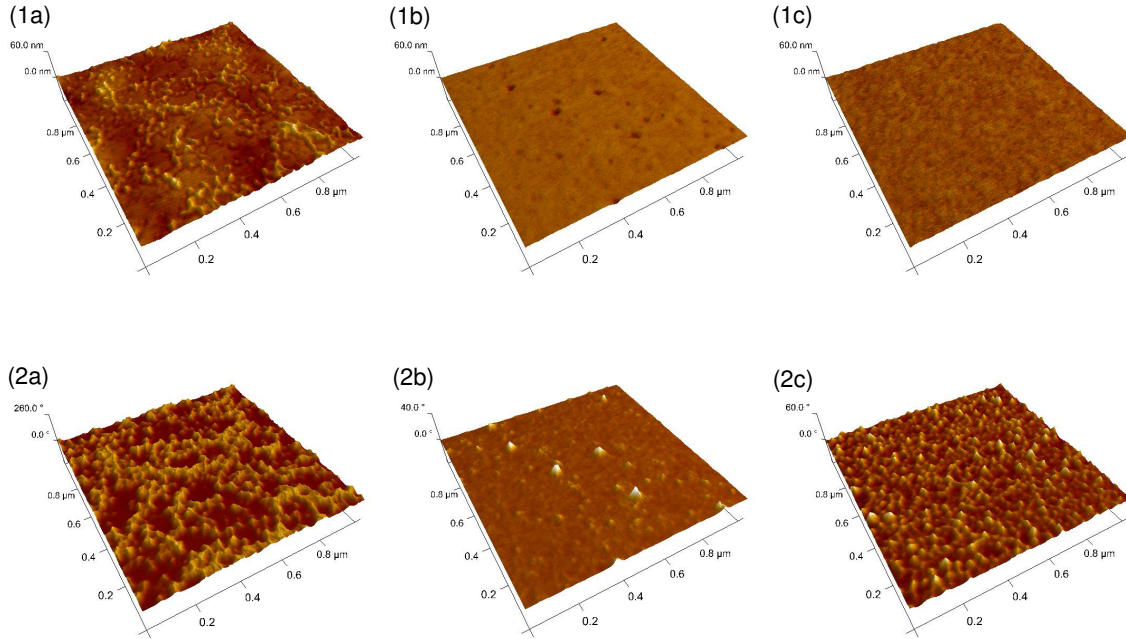


Figure 3.13: First row: Height AFM images of sample 2a_3DAMO-T_Al (1a), 2a_3DAMOT_dc (1b) and 2a_3AMMO_Al (1c), second row: phase images of sample 2a_3DAMO-T_Al (2a), 2a_3DAMOT_dc (2b) and 2a_3AMMO_Al (2c).

According to the phase image (2c), a two phase system is formed. The light areas in the phase images of the samples can be identified as silicone, whereas the darker parts display the polyurethane polymer bulk.

All samples form siloxane structures at the surface, but DAMO-T as adhesion promoter cured at standard conditions (2a_3DAMO-T_Al) leads to the strongest silicone network formation showing new and unique structures. Less moisture with the same sample composition (2a_3DAMOT_dc) results in reduced silicone formation and the appearance of a plane surface. The surface of 2a_3DAMOT_dc looks much more like sample 2a_3AMMO_Al than like sample 2a_3DAMO-T_Al. In all samples, bulk structures differ strongly from surface structures, which can be observed in AFM images of the cross section of sample 2a_3DAMO-T_Al (figure 3.14).

The cross section investigations demonstrate that there is a phase feature gradient going from the ‘air side’ to the inner part of the sample. This effect correlates with the SEM observations shown in figure 3.4. Siloxane structures (displayed in light yellow in the AFM image) decrease within the sample. At a depth of 25 μm (P2), 525 μm (P3) and 1025 μm

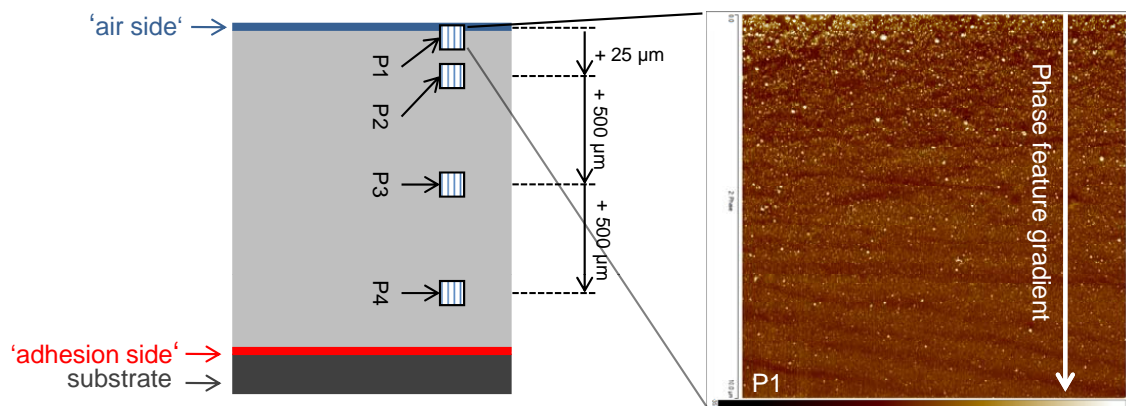


Figure 3.14: AFM cross section measuring points P1-P5 of sample 2a_3DAMO-T_A1 and phase image of P1.

(P4) isolated round light yellow areas in dark bulk structures can be seen. This can be explained by the preparation of the polymers. Due to stirring with the turbo mixer small air bubbles remain in the polymer matrix. In these areas, pockets of moisture remain and promote better siloxane formation.

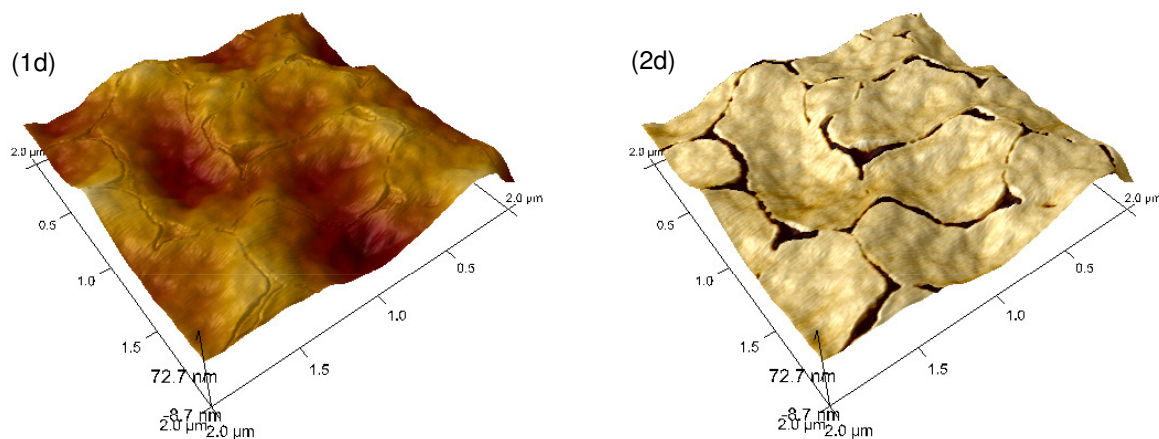


Figure 3.15: AFM height image (1d) and phase image (2d) of the 'air side' of sample 2a_15AMMO_A1.

Silicone accumulation at the sample surface can also be seen by analyzing a sample prepared with a large amount of adhesion promoter AMMO. Sample 2a_15AMMO_A1 was formulated with 15 wt% of AMMO. Whereas sample 2a_3AMMO_A1 (see (1c) in figure 3.13) has a very

planar siloxane-poor surface, the contrary effect can be seen with sample 2a_15AMMO_Al, shown in figure 3.15. A thick siloxane layer is formed at the ‘air side’ surface of the sample, displayed in light yellow in the phase image (2d). Below this film the polyurethane bulk polymer can be seen. The height image (1d) also demonstrates the layered system. Deeper situated areas appear dark in the phase image and vice versa. Furthermore, the surface has a slightly waved appearance compared to the others described above, which can be explained by shrinking effects during the curing process. Due to the two-phase layered system volume shrinkage causes a corrugated surface of the sample.

3.1.3.4 XPS Measurements

X-ray photoelectron spectroscopy (XPS) was employed to support the results obtained by SEM, IR-ATR and AFM analyses. XPS spectra of samples 2a_Al, 2a_3AMMO_Al, 2a_3DAMO-T_Al, 2a_3DAMOT_dc were recorded and compared with respect to their silicon concentration. Silicon accumulation at the ‘air side’ surface is further corroborated by XPS analyses.

3.1.3.5 NMR Measurements

Liquid ^1H and ^{29}Si NMR and solid state ^{29}Si NMR analyses were applied to obtain new knowledge about the hydrolysis and condensation behavior of the adhesion promoters. As described in the literature overview, the alkoxygroups OR enable the silane to be linked to surfaces bearing hydroxyl groups. Organic functionalities like amines or epoxy groups copolymerize with the organic polymer backbone and thus enhance interfacial adhesion between polymer and substrate.

This section will focus on the hydrolysis and condensation characteristics of adhesion promoters AMMO, DAMO-T, 1189, Alink-15 and propyltrimethoxysilane, as it is well known that these two reactions are affected by the structure of the organic part of the silane and by medium characteristics like temperature, pH, concentration, amount of water and catalyst.²⁴ Chemical Formulas and NMR shifts are summarized in tables 3.6 and 3.7.

In the literature, silanol function formation during the hydrolysis process is described and proves to be very reactive in establishing bonds between substrate and adhesion promoter.²¹ Hence, knowledge about the silanol formation and the degree of oligomerization is of decisive importance for practical use of alkoxyxilanes as adhesion agents with respect to curing times and surface appearance characteristics like turbidity or tack behavior, as described in section 3.2.

Table 3.6: Silane coupling agents employed for hydrolysis.

silane	formula
N-cyclohexylaminomethyltriethoxysilane	
AMMO	
DAMO-T	
A-link 15	
1189	
PTMS	

Table 3.7: ^1H and ^{29}Si NMR shifts of the used methoxysilanes in ppm (D_2O , 25°C).

name	$\delta^{29}\text{Si}$ [ppm]	$\delta^1\text{H}$ [ppm]				
		αCH_2	βCH_2	γCH_2	$\text{CH}_3\text{O}-$	R
AMMO	-41.7	0.79	1.65	2.79	3.72	
DAMO-T	-41.8	0.74	1.65	2.80	3.65	a)2.68 b)2.68
A-link 15	-42.1	0.58 and 1.02	1.95	2.60	3.72	a)2.77 b)1.23 c)1.15
1189	-42.0	0.81	1.60	2.75	3.72	a)2.75 b)1.60 c)1.72 d)1.12
PTMS	-42.5	0.94	1.80	1.33	3.90	

Unfortunately, solid state NMR measurements were not successful as no silicon signal could be detected of samples prepared with 3wt% of alkoxy silanes. As a consequence, the reaction progress was observed by ^1H and ^{29}Si liquid NMR measurements. Pretests in CD_3OD as solvent as performed by Salon et al.^{24,25} led to very poor ^{29}Si signals and consequently difficult interpretation. Furthermore, traces of CH_3OH in the deuterated solvent caused misinterpretations. Ongoing tests without solvent were successful.

In regular intervals ^1H and ^{29}Si spectra were recorded. Hydrolysis was followed by monitoring the liberation of CH_3OD and by the disappearance of the methoxy signal $\text{CH}_3\text{O}-$ in the ^1H spectra. In the case of AMMO, DAMO-T, Alink-15 and 1189 the methoxy group $\text{CH}_3\text{O}-$ leads to a signal at ~ 3.7 ppm whereas the released deuterated methanol CH_3OD causes a singlet at 3.4 ppm. This can be seen in figure 3.16 in which a ^1H array of the hydrolysis of AMMO with 1 equivalent of D_2O is displayed.

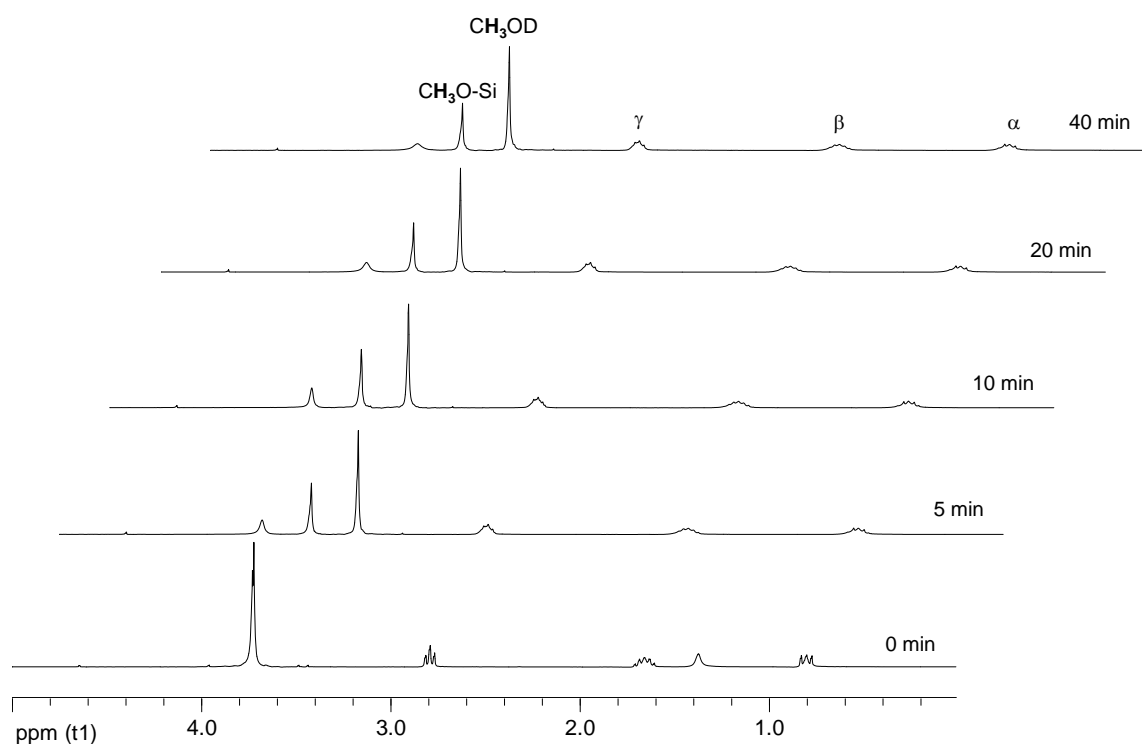


Figure 3.16: ^1H array of hydrolysis of AMMO with 1 eq. D_2O within 40 minutes.

The condensation degree cd was calculated by analysis of the ^{29}Si spectra with the help of equation 3.1. T^n (n =number of siloxane bonds attached to silicon) describes the degree of

silicon cross-linking. Possible T^n structures are shown in figure 3.17.

$$cd = \frac{\frac{1}{3} \cdot \int(T^1) + \frac{2}{3} \cdot \int(T^2) + \frac{3}{3} \cdot \int(T^3)}{\sum \int(T^0, T^1, T^2, T^3)} \quad (3.1)$$

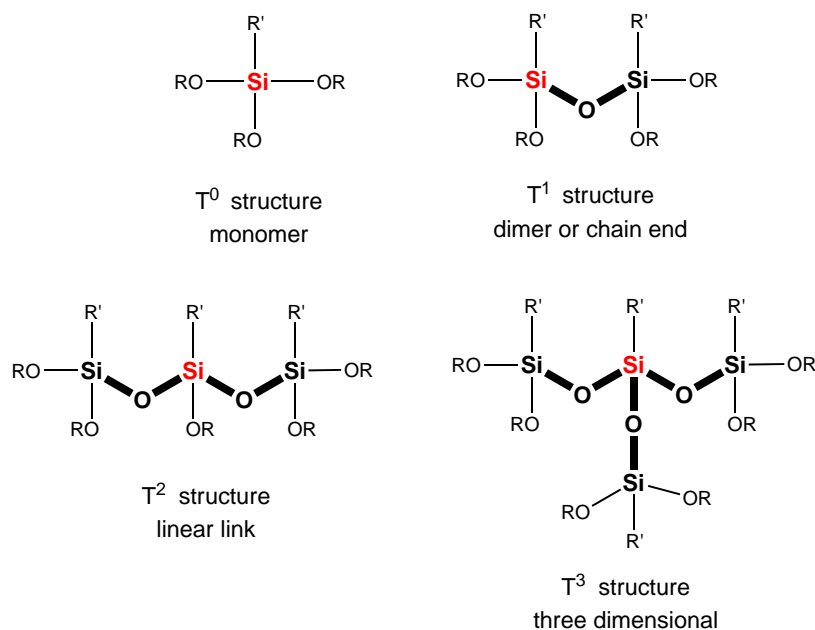


Figure 3.17: Schematic overview of T^n structures.⁷⁴

For the γ -silanes AMMO, DAMO-T, A-link 15, 1189 and PTMS the educt of the type T^0 gives a single peak at ~ -42 ppm in the ^{29}Si NMR spectra. The first condensation product T^1 leads to peaks in the area of -50 ppm. Condensation products of the type T^2 appear at about -59 ppm. T^3 structures with stronger high-field shifts were not detected. The silanol species Si-OH always appear in the same area as the methoxy substituted silanes Si-OR but slightly low-field shifted because of the electron-donating properties of OR .^{22,24} A ^{29}Si array of the hydrolysis of AMMO with 1 eq. D_2O is demonstrated in figure 3.18. α -silane N-cyclohexylaminomethyltriethoxysilane gives a peak at -50 ppm measuring the silicon nucleus. All condensation products are consequently high-field shifted with respect to the γ -silanes.

Partial Hydrolysis

1 eq. adhesion promoter (2000 mg of AMMO, DAMO-T, A-link 15, 1189, PTMS or N-cyclohexylaminomethyltriethoxysilane) was hydrolyzed with 1 eq. D_2O without solvent in a vial. The aim was to have a closer look at the initial hydrolysis and condensation. D_2O was added to the adhesion promoters, then the solution was mixed and transferred directly into

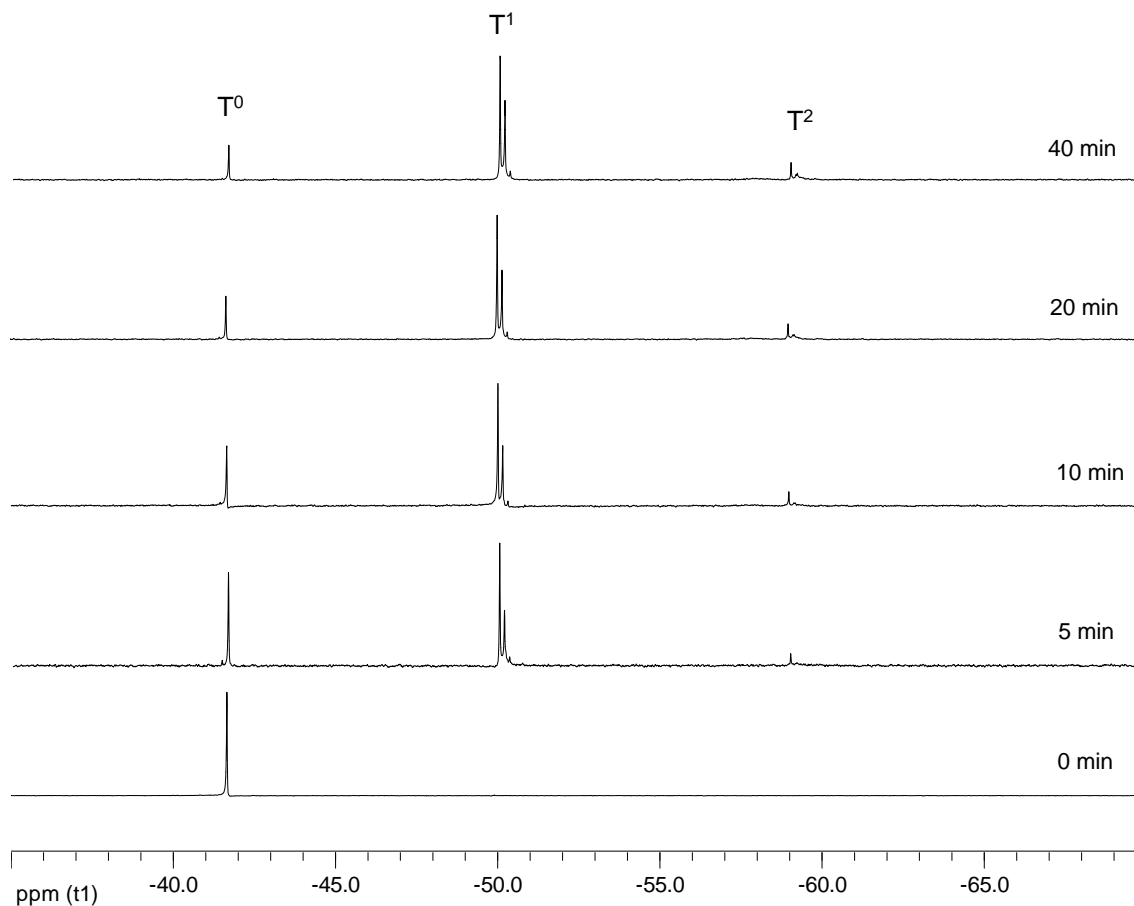


Figure 3.18: ^{29}Si array of hydrolysis of AMMO with 1 eq. D_2O within 40 minutes.

an NMR tube containing a D_2O capillary. All reactions done with N-bearing alkoxy silanes were strongly exothermic. Hydrolysis of PTMS did not lead to heating of the reaction mixture.

In contrast to the behavior of most other organofunctional silanes, the hydrolysis and condensation of silanes bearing primary amino functions are autocatalysed and consequently very fast. This is also caused by strong polarization of the molecule (electrostatic interaction between Si and NH_2). Furthermore, the NH_2 groups initiate strong interactions with water. That is why hydrolysis and condensation products have good water solubility.²¹ For all aminoalkoxy silanes investigated in these experiments the partial hydrolysis is very fast. In all experiments, rapid build-up of oligomers (T^1 and T^2) is detectable.

The α -silane N-cyclohexylaminomethyltriethoxysilane shows the fastest hydrolysis rate followed by the hydrolysis of AMMO. In the case of AMMO, within 5 minutes 65% of CH_3OD is

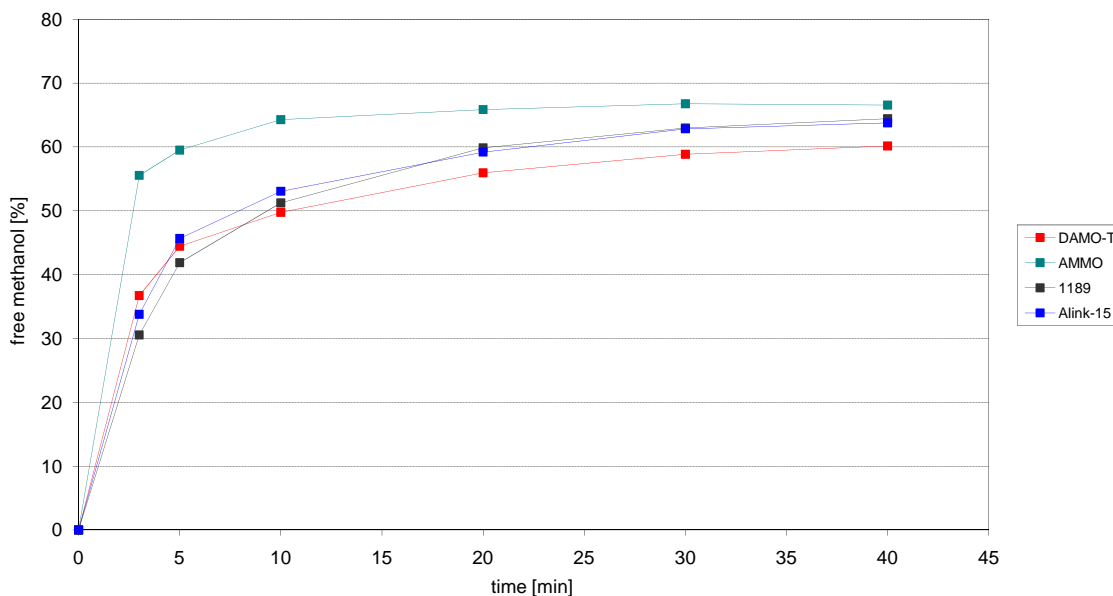


Figure 3.19: Partial hydrolysis of 1 eq. adhesion promoter with 1 eq. D_2O : Methanol CH_3OD liberation versus time.

formed. In the same time the condensation degree increases to 0.25, showing T^1 -structures as main product. After a period of 5 minutes also T^2 -structures can be detected. After 30 minutes the partial hydrolysis finishes. The hydrolysis and condensation behavior of all samples are summarized in figure 3.19 and 3.20.

DAMO-T, 1189 and A-link 15 hydrolyze slightly slower. After 5 minutes between 41 and 45% of free methanol can be detected and the condensation degree is between 0.15 and 0.20. After a reaction period of 5 minutes, a lot of educt of the type T^0 can still be seen along with T^1 - and T^2 -structures in the ^{29}Si NMR spectra. In contrast to the aminoalkoxysilanes, PTMS does not hydrolyze within a period of 40 minutes. No methanol can be detected in the 1H NMR spectra and no oligomeric siloxane structures can be seen in the ^{29}Si NMR spectra.

These results go hand in hand with literature. According to Wacker Chemie AG,⁴³ α -silanes like N-cyclohexylaminomethyltriethoxysilane show very fast hydrolysis rates due to the so called ' α -effect'. They explain that an electronegative donor such as nitrogen or oxygen in the α position relative to the silicon atom activates the alkoxy groups on the silicon atom. This effect is extremely strong if silicon and nitrogen are separated only by a methylene bridge. Due to back-bonding of the free electron pair to silicon the Si-O bond is weakened and hydrolysis is very fast. By increasing the basicity of the nitrogen, this back-bonding

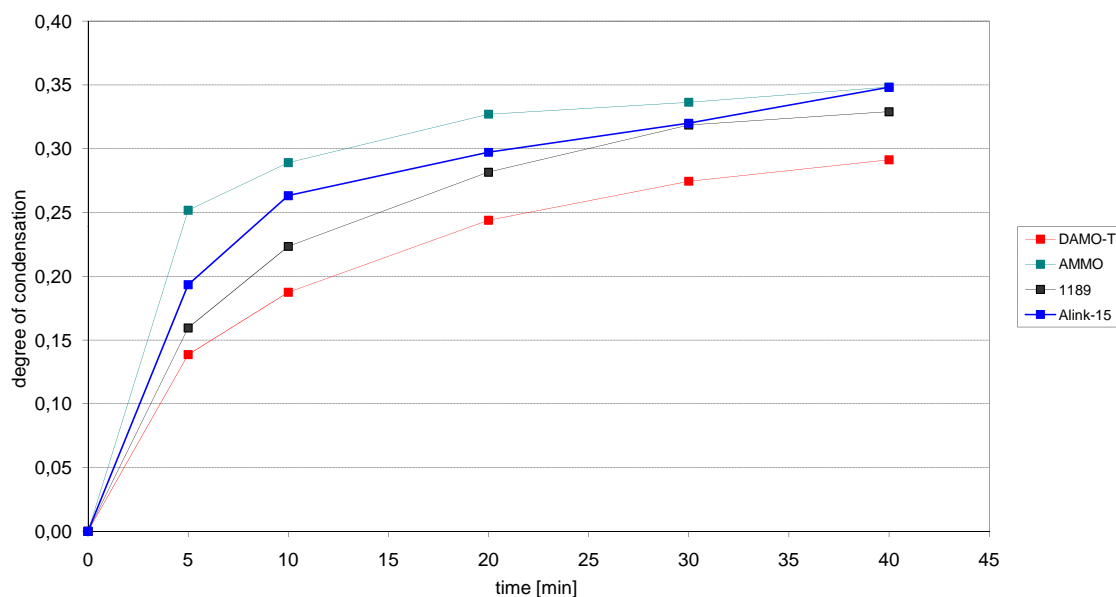


Figure 3.20: Partial hydrolysis of 1 eq. adhesion promoter with 1 eq. D_2O : Increase of the condensation degree versus time.

increases. Furthermore, the reactivity differences between ethoxy- and methoxy-substituted silanes is reduced when α -silanes are applied. This back-bonding effect also explains the high reactivity of AMMO with respect to the other γ -silanes. By increasing the separation between silicon and nitrogen, the back-bonding of the nitrogen's free electron pair decreases. As the primary amine group has higher basicity than the secondary amines of DAMO-T, 1189 and A-link 15, the hydrolysis of AMMO is faster. The primary amine of DAMO-T is situated too far away in order to have a positive effect on the hydrolysis rate.

In summary, the hydrolysis rate decreases from α -silane N-cyclohexylaminomethyl-triethoxysilane to the γ -silanes AMMO, 1189, and A-link 15, and is very slow for alkylsilanes like PTMS. Direct correlations between hydrolysis of the adhesion promoters and tack and adhesion characteristics will be shown in section 3.2 and 3.3.

3.1.4 Summary

Surfaces analyses of the formulated polymers with adhesion promoter concentrations higher than 3 wt% show siloxane structures at the top side of the cured polymer, whereas this effect is not seen at the adhesion side. With SEM-EDX cross section images this phenomenon can be clearly observed. At the 'air side' of sample 2c'_10AMEO_A1, for instance, the percentage of silicon decreases relative to that of carbon and oxygen going towards the inner part. The

silicon concentration at position (1) halves in value at position (6), 100 μm deeper inside the sample, as shown in figure 3.21. This ratio of silicon to carbon and oxygen remains constant within the sample (compare spectrum (3) in figure 3.21).

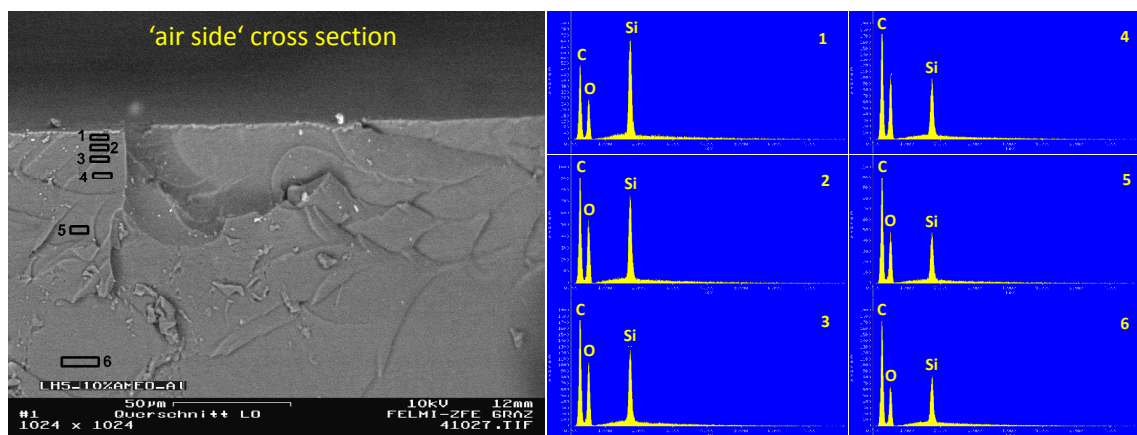


Figure 3.21: Decrease of the silicon content at the ‘air side’ of sample 2c_10AMEO_A1 (BSE cross section image).

The cross section picture of the ‘adhesion side’ shows that silicon is not accumulated at this side. Rather, a contrary effect can be detected, comparing EDX-spectra (1), (2) and (3) in figure 3.22.

This accumulation of silicone at the ‘air side’ can also be proved with other surface analyses like IR-ATR, AFM and XPS. IR-ATR especially, can be employed as a cheap and powerful tool to detect siloxane structures at the ‘air side’ of the cured prepolymers.

Depending on the alkoxy silane used, the accumulation of silicon at the air side may be stronger or weaker. Adhesion promoters with two amine groups like DAMO-T and DAMO-D initiate the strongest silicone network formation at the surface. In the case of monofunctional amines like AMMO, 1189 or A-link-15, the silicone accumulation at the surface is smaller. Alkoxy silanes with stronger polar alkyl chains like DAMO-D or DAMO-T move to the hydrophilic ‘air side’ surface. This effect can also be seen by applying additional pure amines to the alkoxy silanes (see section 3.3.5). Hydrolysis behavior of the adhesion promoters shows that the hydrolysis rate does not correlate with the probability of the agents to accumulate at the surface. Hydrolysis decreases from α -silane N-cyclohexylaminomethyltriethoxysilane to the γ -silanes AMMO, 1189, A-link 15 and is very slow for alkylsilanes like PTMS, a phenomenon which can be explained by back-bonding effects.

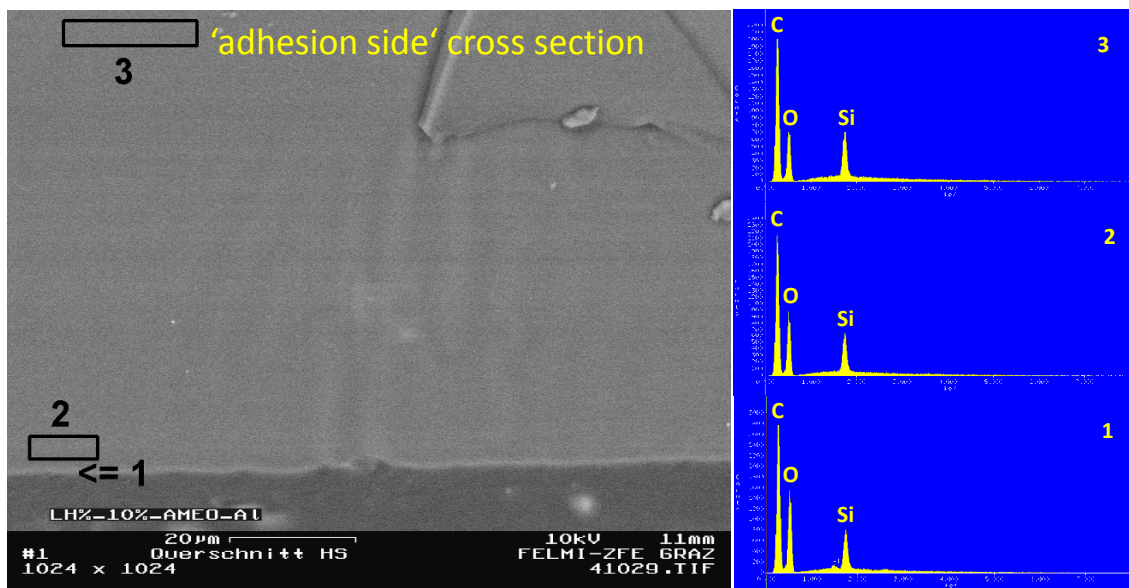


Figure 3.22: Silicon allocation at the 'adhesion side' of sample 2c_10AMEO_Al (BSE cross section image)

3.2 Tack Tests

Tack behavior of different STPU employed as sealants can be a major problem for industrial applications. Investigations show that this effect is linked with the amount and type of adhesion promoter used. Longterm analyses have shown that tack characteristics of polymers can decrease after a period of time whereas others stay sticky even over long periods. Sticky sealants reduce possible application areas. For instance, tacky sealants applied to an externally visible surface, like in bathrooms, attract impurities.

The tack tests done of the polymer surfaces were done either manually or mechanically. Precise proceedings are demonstrated in the ‘Experimental’ section, 4.2.5. The manual tack test was performed by touching the surface of the cured polymers. The stickiness was evaluated by comparing the samples on a scale from 1-3 (1=no stickiness, 2=some stickiness, 3=strong stickiness).

3.2.1 Sample Composition

To investigate tack behavior, various resins with different compositions were prepared. The exact synthesis and proceedings are described in section 4.2. Special sample composition for tack tests are summarized in this section. All analyses of one test series were done under the same conditions after the same curing times if not otherwise stated. In this section the substrate term is eliminated in the preparation tables due to space problems. All samples were cured in aluminum boats. For instance, sample 2a_3AMMO is equivalent to 2a_3AMMO_Al. Increasing amount of AMMO as adhesion promoter was investigated with respect to surface stickiness. Concentrations from 0 to 15 wt% of AMMO were chosen (see table 3.8) and the samples were analyzed.

Table 3.8: Sample preparation for tack tests, increasing amount of AMMO (test series 1).

ITPU	end-capper	adhesion agent	name
IPDI-Acclaim_1.5 (1a)	AMMO (2a)	-	2a
IPDI-Acclaim_1.5 (1a)	AMMO (2a)	3 wt% AMMO	2a_3AMMO
IPDI-Acclaim_1.5 (1a)	AMMO (2a)	5 wt% AMMO	2a_5AMMO
IPDI-Acclaim_1.5 (1a)	AMMO (2a)	7 wt% AMMO	2a_7AMMO
IPDI-Acclaim_1.5 (1a)	AMMO (2a)	10 wt% AMMO	2a_10AMMO
IPDI-Acclaim_1.5(1a)	AMMO (2a)	15 wt% AMMO	2a_15AMMO

Influence of different adhesion promoters and catalysts on the tack behavior was also tested.

Sample preparation is displayed in tables 3.10, 3.9 and 3.11. Test series 3 contains one sample cured under moisture-poor conditions: Sample 2a_3DAMOT_dc was cured in a drying cabinet at 50°C. In test series 4, 1 wt% of VTMO was added directly to the STPU after synthesis to increase storage stability. The formulation with different adhesion agents and catalysts was done as usual. As catalysts dibutyltin dilaurate (DBTL), titanium dibutoxide(bis-2,4-pentanedionate) (TBP), bismuth neodecanoate (BND) and 1,8-diazabicycloundec-7-ene (DBU) were chosen.

Table 3.9: Sample preparation for tack tests, different alkoxy silanes, n(Si)=4.99 mmol (test series 2).

ITPU	end-capper	adhesion agent	name
IPDI-Acclaim_1.5 (1a)	AMMO (2a)	3.00 wt% AMMO	2a_3AMMO
IPDI-Acclaim_1.5 (1a)	AMMO (2a)	4.26 wt% 1189	2a_4.261189
IPDI-Acclaim_1.5 (1a)	AMMO (2a)	3.74 wt% A-link 15	2a_3.74Alink15
IPDI-Acclaim_1.5(1a)	AMMO (2a)	3.76 wt% DAMO-T	2a_3.76DAMOT
IPDI-Acclaim_1.5(1a)	AMMO (2a)	3.50 wt% DAMO-D	2a_3.50DAMOD

Table 3.10: Sample preparation for tack tests, different alkoxy silanes (test series 3).

ITPU	end-capper	adhesion agent	name
IPDI-Acclaim_1.5 (1a)	AMMO (2a)	-	2a
IPDI-Acclaim_1.5 (1a)	AMMO (2a)	3 wt% AMMO	2a_3AMMO
IPDI-Acclaim_1.5 (1a)	AMMO (2a)	3 wt% DAMO-T	2a_3DAMOT
IPDI-Acclaim_1.5 (1a)	AMMO (2a)	3 wt% DAMO-T	2a_3DAMOT_dc

Table 3.11: Sample preparation for tack tests, 1 wt% of AMMO with different catalysts and VTMO as water scavenger (test series 4).

ITPU	end-capper	adhesion agent	catalyst	name
IPDI-Acclaim_2 (1b)	AMMO (2b)	1 wt% AMMO	0.5 wt% DBTL	2b_1VTMO_0.5DBTL
IPDI-Acclaim_2 (1b)	AMMO (2b)	1 wt% AMMO	1 wt% DBTL	2b_1VTMO_1DBTL
IPDI-Acclaim_2 (1b)	AMMO (2b)	1 wt% AMMO	0.5 wt% TBP	2b_1VTMO_0.5TBP
IPDI-Acclaim_2 (1b)	AMMO (2b)	1 wt% AMMO	0.5 wt% BND	2b_1VTMO_0.5BND
IPDI-Acclaim_2 (1b)	AMMO (2b)	1 wt% AMMO	0.5 wt% DBU	2b_1VTMO_0.5DBU

3.2.2 Increasing Amount of Alkoxysilane

The amount of alkoxysilane added to the silyl-terminated polyurethane has significant influence on the tack behavior of the ‘air side’ surface. In all investigations sample 2a without adhesion promoter has very strong tack behavior. Increasing the weight percent of adhesion promoters like AMMO decreases the stickiness of the surface. At the same time the polymer characteristics change. Sample 2a has a transparent, smooth appearance. Increasing amount of alkoxysilane in the cured polymer leads to turbid, white and waved surfaces.

Table 3.12 displays the tack decrease with respect to increasing amounts of AMMO. Sample 2a shows the strongest tack behavior. At 7 wt% (see sample 2a_7AMMO) stickiness tends toward zero and simultaneously the sample appearance changes to turbid. The stickiness was evaluated after a curing period of 10 days. The tack behavior changes rapidly within the the first curing week but then stays constant. Samples that have a sticky surface after one week of curing also show this property after several monts.

Table 3.12: Manual tack test results, increasing amount of AMMO (test series 1).

name	adhesion agent	manual tack test ¹
2a	-	3
2a_3AMMO	3 wt% AMMO	2
2a_5AMMO	5 wt% AMMO	2
2a_7AMMO	7 wt% AMMO	1
2a_10AMMO	10 wt% AMMO	1
2a_15AMMO	15 wt% AMMO	1

Surface analyses of the samples (see section 3.2.5) have proved that siloxane layers are formed at the ‘air side’ of the cured polymer. Depending on the formulation different silicon concentrations could be detected. There is a direct correlation between turbid cured polymers, strong silicon accumulation and low stickiness. This leads to the conclusion that unreacted silanol groups on the surface of the resin may be the reason for the stickiness (see figure 3.23). Due to the polymer network the alkoxysilane end-cappers are too isolated from each other to cause condensation of silanol groups. Consequently, many unreacted silanol groups as result of the alkoxysilane hydrolysis can be found.

¹1=no stickiness, 2=some stickiness, 3=strong stickiness

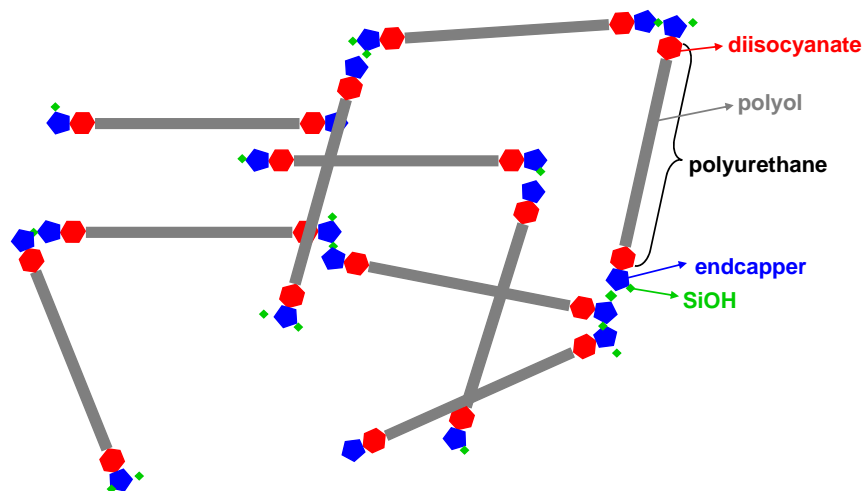


Figure 3.23: Schematic description of sample 2a having a high number of free silanol groups.

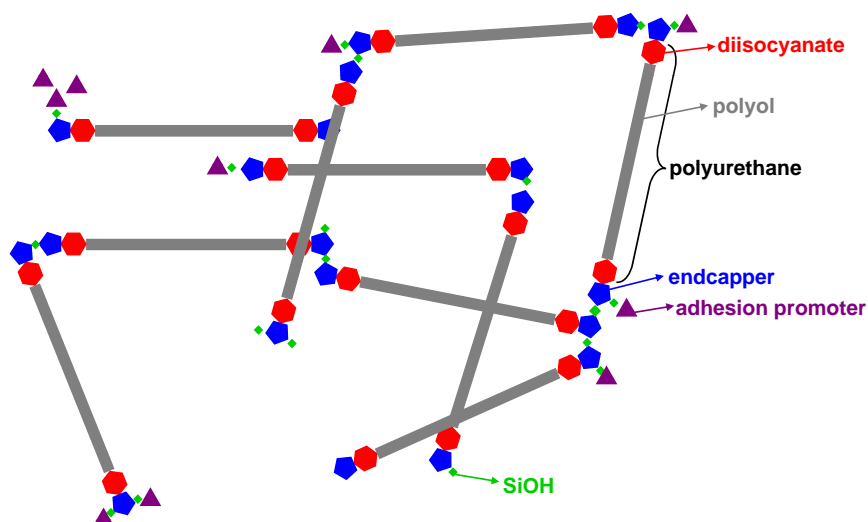


Figure 3.24: Schematic description of samples formulated with high amounts of adhesion promoter.

By adding an adhesion promoter, siloxane formation is more highly encouraged (see figure 3.24). The adhesion promoter is multi-directionally movable and high amounts lead to the formation of a silicone network at the surface. Consequently, few or no free silanol groups should be available any more. Furthermore, the stickiness of all samples decreases as a function of time within the first curing week which could also be a hint that free silanol groups have reacted in the meantime. According to the literature search in section 2.3, contact angle analyses of the surface could give information about the silanol concentration

of polymer surfaces. Unfortunately, no direct correlations between hydrophilic behavior and silanol concentration could be drawn. Undesired bubbles in the polymer matrix due to stirring during the formulation process affected the analyses. During the wetting with water it could be observed that the drop somewhat drawn into the sample, which makes an interpretation of results unreasonable. Solid state NMR analyses of the samples also gave no results. Nevertheless, a siloxane network favors unsticky but turbid samples. These results are substantiated by AFM, SEM, IR-ATR and XPS analyses.

3.2.3 Influence of Different Alkoxysilanes

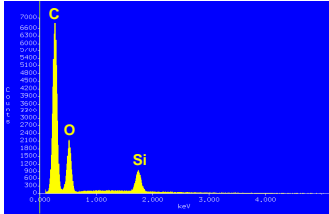
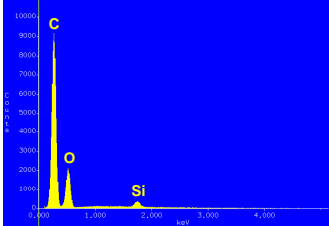
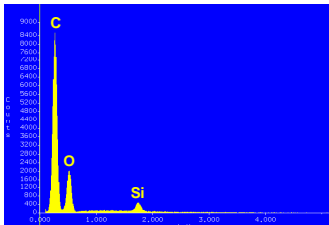
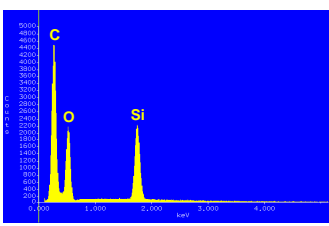
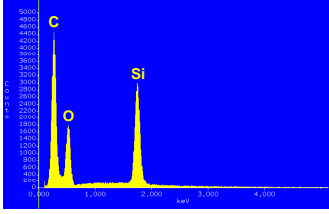
Application of different adhesion promoters has a strong impact on the sample characteristic and especially on the tack behavior. The influence of adhesion agents like AMMO, DAMO-T, A-link 15, 1189 etc. was investigated. Correlations between the surface analyses in section 3.1 and sample appearance were drawn.

In all test series the stickiness of sample 2a bearing no adhesion promoter was also considered. In this sample the strongest stickiness was detected. By adding 3 wt% of adhesion promoters the stickiness decreased. To compare the tack behavior of the samples directly, several samples were prepared with the same molar amount of silicon (4.99 mmolar) as summarized in table 3.9. The results of the manual tack tests are shown in table 3.13.

The tack behavior of all samples of test series 2 in table 3.9 can be described on the stickiness scale between 1 and 2. Sample 2a_3.76DAMOT and 2a_3.50DAMOD have turbid plane surfaces. 2a_3.76DAMOT appears as an unsticky surface, whereas on sample 2a_3.50DAMOD tacky and rough areas can be seen. All the other samples show stronger tack behavior than sample 2a_3.76DAMOT formulated with 3.76 wt% of DAMO-T. This effect can also be seen by comparing sample 2a_3DAMOT and 2a_3DAMOT_dc of test series 3 in table 3.10. The two samples have the same composition with the difference that sample 2a_3DAMOT was cured at standard conditions in the laboratory whereas sample 2a_3DAMOT_dc was stored in a moisture-poor atmosphere in a drying cabinet at 50°C. The tack behavior of sample 2a_3DAMOT was evaluated as a 1 on the stickiness scale after a curing period of 1 week. Contrary to this result, the stickiness of sample 2a_3DAMOT_dc was very strong and described as a 3 on the stickiness scale.

SEM and IR-ATR surface analyses of the samples were described in section 3.1.3.1 and 3.1.3.2. According to these results, in all samples, silicone accumulation at the ‘air side’ can be detected by SEM and IR-ATR, but DAMO-T and DAMO-D show strongest silicon concentration in all investigations.

Table 3.13: Manual tack test in correlation with silicon accumulation detected by SEM-EDX (test series 2).

name	adhesion agent	tack test ¹	EDX spectra
2a_3AMMO	3 wt% AMMO	2	
2a_4.261189	4.26 wt% 1189	1.5	
2a_3.74Alink15	3.74 wt% A-link 15	1.5	
2a_3.76DAMOT	3.76 wt% DAMO-T	1	
2a_3.50DAMOD	3.50 wt% DAMO-D	2 ²	

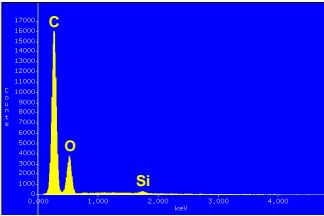
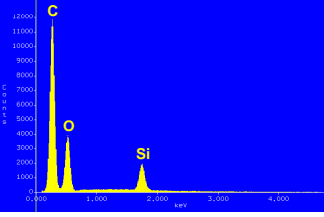
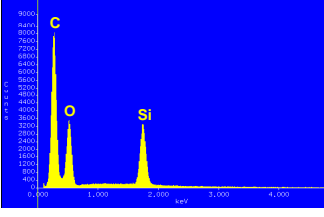
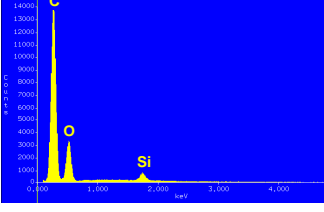
EDX-SEM spectra of the two chemically identical samples 2a_3DAMOT and 2a_3DAMOT_dc show impressively the stronger silicone accumulation in sample 2a_3DAMOT. The results of the EDX spectra are summarized in table 3.13 and 3.14. Obviously, the amine groups of

¹manual tack test: 1=no stickiness, 2=some stickiness, 3=strong stickiness

²Sample contains sticky and unsticky areas.

the adhesion agents do have an influence on the silicone accumulation. Alkoxysilanes with a stronger polar alkyl chain like DAMO-D or DAMO-T move to the strong hydrophilic ‘air side’ surface and tend to be less sticky. Hydrolysis rates do not have an influence on the accumulation, as AMMO hydrolyzes faster than DAMO-T and especially DAMO-D but shows less silicon accumulation. This was shown in section 3.1.3.5.

Table 3.14: Manual tack test in correlation with silicon accumulation detected by SEM-EDX (test series 3).

name	adhesion agent	tack test ¹	EDX spectra
2a	-	3	
2a_3AMMO	3 wt% AMMO	2	
2a_3DAMOT	3 wt% DAMO-T	1	
2a_3DAMOT_dc	3 wt% DAMO-T	3	

3.2.4 Influence of Catalysts

For the curing process several catalysts are applied in industry. The influence of curing catalysts like dibutyltin dilaurate (DBTL), titanium dibutoxide(bis-2,4-pentanedionate) (TBP),

¹manual tack test: 1=no stickiness, 2=some stickiness, 3=strong stickiness

bismuth neodecanoate (BND) and 1,8-diazabicycloundec-7-ene (DBU) on the tack behavior was investigated. The tack tests were performed mechanically and manually and are summarized in table 3.15

Table 3.15: Manual and mechanical tack test results, different curing catalysts (test series 4).

name	adhesion agent	curing catalyst	manual tack test ¹	mechanical tack test ³
2a	1 wt% AMMO	0.5 wt% DBTL	2.5	0.52
2a_3AMMO	1 wt% AMMO	0.1 wt% DBTL	2.5	0.56
2a_5AMMO	1 wt% AMMO	0.5 wt% TBP	2.5	0.52
2a_7AMMO	1 wt% AMMO	0.5 wt% BND	2.5	0.53
2a_10AMMO	1 wt% AMMO	0.5 wt% DBU	1.5	0.38

The addition of catalysts does not have a positive effect on the tack behavior of the cured polymers. Faster hydrolysis and condensation of the alkoxysilane groups due to catalysis does not reduce stickiness of the polymers as polymers without catalysts show stickiness of 3 on the tack scale. The amount of added catalyst also did not have a detectable impact on the stickiness behavior and differences with respect to hydrolysis or condensation behavior were not monitored. By using amine catalysts like DBU a slightly positive trend was observed; however, it was clear that fast hydrolysis and surface stickiness are not in connection with each other.

3.2.5 Summary

Investigations of tack behavior of cured silyl-terminated polyurethanes show that this effect is linked with the amount and type of adhesion promoter used.

In all investigations pure silyl-terminated polyurethanes applied without adhesion promoter show very strong tack behavior. By increasing the weight percent of adhesion promoters like AMMO the stickiness of the surface decreases. A siloxane network is formed which favors unsticky but turbid samples. These results are substantiated by AFM, SEM, IR-ATR and XPS analyses.

According to these analyses, DAMO-T and DAMO-D show strongest silicone accumulation at the ‘air side’ in all investigations. Alkoxysilanes with a stronger polar alkyl chain like DAMO-D or DAMO-T move to the strong hydrophilic ‘air side’ surface and tend to make

¹manual tack test: 1=no stickiness, 2=some stickiness, 3=strong stickiness

³mechanical tack test: F_{max} in F/mm^2

the surface less sticky. Hydrolysis rates do not correlate with the accumulation as AMMO hydrolyzes faster than DAMO-T and especially DAMO-D. The addition of catalysts does not have a positive effect on the tack behavior of the cured prepolymers, as faster hydrolysis and condensation of the alkoxy silane groups to siloxanes does not reduce stickiness of the polymers.

3.3 Adhesion Tests

Describing the mechanism of adhesion in simple terms is difficult and the ultimate goal of finding one single mechanism to understand adhesion phenomena is not accomplished yet as summarized in section 2.2. The question of whether chemical or physical interactions are responsible for good adhesion abilities on several surfaces or even a combination of various effects is still open for discussion.

So far, it is known that adhesion of silyl-terminated polyurethanes to different substrates is influenced by the addition of adhesion promoters. The aim of this thesis is the development of a sealant based on a STPU system which can be applied without primers on various materials.

In order to investigate the adhesion process, prepolymers mixed with various adhesion promoters were deposited on different substrates like polyethylene, aluminum, copper, etched copper, steel and silver. The pull-off procedure was performed either mechanically with an adhesive tensile strength engine or manually. The exact proceeding is described in section 4.2.4. Additionally, several agents and combinations of them were tested in order to increase adhesion of the samples. Furthermore, the substrates were analyzed by SEM in order to detect polymer residues or hints of the formation of Al-O-Si bonds. Samples of each test series were analyzed after the same curing times and at the same conditions.

3.3.1 Sample Composition

The preparation of the samples for several adhesion tests are described in this subsection. To analyze the substrates, aluminum and polyethylene disks were coated with thin layers of AMMO and (N,N-dimethyl-3-aminopropyl)trimethoxysilane. These two silanes were selected to investigate different adhesion abilities of primary and tertiary amines to aluminum and polyethylene. The samples were stored 12 hours in acetone and the polymeric layer was removed with cellulose before SEM investigations. The disks are displayed in figure 3.25, and the labeling of the samples is listed in table 3.16. Before SEM analysis, samples Al1, PE1 and PE2 were deposited with carbon, whereas sample Al2 was measured without carbon deposition. In this case, the samples did not show any charging problems and the missing carbon layer did not have an effect on the measurements.

To have a closer look at the influence of the roughness of the substrates on the adhesion abilities of the polymers, various mixtures were prepared according to table 3.17. 3 wt% of the adhesion promoters were added and poured into forms made of acrylic glas fixed on aluminum, copper, steel and polyethylene boards. These materials were chosen due to their

Table 3.16: Sample preparation for SEM measurements, surface coating of aluminum and polyethylene.

silane	name (Al disks)	name (PE disks)
(N,N-dimethyl-3-aminopropyl)trimethoxysilane	A11	PE1
AMMO	A12	PE2

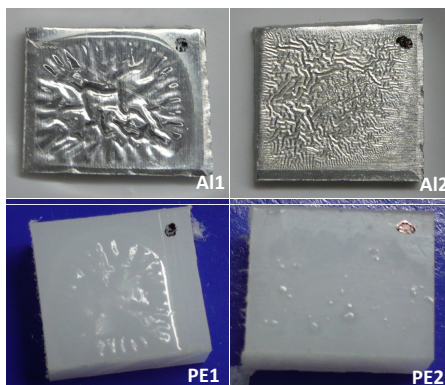


Figure 3.25: Surface coating of aluminum and polyethylene with (N,N-dimethyl-3-aminopropyl)trimethoxysilane and AMMO.

different reactivities towards silicon-bearing sealants. So far, Al-O-Si bonds are described in literature (see section 2.2.1.4). In the case of copper and steel surfaces reactions between the metal surface and the polymer should be more improbable and can be ruled out with respect to polyethylene. Additionally, adhesion promoter free samples were investigated.

Table 3.17: Sample preparation for roughness test, different alkoxy silanes on various curing substrates (test series 1).

ITPU	end-capper	adhesion agent	substrate ⁴
IPDI-Acclaim_1.5 (1a)	AMMO (2a)	-	Al/Cu/steel/PE
IPDI-Acclaim_1.5 (1a)	AMMO (2a)	3 wt% AMMO	Al/Cu/steel/PE
IPDI-Acclaim_1.5 (1a)	AMMO (2a)	3 wt% DAMO-T	Al/Cu/steel/PE
IPDI-Acclaim_1.5 (1a)	AMMO (2a)	3 wt% A-link 15	Al/Cu/steel/PE

The substrates were cleaned with acetone and methanol in advance. Commercially available steel, copper, aluminum and polyethylene plates were selected and the surface roughness was changed by treating the different boards with a small sized abrasive paper (particle size of

⁴rough and plane surface

K15). The result was documented with a light microscope 1000-times magnified, shown in figure 3.26. All samples were investigated after curing on plane and rough substrate surfaces.

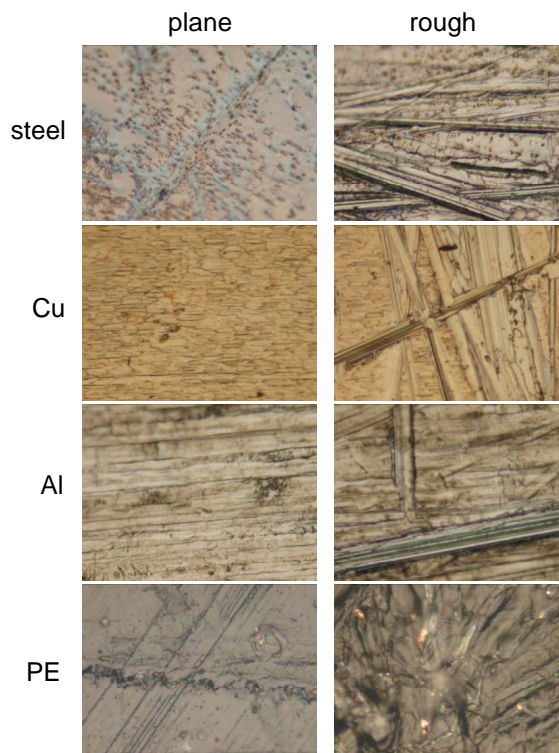


Figure 3.26: Curing boards of steel, aluminum, copper and polyethylene with plane and rough surface.

As the type of adhesion promoter applied does have a major impact on the adhesion abilities of a sealant, several different types of agents were analyzed, summarized in table 3.18. Adhesion promoters containing amine groups like AMMO, DAMO-D and DAMO-T were chosen to verify the assumption that amine-containing promoters lead to very good adhesion. In contrast amine free alkoxy silanes like GLYMO and PTMS were investigated. A mixture of (n-cyclohexylaminomethyl)methyltriethoxysilane (' α -silane'), DAMO-T and DAMO-D (abbreviation 'mixture' in figure 3.29) was also used to investigate the influence of strong-amine containing adhesion promoter formulations. The polymers were cured on aluminum and copper boards; additionally, etched copper disks were used. To eliminate the copper oxide surface the copper disks were etched with diluted sulphuric acid. As a consequence, a chemical Cu-O-Si bond should be improbable.

The third test series investigated the influence of amines on the adhesion abilities of the cured prepolymer. Alkoxy silane-amine mixtures were prepared to detect the role of the amine part

in curing procedures. All mixtures were referred to the pure alkoxy-silanes applied as adhesion promoters.

Table 3.18: Sample preparation to detect the influence of different alkoxy-silanes on the adhesion abilities (test series 2).

ITPU	end-capper	adhesion agent	substrate
IPDI-Acclaim_1.5 (1a)	AMMO (2a)	-	Al/Cu/Cu _{etched}
IPDI-Acclaim_1.5 (1a)	AMMO (2a)	3 wt% AMMO	Al/Cu
IPDI-Acclaim_1.5 (1a)	AMMO (2a)	3 wt% GLYMO	Al/Cu
IPDI-Acclaim_1.5 (1a)	AMMO (2a)	3 wt% DAMO-D	Al/Cu
IPDI-Acclaim_1.5 (1a)	AMMO (2a)	each 1 wt% DAMO-T DAMO-D, α -silane	Al/Cu
IPDI-Acclaim_1.5 (1a)	AMMO (2a)	3 wt% DAMO-T	Al/Cu
IPDI-Acclaim_1.5 (1a)	AMMO (2a)	10 wt% DAMO-T	Al/Cu
IPDI-Acclaim_1.5 (1a)	AMMO (2a)	15 wt% DAMO-T	Al/Cu

Table 3.19: Sample preparation to detect the influence of different alkoxy-silane-amine mixtures on the adhesion abilities (test series 3).

ITPU	end-capper	adhesion agent	substrate
IPDI-Acclaim_1.5 (1a)	AMMO (2a)	-	Al/Cu/Cu _{etched}
IPDI-Acclaim_1.5 (1a)	AMMO (2a)	3 wt% DAMO-T	Al/Cu/Cu _{etched}
IPDI-Acclaim_1.5 (1a)	AMMO (2a)	3.17 wt% GLYMO	Al/Cu/Cu _{etched}
IPDI-Acclaim_1.5 (1a)	AMMO (2a)	3.17 wt% GLYMO + 2.96 wt% 4,7,10-trioxatridecan-1,13-diamine	Al/Cu/Cu _{etched}
IPDI-Acclaim_1.5 (1a)	AMMO (2a)	3.17 wt% GLYMO + 2.57 wt% Jeffcat ZF-10	Al/Cu/Cu _{etched}
IPDI-Acclaim_1.5 (1a)	AMMO (2a)	3.17 wt% GLYMO + 1.42 wt% N-(2-hydroxyethyl)ethylenediamine	Al/Cu/Cu _{etched}
IPDI-Acclaim_1.5 (1a)	AMMO (2a)	2.82 wt% TEOS	Al/Cu/Cu _{etched}
IPDI-Acclaim_1.5 (1a)	AMMO (2a)	2.82 wt% TEOS + 2.96 wt% 4,7,10-trioxatridecan-1,13-diamine	Al/Cu/Cu _{etched}
IPDI-Acclaim_1.5 (1a)	AMMO (2a)	2.82 wt% TEOS + 2.57 wt% Jeffcat ZF-10	Al/Cu/Cu _{etched}
IPDI-Acclaim_1.5 (1a)	AMMO (2a)	2.82 wt% TEOS + 1.42 wt% N-(2-hydroxyethyl)ethylenediamine	Al/Cu/Cu _{etched}

The sample composition is summarized in table 3.19. The same silicon and amine concentrations were used to allow an exact comparison of the cured polymers prepared with different additives. As alkoxysilanes, DAMO-T, GLYMO and TEOS were employed. Amines were selected to have good miscibility with the polyurethane backbone. Hence, 2-((2-(dimethylamino)ethoxy)ethyl)(methylamino)ethanol (Jeffcat ZF-10), 4,7,10-trioxatridecan-1,13-diamine and N-(2-hydroxyethyl)ethylenediamine were mixed with TEOS and GLYMO, respectively. Besides aluminum, copper and etched copper surfaces, silver disks were also investigated as substrates for curing. Chemical interaction between silver and silicon-bearing polymer can be ruled out. Therefore, copper disks were coated in the run-up as described in section 4.3.2. Gold sputtering was not successful as the gold layer showed bad adhesion to the copper disks. During the pull-off procedure the gold layer departed from the copper substrate. All samples within one test series were analyzed after the same curing time and under the same conditions.

3.3.2 Analyses of the Substrates

The literature overview in chapter 2.2.1.4 already displayed research in the field of polymer-metal interfaces. According to literature M-O-Si bonds (M=Al) may be detected by SIMS.^{46,48,49} Due to the fact that no adhesion promoter accumulation was detected at the ‘adhesion side’ of the samples, the substrates aluminum and polyethylene were investigated by SEM.

3.3.2.1 SEM Measurements

To have a closer look at the polymer-metal interface, two different alkoxysilanes were applied to aluminum and PE disks. On the aluminum disk Al1 coated with (N,N-dimethyl-3-aminopropyl)trimethoxysilane and washed with acetone a polymer layer could be detected optically and by EDX. The ‘interaction’ between polymer and metal surface seems to be very strong and could not be destroyed by washing with acetone.

In the case of AMMO an area was analyzed in which the silicone layer was dissolved in acetone over night and could be removed with cleaning tissues. The BSE image in figure 3.27 shows silicon occurrence on the aluminum board. In section (3) and (1) a very small amount of silicon can be detected whereas the darker area (2) provides the highest silicon percentage. Besides, a small amount of carbon can be seen in this area (2).

A closer look at the PE substrates leads to the same conclusion as small amounts of silicon could be detected on the cleaned surfaces. Some silicone remained in the gaps or deepening

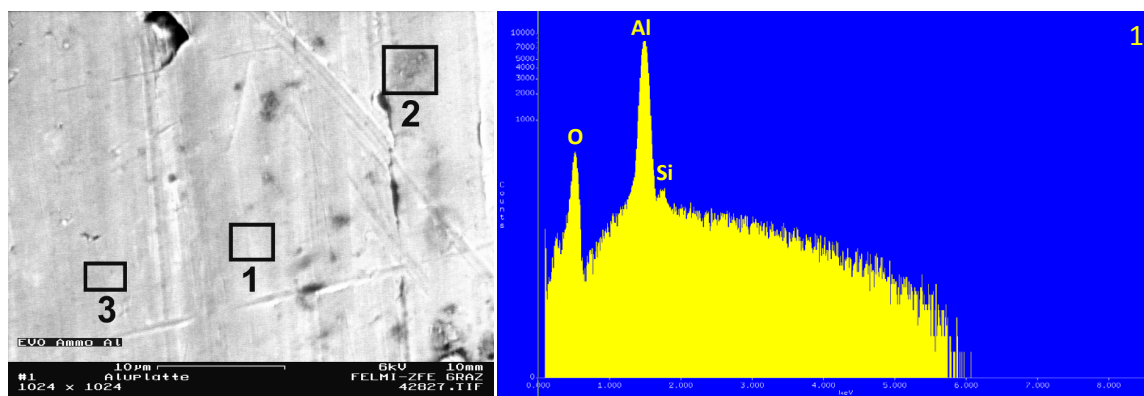


Figure 3.27: BSE image of sample Al6 and EDX spectrum of marked area (1), logarithmic scale.

of the aluminum or polyethylene surface and thus could not be washed away by acetone. Otherwise, the silicon detection by EDX would have been considerably higher, although monolayers cannot be detected with this method. Nevertheless, no proof or direct hints for the formation of Al-O-Si monolayers were found. Mechanical anchorage leading to adhesion seems to be more probable.

3.3.3 Influence of Substrate Roughness

It is known that the roughness of the adhesion surface has a direct influence on adhesion abilities. Hence, the adhesion of silyl-terminated polyurethanes on different materials (aluminum, copper, steel and PE) was investigated paying particular attention on the surface roughness of substrates. Strong mechanical interactions and consequently strong adhesion were desired.

In figure 3.28 the results of the manual pull-off test of test series 1 (see table 3.17) are displayed. The pure silyl-terminated polyurethanes with no additional adhesion promoter display weak interaction between polymer and substrate for aluminum, copper, steel and polyethylene.

By adding 3 wt% of AMMO, A-link 15 or DAMO-T the adhesion abilities of the polymers increase clearly to aluminum, copper and steel. In the case of polyethylene as curing board, no adhesion on plane or rough surfaces was observed.

Adhesion of the samples to rough surfaces is slightly stronger. This effect can mainly be seen on aluminum as substrate, and may be due to a combination of mechanical and chemical

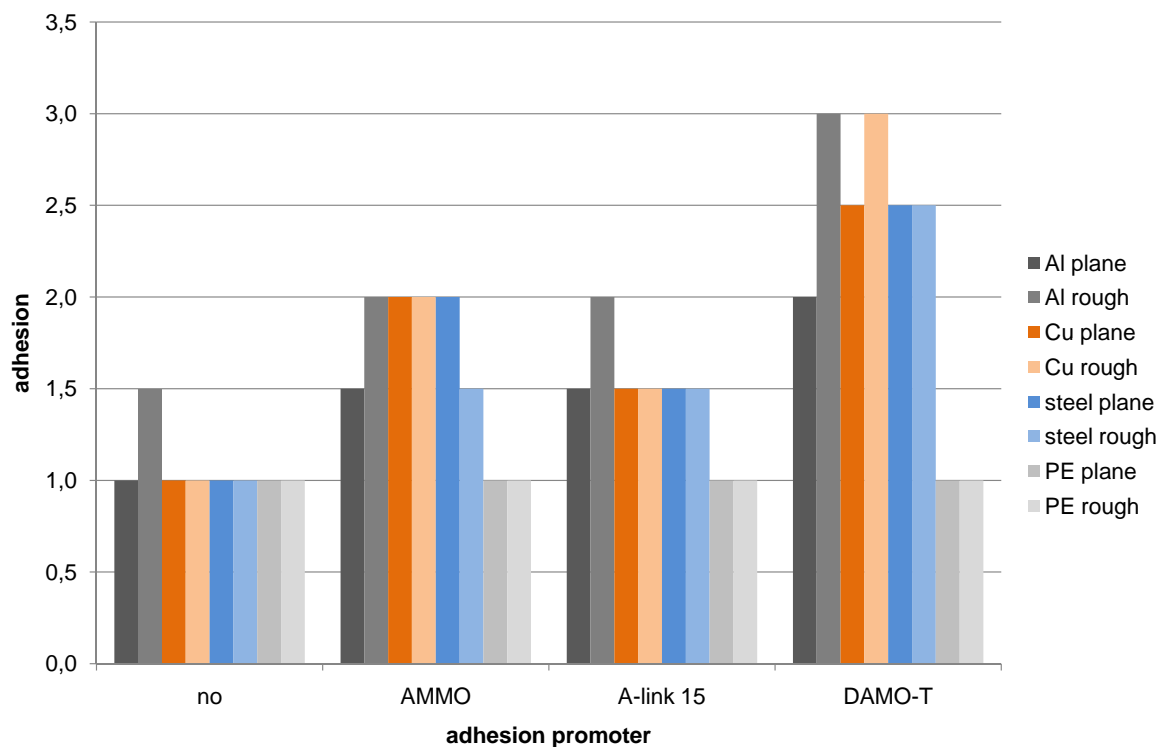


Figure 3.28: Adhesion of various cured prepolymers on plane and rough surfaces of aluminum, copper, steel and polyethylene (1=no adhesion, 2=some adhesion, 3=strong adhesion).

adhesion. The adhesion of the cured prepolymer on the plane surface seems to be rather poor whereas it increases with the degree of roughness. This outcome is not seen using copper, steel or polyethylene as curing boards. Strong adhesion differences between metals like aluminum, copper and steel were not detected. Whereas the adhesion ability of the STPU is satisfying to these three, no adhesion could be detected by using plastics like polyethylene. Hence, chemical interaction between the metal surface and the polymer seems likely. Additional roughness of the substrate may lead to stronger adhesion.

Eye-catching is the fact that DAMO-T as adhesion promoter leads to the best adhesion. This might be explained by the two amine groups and the possibility of forming an amine complex of the adhesion promoter with the metal substrate. Good adhesion abilities of primary di- and trifunctional aminoalkoxysilanes applied as adhesion promoters in silylated urethane polymer systems were also reported by Landon et al.⁷⁵ in 1996. They demonstrated excellent adhesion to aluminum, glass, polyvinyl chloride, acrylonitrile-butadiene-styrene and polystyrene.

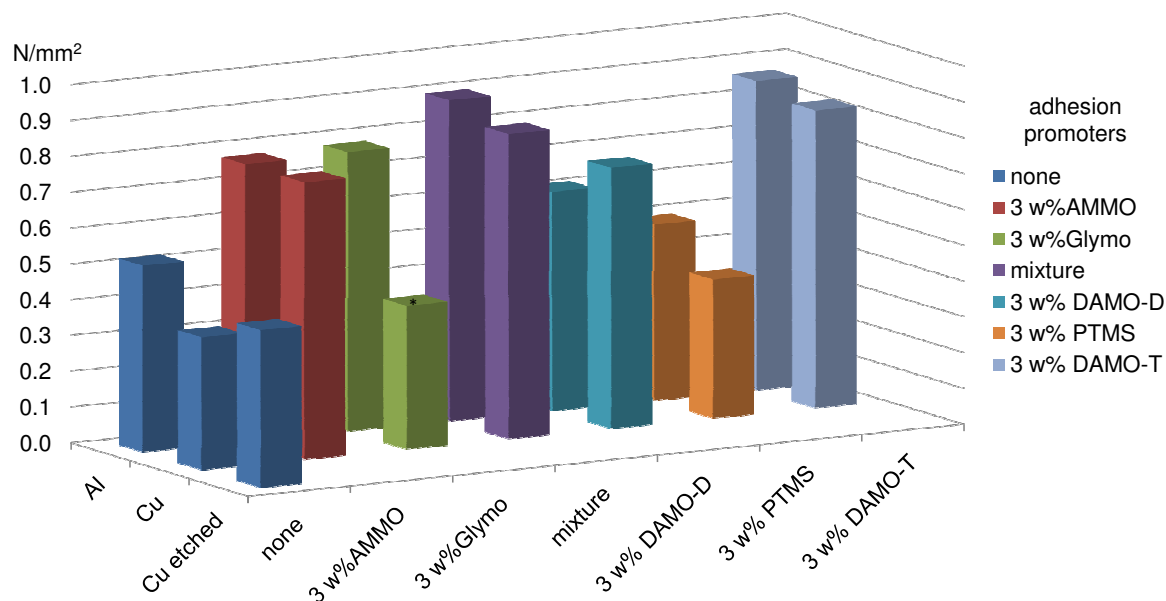


Figure 3.29: Adhesion of different cured prepolymer to aluminum, copper and etched copper.

3.3.4 Influence of Different Alkoxysilanes

Obviously, different alkoxysilanes do have a large impact on adhesion abilities. The results of the manual pull-off test with respect to different adhesion promoters were confirmed more precisely by applying a mechanical pull-off test described in detail in section 4.2.4.

Five values were determined per formulation and the outliers were eliminated. Additionally, the stripped disks were analyzed for polymer residues on the aluminum or copper disks as seen in figure 3.30. These results can give hints regarding adhesion or cohesion abilities of the samples. Furthermore, increasing amounts of adhesion promoter added to the STPU were investigated.

As figure 3.29 shows, adhesion promoters containing amine groups, like AMMO, DAMO-D and DAMO-T provide very good adhesion abilities. DAMO-T and a mixture of (n-cyclohexylaminomethyl)-methyltriethoxysilane, DAMO-T and DAMO-D ('mixture') achieve the best results with respect to aluminum and copper substrates. GLYMO applied as adhesion promoter also leads to good adhesion to aluminum surfaces. The results of the interaction between polymer and copper surface (marked * in figure 3.29) are afflicted with an imperfection due to the fact that the polymer layer was applied too thin to the concrete slabs. In the case of PTMS good adhesion could not be achieved.

Basically adhesion on aluminum seems to be better than on copper. In the case of DAMO-D

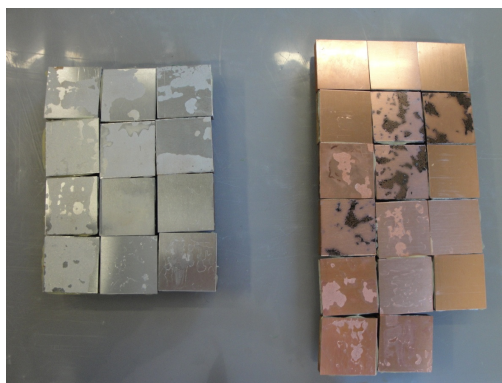


Figure 3.30: Polymer residues on aluminum (left side) and copper (right side) disks.

the adhesion pull-off test had to be done twice due to the fact that the first trial was not successful (copper as substrate: all five first stripping tests had to be redone as the pull studs disconnected from the copper disks during the pull off procedure, aluminum as substrate: three out of five tests had to be done twice). This may be an explanation for the slightly lower adhesion values of DAMO-D as adhesion promoter in figure 3.29. To eliminate the copper oxide surface several copper disks were etched with diluted sulphuric acid; this would make a chemical Cu-O-Si bond improbable. No significant difference between adhesion on copper and etched copper surfaces was observed.

The better adhesion of the samples on aluminum surfaces can also be seen in figure 3.30, showing several pulled-off aluminum and copper disks. The proportion of polymer residue on the aluminum disks is significantly higher than on copper as substrate. Adhesion promoters like DAMO-D, DAMO-T and a mixture of amine-containing adhesion agents lead to large amounts of polymer residue on the aluminum disks after pulling them off with the stripping engine, which is an indicator for good cohesion abilities of these polymers. This effect can also be seen with alkoxysilanes such as GLYMO or propyltrimethoxysilane. In the case of AMMO good cohesion was not observed.

Obviously, adhesion promoter DAMO-T seems to be the best choice to obtain good adhesion on metals like aluminum or copper. By increasing the proportion of DAMO-T in the resin adhesion abilities can be even more improved. This effect is seen in the figure 3.31. The adhesion ability of the samples increases with the addition of adhesion promoter, but at the same time some elasticity is lost. As described in section 3.2.5, a brittle siloxane film is formed when adding higher amounts of adhesion promoter.

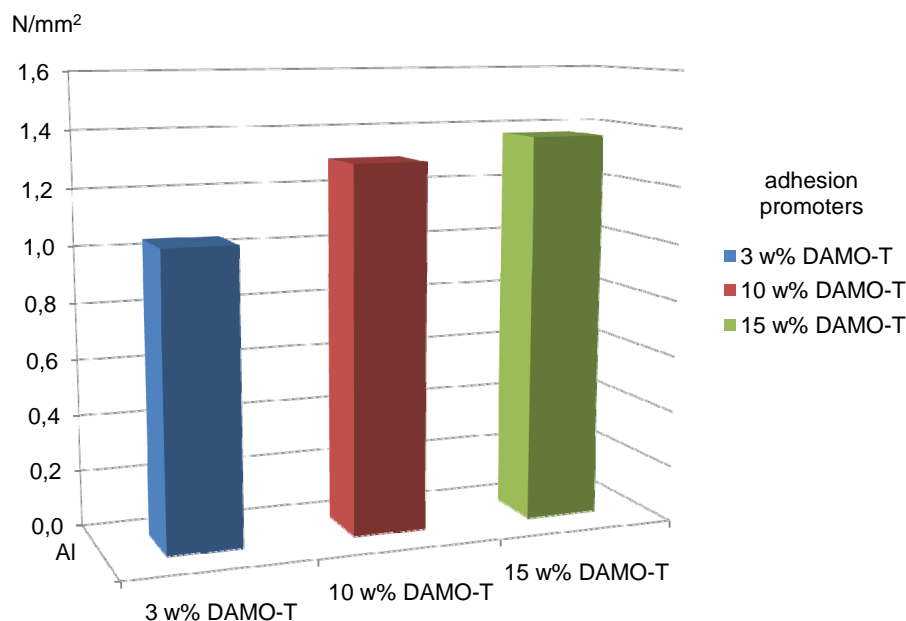


Figure 3.31: Adhesion of cured prepolymers with 3, 10 and 15 wt% DAMO-T to aluminum.

3.3.5 Influence of Different Amines

As described in section 3.3.4, amine-bearing alkoxy-silanes applied as adhesion promoters seem to be very appropriate to achieve good adhesion of silyl-terminated polyurethanes to metal surfaces. In order to consider economic aspects, new amine-alkoxy-silane mixtures were tested. As GLYMO and TEOS are quite cheap chemicals, these two were employed as an alkoxy-silane part and mixed with amines. Amines were selected for good miscibility with the polyurethane backbone. Hence, 2-((2-(dimethylamino)ethoxy)ethyl)(methylamino)ethanol (Jeffcat ZF-10), 4,7,10-trioxatridecan-1,13-diamine and N-(2-hydroxyethyl)ethylenediamine were employed. The exact sample compositions are summarized in table 3.19. In test series 3 amine-free alkoxy-silanes like TEOS or GLYMO also provide good adhesion abilities to metal surfaces which can be seen in figure 3.32.

In general the adhesion decreases from aluminum to copper and etched copper. The addition of the adhesion promoter leads to stronger metal-polymer interaction and consequently adhesion. Tests with silver surfaces were also done. Silver substrates provide good adhesion to silyl-terminated polyurethanes as do etched copper surfaces. This was not expected since M-O-Si bonds (M=Cu,Ag) should not be formed. However, both mechanical and chemical aspects influence adhesion abilities.

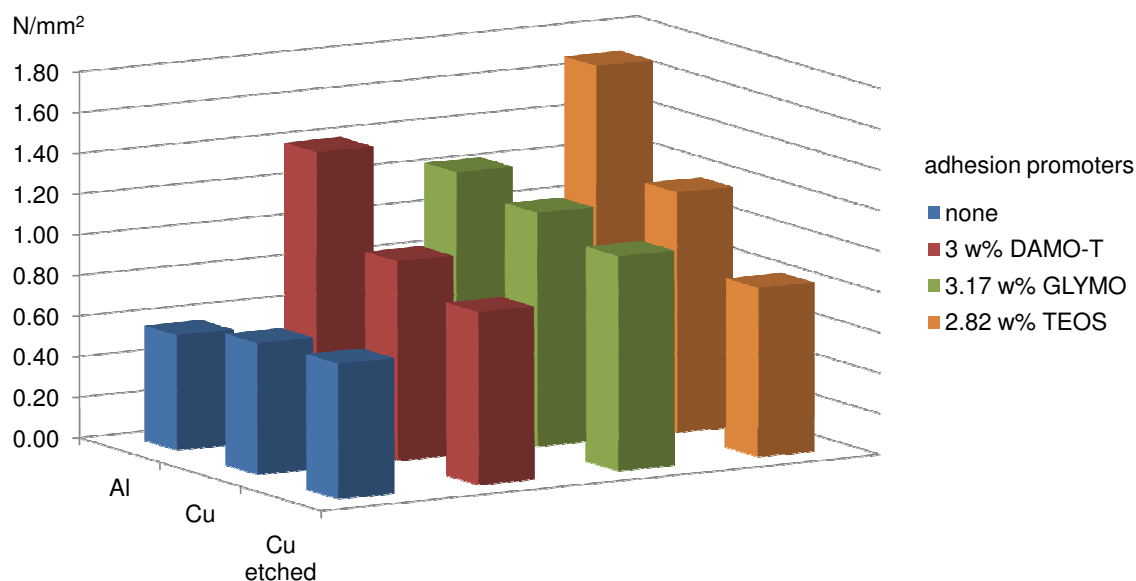


Figure 3.32: Adhesion of different cured polymers to aluminum, copper and etched copper with same silicon concentration.

The amine-alkoxysilane mixtures applied as adhesion promoters, as displayed in figures 3.33 and 3.34, lead to better adhesion abilities of the samples than adhesion promoter-free formulations. Unfortunately, adhesion strength can only be put on the same level as pure TEOS; by the addition of amines, adhesion does not increase. In the case of GLYMO (see figure 3.33) adhesion even decreases by adding Jeffcat ZF-10 or 4,7,10-trioxatridecan-1,13-diamine.

In general, all samples with additional amines lead to fluid accumulation at the 'air surface'. By ^1H and ^{13}C NMR spectroscopy the liquids can be identified as the respective amines. As seen in section 3.2.5, polar amines migrate to the hydrophilic 'air side'. Furthermore, the amines react with the copper and etched copper surfaces resulting in green to black copper surfaces and polymer residues which could be detected after the pull-off test. Obviously, the addition of amines besides the alkoxysilanes as adhesion promoters does not lead to the expected increase in adhesion. Rather, an accumulation of the amines at the 'air side' can be seen. Pure alkoxysilanes seem to be the method of choice since they allow chemical bonding with the metal substrates. Furthermore, surface tension agents such as Byk 333 or Coatosil 1211 as additives do not lead to better adhesion of the STPU to any substrate. The approach of reducing the surface tension of the polymer (see section 2.2.1.3) to get better adhesion was not successful.

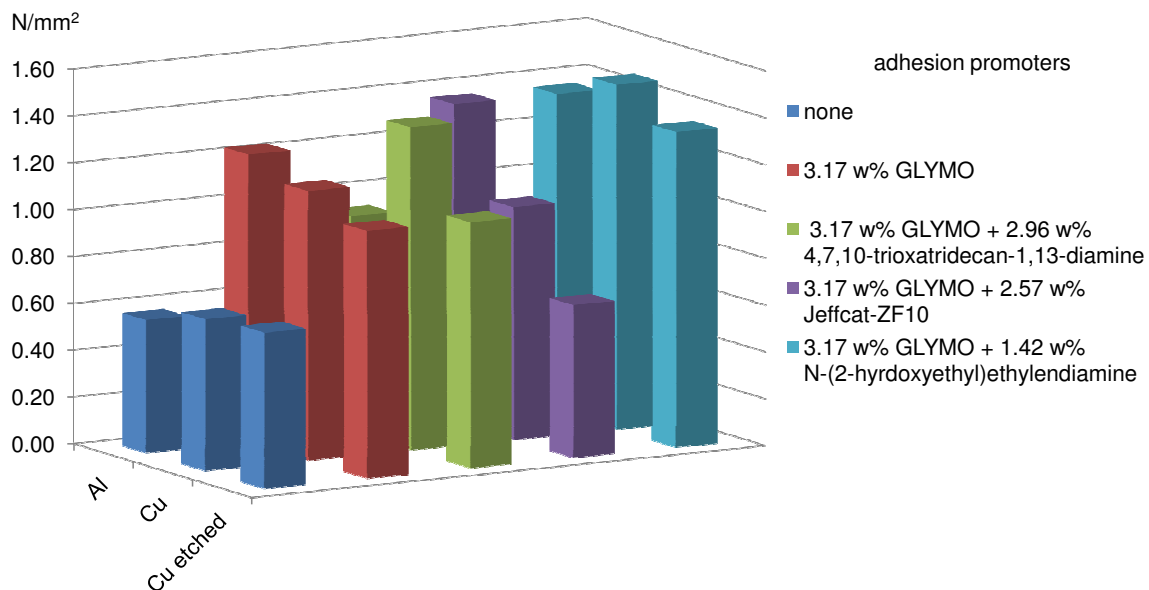


Figure 3.33: Adhesion of GLYMO and GLYMO-amine mixtures to aluminum, copper and etched copper with same silicon concentration.

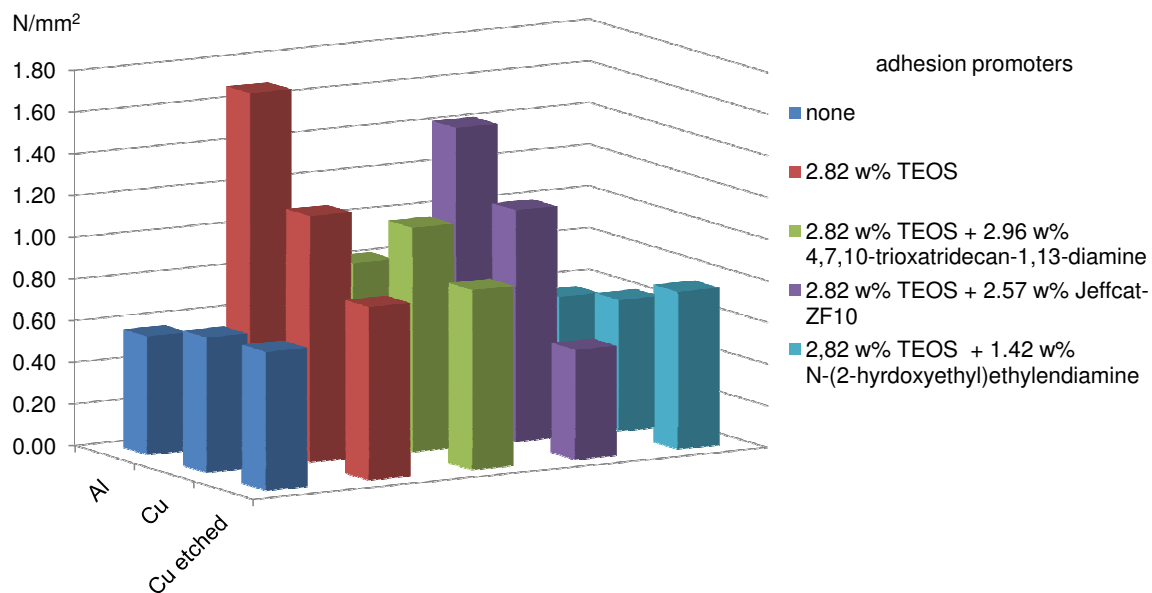


Figure 3.34: Adhesion of TEOS and TEOS-amine mixtures to aluminum, copper and etched copper with same silicon concentration.

The question of whether chemical or physical interactions are responsible for the adhesion abilities of the STPUs is still open. In all test series, a combination of these effects was observed.

3.3.6 Summary

Due to the complexity of this topic, no definitive adhesion mechanism can be reported; rather, a combination of physical and chemical effects was detected in the adhesion of STPU to substrates.

In all investigations, the pure silyl-terminated polyurethanes with no additional adhesion promoter display weak interaction between polymer and substrates of aluminum, copper, steel and polyethylene. By adding 3 wt% of AMMO, A-link 15 or DAMO-T the adhesion abilities of the polymers increase significantly to aluminum, copper and steel. However, no adhesion could be detected to plastics like polyethylene, which suggests chemical interaction between the metal surface and the polymer. Additional roughness of the substrate leads to slightly better adhesion.

In general, the adhesion decreases from aluminum to copper and etched copper substrates. The addition of the adhesion promoter leads to stronger metal-polymer interaction and consequently adhesion. Etched copper surfaces and silver substrates provide good adhesion to silyl-terminated polyurethanes. This was not expected since M-O-Si bonds (M=Cu,Ag) should not be formed. Obviously, both physical and chemical aspects influence adhesion abilities.

Amine-bearing alkoxy silanes applied as adhesion promoters seem to be very appropriate to promote good adhesion of silyl-terminated polyurethanes to metal surfaces. The addition of amines besides the alkoxy silanes as adhesion promoters does not lead to the expected increase of adhesion. Rather, an accumulation of the amines at the 'air side' is observed.

Pure amine-bearing alkoxy silanes are the adhesion promoters of choice since they allow chemical bonding with the metal substrates. By considering economic aspects, GLYMO is best suited.

Chapter 4

Experimental

In this chapter the experimental procedures are described. Synthesis of all products was carried out under inert atmosphere using standard Schlenk technique. The curing of the polymers was performed at ambient atmosphere. All alkoxy silanes were monitored for purity by NMR spectroscopy and if necessary distilled prior to use. All other reagents and materials were utilized without further purification.

4.1 Chemicals

Isophorone diisocyanate (IPDI) and dibutyltin dilaurate (DBTL) were purchased from Sigma-Aldrich. The polyols Acclaim 8200 N (linear polypropylene ether polyol, hydroxyl number = 14.0 ± 1.5 mgKOH/g, viscosity at 25 °C = 2850 ± 850 mPa·s) and Desmophen 3600Z (bifunctional polyether polyol, hydroxyl number = 56 ± 2 mgKOH/g, viscosity at 25 °C = 310 ± 25 mPa·s) were supplied from Bayer Material Science. Additionally, the polyisocyanate-prepolymer Desmodur VP LS 2371 (NCO% = approx. 3.7, viscosity at 23 °C = 11000 mPa·s) was provided from Bayer Material Science.

The alkoxy silanes AMMO (3-aminopropyltrimethoxysilane), AMEO (3-aminopropyltriethoxysilane), DAMO-T (N-(2-aminoethyl)-3-aminopropyltrimethoxysilane), 1146 (co-oligomeric diamino/alkylfunctional silane), 1189 (N-(n-butyl)-3-aminopropyltrimethoxysilane), GLMYO (3-Glycidyloxypropyltrimethoxysilane) and TEOS (tetraethyl orthosilicate) were contributed by Evonik. All other alkoxy silanes and titanium di-n-butoxide-bis-2,4-pentanedionate were purchased from ABCR. N-ethyl-3-trimethoxysilyl-2-methylpropanamine (A-link 15) and CoatOsil 1211 (organomodified polydimethylsiloxane) were received from Momentive Performance Materials. BYK-333 (polyether modified polydimethylsiloxane) was supplied by POLYChem. Bismuth neodecanoate and all amines

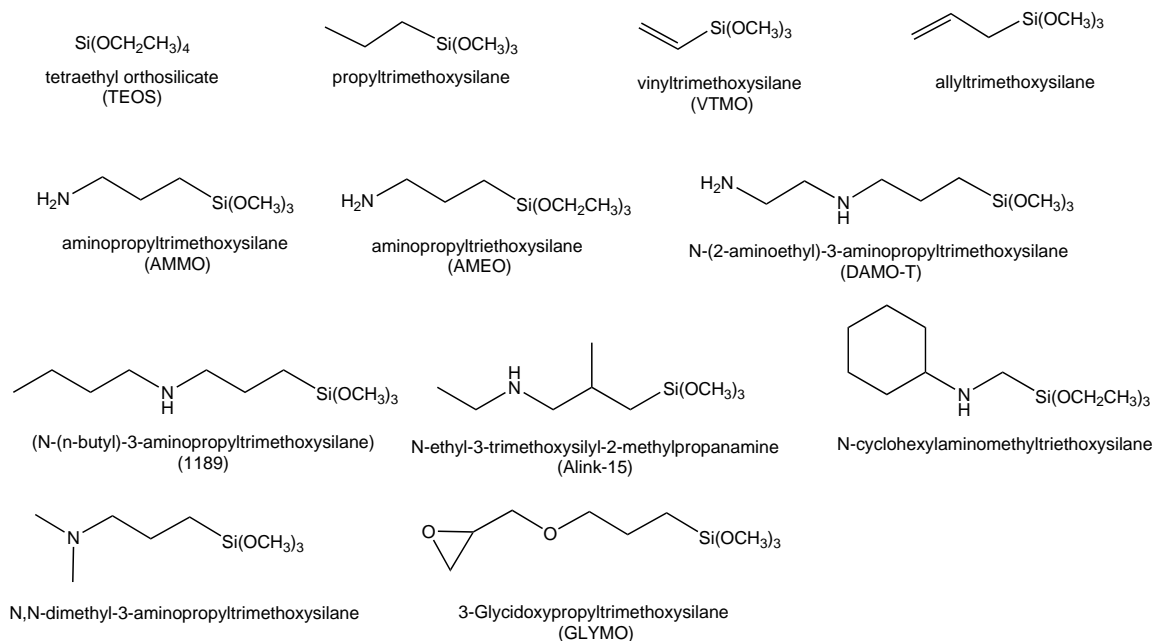


Figure 4.1: Tetraalkoxy- and trialkoxysilanes employed as adhesion promoters.

used were provided by BASF Construction Chemicals. The monomeric trialkoxysilanes, dialkoxysilanes and amines applied are summarized in figure 4.1, 4.2 and 4.3, respectively.

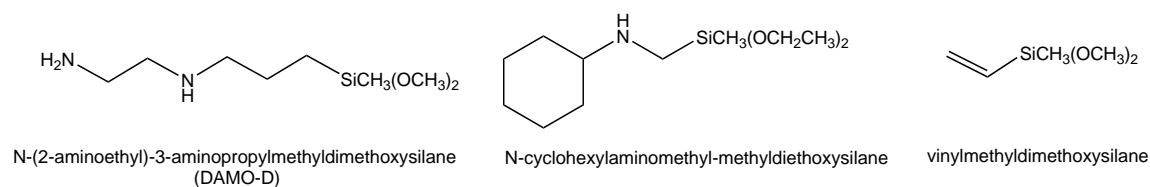


Figure 4.2: Dialkoxysilanes employed as adhesion promoters.

4.2 Synthesis of the Cured Prepolymers

The synthesis of the resins analyzed in this thesis can be summarized in three steps. The first step includes the synthesis of a polyurethane prepolymer by the reaction of a diisocyanate and a polyol compound yielding the polyurethane backbone bearing free isocyanate groups. In the second step the isocyanate-terminated polyurethane reacts with the silane end-capper and

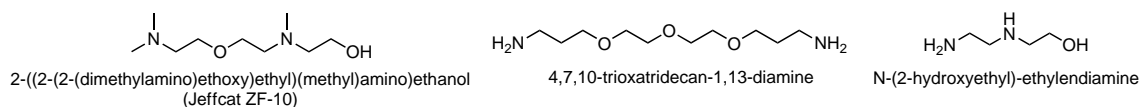


Figure 4.3: Amines employed as additives.

yields the inorganic-organic hybrid material. The curing of the silyl-terminated polyurethane prepolymer with different additives can be regarded as the third step. The three substeps of the synthesis are described in detail in section 4.2.1, 4.2.2 and 4.2.3.

4.2.1 Preparation of Isocyanate-Terminated Polyurethanes

The isocyanate-terminated polyurethane (ITPU) was prepared by the reaction of a polyol and a diisocyanate (IPDI) in the presence of a tin catalyst (DBTL). As polyol components, Acclaim 8200 N (hydroxyl value = 14.0 ± 1.5 mgKOH/g) or Desmophen 3600Z (hydroxyl number = 56 ± 2 mgKOH/g) were employed. The NCO/OH ratio was set at either 1.5 or 2.0. The synthesis of polyurethane **1a** is described as an example in section 4.2.1.1. All prepared isocyanate-terminated polyurethanes are summarized in table 4.1.

Table 4.1: Isocyanate-terminated Polyurethanes **1a-1d**.

diisocyanate	polyol	NCO/OH ratio	name
IPDI	Acclaim 8200 N	1.5	1a
IPDI	Acclaim 8200 N	2.0	1b
IPDI	Desmophen 3600Z	1.5	1c
IPDI	Desmophen 3600Z	2.0	1d

4.2.1.1 Isocyanate-Terminated Polyurethane **1a**

800 g of Acclaim 8200 N were reacted with 31.80 ml IPDI (NCO/OH molar ratio = 1.5) in a three neck 1000 ml vessel reactor with dropping funnel, bubble counter and KPG-stirrer. The polyol and 40 mg tin catalyst (50 ppm for 800 g polyol) were put into the reactor and the diisocyanate was added dropwise. After five minutes the reaction started (**0a**) and the solution was heated to 50 °C for three hours, producing a viscous clear liquid **1a**. The isocyanate content evaluated by titration was 0.57 wt%. The titration process is described in section 4.3.1.

Isocyanate-terminated polyurethane **0a** (tr=5min): IR (NaCl plate, in cm^{-1}): 3482 (-OH), 2973, 2930, 2873, 2259 (-NCO), 1720, 1453, 1373, 1344, 1297, 1258, 1112, 1014, 927, 866, 828 cm^{-1} . ^1H NMR (CDCl_3 , δ in ppm): 0.86-3.62 [aliphatic CHs, IPDI], 1.00-1.02 [d, 3H, $(\text{CH}_3)\text{CHCH}_2$, polyol], 3.26-3.59 [m, $(\text{CH}_3)\text{CHCH}_2$, polyol]; ^{13}C NMR (CDCl_3 , δ in ppm): 16.93-18.44 [$(\text{CH}_3)\text{CHCH}_2$, polyol], 23.22-56.66 [aliphatic CHs, IPDI], 72.83-75.35 [$(\text{CH}_3)\text{CHCH}_2$, polyol], 116.86-123.87 [NCO, IPDI].

Isocyanate-terminated polyurethane **1a**: IR (NaCl plate, in cm^{-1}): 3344 (-NH-), 2972, 2932, 2870, 2268 (-NCO), 2015, 1721 (-NHC(O)O-), 1522 (-NHC(O)O-), 1454, 1373, 1343, 1297, 1240, 1123, 1015, 927, 868, 833, 661 cm^{-1} . ^1H NMR (CDCl_3 , δ in ppm): 0.88-3.62 [aliphatic CHs, IPDI], 1.06-1.08 [d, 3H, $(\text{CH}_3)\text{CHCH}_2$, polyol], 3.24-3.64 [m, $(\text{CH}_3)\text{CHCH}_2$, polyol]; ^{13}C NMR (CDCl_3 , δ in ppm): 17.19-18.48 [$(\text{CH}_3)\text{CHCH}_2$, polyol], 23.31-56.97 [aliphatic CHs, IPDI], 72.89-75.41 [$(\text{CH}_3)\text{CHCH}_2$, polyol], 121.99 [NCO, IPDI].

4.2.2 Preparation of Silyl-Terminated Polyurethanes

Silyl-terminated polyurethane polymers (STPU) were prepared by the reaction of isocyanate-terminated polyurethanes with different silane end-cappers. The synthesis of AMMO-end-capped polyurethane **2a** is summarized in section 4.2.2.1. A summary of all prepared STPU with different end-cappers is given in table 4.2.

4.2.2.1 Silyl-Terminated Polyurethane **2a**

833 g of isocyanate-terminated polyurethane **1a** and 20 ml of silane end-capper AMMO (equimolar amount of the isocyanate groups) were reacted at 50 °C for one hour. AMMO was added directly with the dropping funnel to **1a**. The 100% conversion of the free isocyanate-groups was monitored by IR spectroscopy (disappearance of -NCO band at 2268 cm^{-1}) and NCO-titration, yielding a viscous liquid **2a** as crude product. The complete reaction pathway to obtain compound **2a** is shown in figure 4.4 and IR monitoring is demonstrated in figure 4.5. The bands were read according to literature.^{73,76} The obtained polymer was stored in glass bottles as the product stays stable over a period of several months even without addition of water scavengers like vinyltrimethoxysilane (VTMO).

Silyl-terminated polyurethane **2a**: IR (NaCl plate, in cm^{-1}): 3365, 2978, 2908, 2021, 1721 (-NHC(O)O-), 1688 (-NHC(O)NH-), 1654 (-NHC(O)NH-), 1534, 1455, 1375, 1342, 1297, 1240, 1148, 1013, 927, 867, 824, 664; ^1H NMR (CDCl_3 , δ in ppm): 0.57 [t, 0.02H, $\text{SiCH}_2\text{CH}_2\text{CH}_2\text{NH}_2$, AMMO], 0.85-3.64 [aliphatic CHs, IPDI], 1.05-1.07 [d, 3H, $(\text{CH}_3)\text{CHCH}_2$, polyol], 1.47 [m, 0.02H, $\text{SiCH}_2\text{CH}_2\text{CH}_2\text{NH}_2$, AMMO], 2.60 [t, 0.02H,

Table 4.2: Silyl-terminated Polyurethanes **2a-2d'''**.

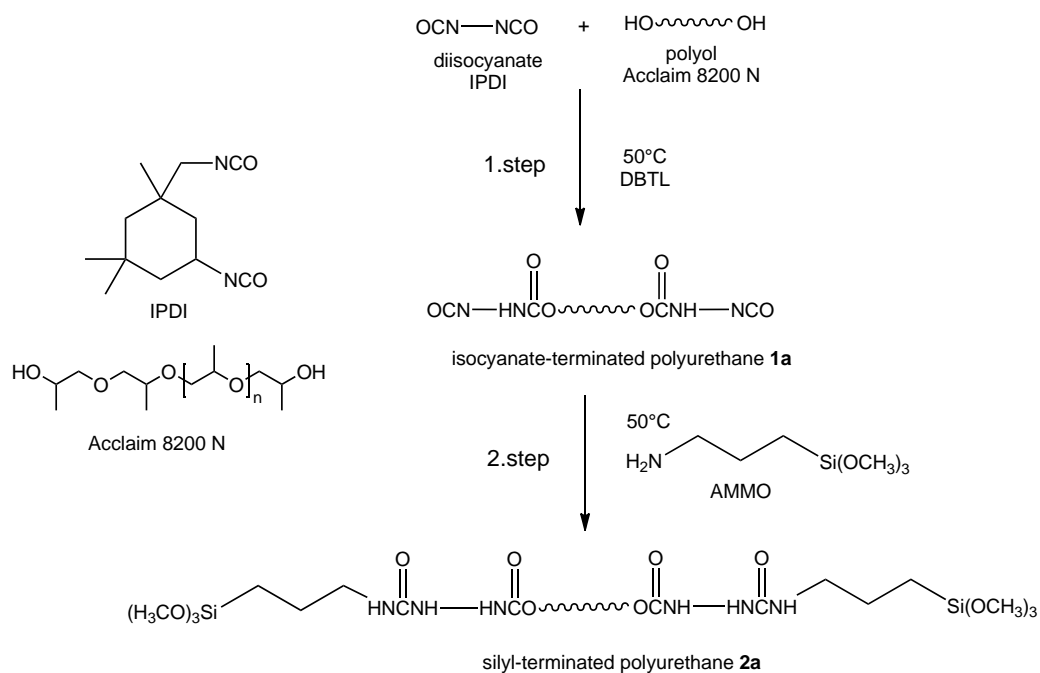
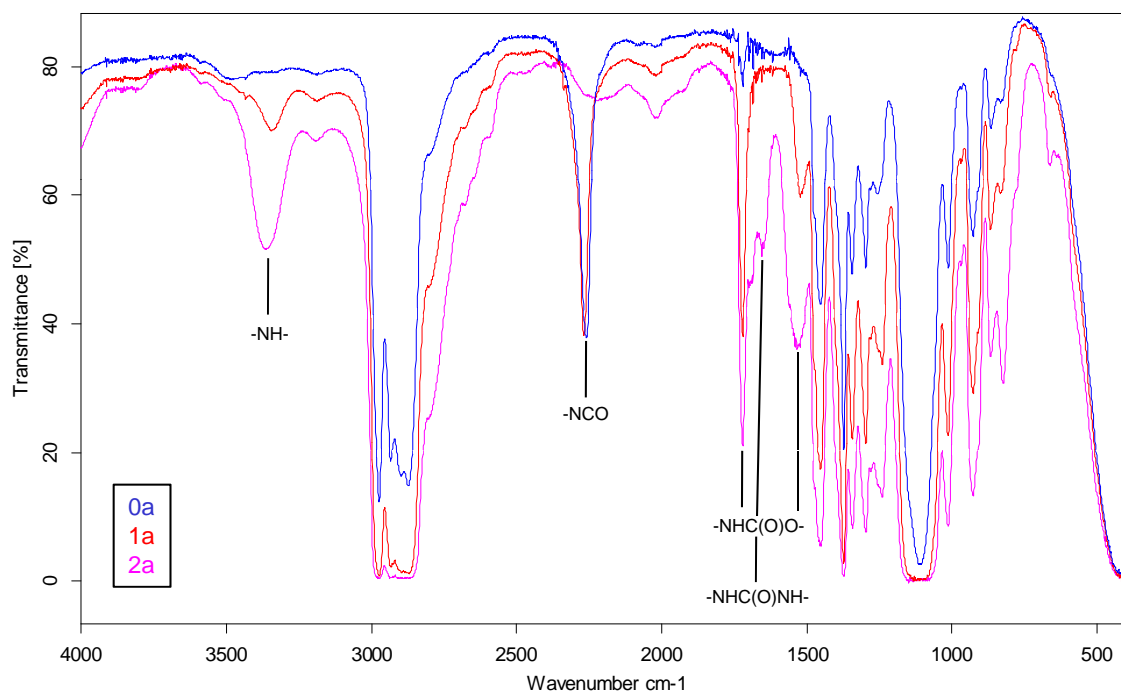
IPTU	end-capper	name
1a	AMMO	2a
1b	AMMO	2b
1c	AMMO	2c
1d	AMMO	2d
1a	AMEO	2a'
1b	AMEO	2b'
1c	AMEO	2c'
1d	AMEO	2d'
1a	1189	2a''
1b	1189	2b''
1c	1189	2c''
1d	1189	2d''
1a	Alink-15	2a'''
1b	Alink-15	2b'''
1c	Alink-15	2c'''
1d	Alink-15	2d'''

SiCH₂CH₂CH₂NH₂, AMMO], 3.21-3.66 [m, (CH₃)CHCH₂, polyol]; ¹³C NMR (CDCl₃, δ in ppm): 6.31 [SiCH₂CH₂CH₂NH₂, AMMO], 17.18-18.46 [(CH₃)CHCH₂, polyol], 23.54-50.43 [aliphatic CHs, IPDI], 26.88 [SiCH₂CH₂CH₂NH₂, AMMO], 44.89 [SiCH₂CH₂CH₂NH₂, AMMO], 72.87-75.42 [(CH₃)CHCH₂, polyol]; ²⁹Si NMR (CDCl₃, δ in ppm): -42.16 [s, SiCH₂CH₂CH₂NH₂, AMMO].

4.2.3 Curing of Silyl-Terminated Polyurethanes

The curing of the STPU was performed by addition of different additives as adhesion promoters. Pure alkoxy silanes (1.), surface tension reduction agents (2.) or a mixture of alkoxy silanes and amines (3.) were mixed with the STPU.

1. Alkoxy silanes (AMMO, AMEO, 1189, 1146, DAMO-T, DAMO-D, TEOS, VTMO, GLYMO, propyltrimethoxysilane, N,N-dimethyl-3-aminopropyltrimethoxysilane, vinylmethyldimethoxysilane, allyltrimethoxysilane, N-cyclohexylaminomethyltriethoxysilane or N-cyclohexylaminomethyl-methyldiethoxysilane). The silyl-

Figure 4.4: Reaction pathway of **2a**.Figure 4.5: IR progress during the preparation of **2a**.

terminated polyurethanes were directly weighed in plastic boxes and adhesion promoters (1 to 15 wt% with respect to the STPU) were added.

2. Surface tension reducing agents (Byk-333 or CoatOsil). To the silyl-terminated polyurethane, 1 to 10 wt% of the agents were added.
3. Mixtures of alkoxysilanes (GLYMO or TEOS) with amines (4,7,10-trioxatridecan-1,13-diamine, Jeffcat ZF-10 or N-(2-hydroxyethyl)-ethylendiamine). Between 2 and 3 %w of the alkoxysilanes with respect to the STPU prepolymer were mixed with 1 to 3 w% of the amines.

The various mixtures were stirred for five minutes with a turbo mixer at about 400 rpm. Curing times varied between one week and one month. As substrates aluminum, copper, polyethylene and steel surfaces were chosen. Aluminum as substrate is shown in figure 4.6.

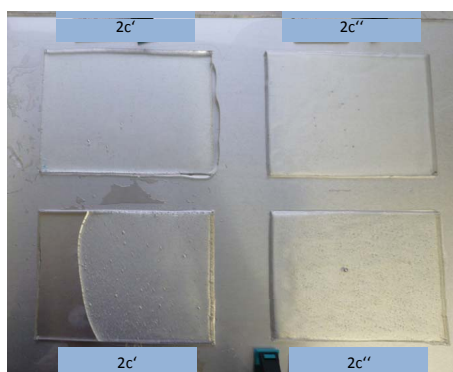


Figure 4.6: STPU **2c'** and **2c''** on aluminum substrate.

4.2.4 Pull-off Tests

The pull-off tests of the polymers deposited on various substrates were done either manually or mechanically. The manual test was performed by pulling off the cured prepolymer manually from the substrate. The force necessary was referred to a scale from 1-3 (1=no adhesion, 2=some adhesion, 3=strong adhesion).

The mechanical pull off test was performed modeled after DIN EN 1346 (“Mörtel und Klebstoffe für Fliesen und Platten - Bestimmung der offenen Zeit, 2007”).

40 x 40 cm concrete slabs were dried for several hours at 70 °C in the drying oven. Afterwards, the concrete was coated with layers of different polymer mixtures with wooden spatulas (the layers must not be too thin). 5 x 5 cm disks of copper and aluminum were roughed on one

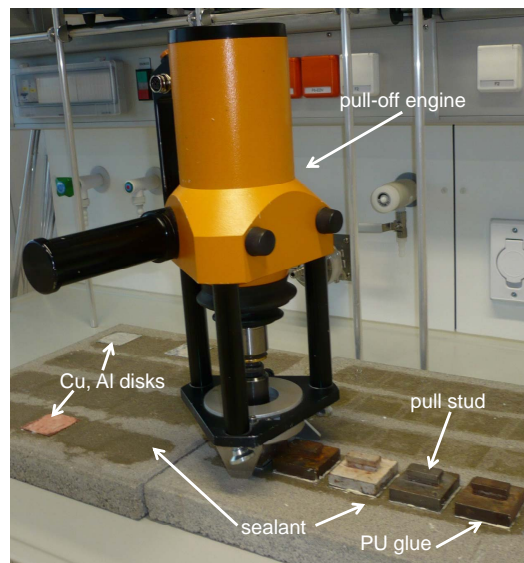


Figure 4.7: Pull-off test setup.

side with abrasive paper with grain size of 120 (to provide better adhesion of the disks to the pull stud) and cleaned with acetone. Several copper disks were additionally etched with diluted sulphuric acid. The smooth surface of the disks was pushed into the polymer layer and weighed down one minute with a stamp of 1,5 kg. The concrete slabs as shown in the following figure were stored at room temperature for about 25 days.

The adhesion test was performed with an adhesive tensile strength engine of the type Freundl F20D EASY M2000 at a stripping speed of 250 N/s. Therefore, pull studs were adhered to the roughened disks with the help of two different glues (“SaBEsto 2K-Epoxydharzklebstoff Würth” or “PUR-SPEED SaBesto Würth”) with a curing time of 2 or 24 hours, respectively. The set up is shown in figure 4.7. Due to bad adhesion of the pull studs on the aluminum and copper disks several measurements had to be redone. After longer curing times of the glue and by spraying the bonding parts with water the PU glue was found to be more appropriate than the 2K.

4.2.5 Tack Tests

The tack tests done of the sample surfaces were done either manually or mechanically. The manual tack test was performed by touching the surface of the cured polymers. The stickiness was evaluated by comparing the samples on a scale from 1-3 (1=no stickiness, 2=some stickiness, 3=strong stickiness).

The mechanical tack test was done on a Zwick 1120. Therefore, a method close to DIN Norm

Table 4.3: Tack test scale.

Manual	Mechanical $F_{max}[\text{N}/\text{mm}^2]$
1	0.38-0.43
2	0,44-0,54
3	$\geq 0,54$

ASTM D 2979 was chosen.⁷⁷ The sample was fixed on a T-section, which was clamped into the lower gripping device of the tension testing machine. As stickiness sensor a metal rod having a diameter of 2 mm was clamped into the upper gripping device. The preforce velocity of the metal rod was 10 mm/min. The rod was pushed into the cured polymer until a perforce of -0,4 N was obtained. Then the force was set automatically to zero and the metal rod was removed with 250 mm/min from the test specimen. The measured maximal force F_{max} is linked to the stickiness of the sample. 5 to 10 spots were measured for each sample. The set-up is shown in figure 4.8. The correlation between the two test methods is shown in table 4.3.

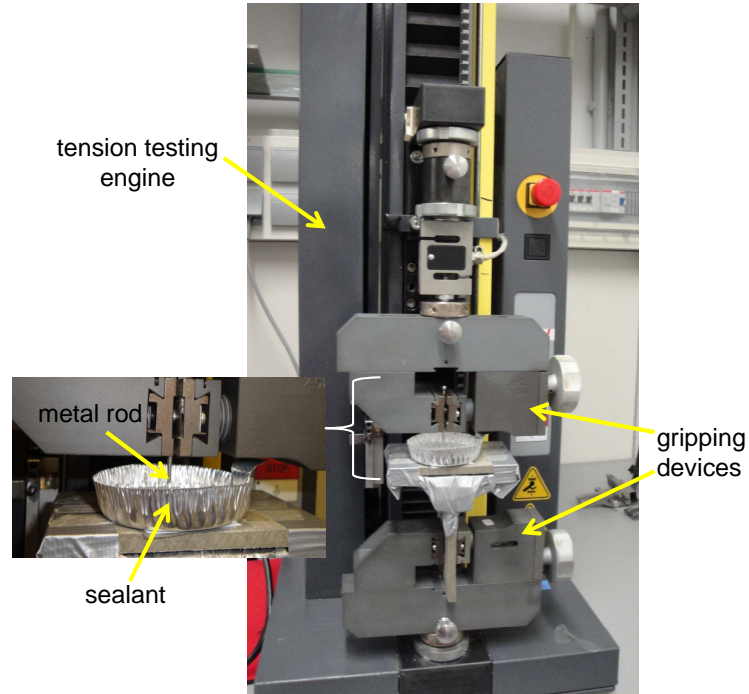


Figure 4.8: Tack test setup.

4.3 Analytics and Preparations

4.3.1 NCO Determination by Titration

To determine the isocyanate content of the isocyanate-terminated polyurethane (ITPU), between 0.5 and 5 g sample were weighed precisely in an Erlenmeyer flask. Afterwards, 10 ml of a dibutylamine solution (26.0 g dibutylamine/1000 ml toluene) and 10 ml of toluene were added. The sample was dissolved completely by stirring and heating and 70 ml of isopropanol and 3-8 drops of a bromophenol blue solution (0.5 w% in isopropanol) were added. The excess of dibutylamine was retitrated with 0.1 N hydrochloric acid producing a colour change from blue to green and finally yellow. The isocyanate content was calculated according to equation 4.1.

$$w\%NCO = \frac{(\text{blank}(ml) - \text{sample}(ml)) \cdot 100 \cdot 4.2}{\text{sample weight}(mg)} \quad (4.1)$$

4.3.2 Silver Coating

Silver coating of copper disks (5x5 cm) was done by galvanic deposition.

1. sample pretreatment
 - (a) alkaline degreasing (10 minutes, 65°C, Uniclean 155)
 - (b) deoxidation (1 minute, rt, 10 wt% H₂SO₄)
2. coating sequence
 - (a) 8 min nickel sulfamate bath (50°C, 3 A/dm²)
 - (b) 1 min 10 wt% H₂SO₄ (rt)
 - (c) rinsing with deionized water
 - (d) 7 s presilver bath (AG O-56, rt, 4 V constant)
 - (e) 20 min silver bath (AG O-56, rt, 1 A/dm²)
 - (f) 3 min Uniclean 155 bath (65°C)
 - (g) 1 min 10 wt% H₂SO₄ (rt)
 - (h) rinsing with deionized water

Table 4.4: Frequencies for NMR nuclei.

nucleus	frequency [Hz]
^1H	300.22
^{13}C	75.50
^{29}Si	59.64

4.3.3 NMR Spectroscopy

^1H , ^{13}C and ^{29}Si NMR spectra were recorded on a Varian Mercury 300 spectrometer in deuterated solvents (CDCl_3 or D_2O) at 25 °C and referenced against Me_4Si . The ^{29}Si spectra were recorded using the Insensitive Nuclei Enhancement by Polarization Transfer (INEPT) or Distortionless Enhancement by Polarization Transfer (DEPT) method. The frequencies of the nuclei are given in table 4.4.

4.3.4 IR Spectroscopy

The liquid IR spectra were recorded on an 883 Infrared Spectrophotometer from Perkin Elmer. The samples were put between two KBr or NaCl pellets. The IR-ATR measurements were done on a Bruker Alpha FT-IR Specrometer with an ATR platinum diamond.

4.3.5 SEM

Scanning electron microscopy (SEM) measurements were done with a Zeiss DSM 982 Gemini Microscope at the Austrian Centre for Electron Microscopy and Nanoanalysis (FELMI-ZFE). Secondary electron (SE) and Backscattered electron (BSE) images were recorded and EDX spectra were taken with a Noran Voyager Detector. EDX spectra were analyzed with Noran Voyager Software using the matrix-correction PHIRHOZ-method (PROZA). The background netcount determination was done with top hat filters. Magnification was regulated between 50x and 2000x. The exact conditions are displayed on every image.

Small light crumbs were identified as CaCO_3 due to sample preparation on a sheet of paper. As the sample is sticky, small pieces of CaCO_3 adhered to the surface. Every time calcium is detected this may refer to CaCO_3 . Furthermore, traces of chloride were detected on several ‘air side’ images, caused by the laboratory air.

4.3.6 AFM

Atomic force microscopy (AFM) measurements were performed with a Dimension 3100 microscope (Digital Instruments, Bruker AXS) equipped with a Hybrid XYZ scan head operated by a Nanoscope IVa controller in tapping mode. An Olympus cantilever with a spring constant of ~ 40 N/m was used with lowest energy dissipation possible. The images have been post processed by NanoScope Analyses (V1.2).

4.3.7 XPS

All measurements were performed in a multichamber ultrahigh vacuum (UHV) system at a pressure of $< 10^{-9}$ mbar.

The samples were introduced via a fast entry load lock and stored on a sample stage for 4-10 h (outgassing of the samples) before transfer to the measurement chamber. The XPS experiments were carried out using Mg K_{α} radiation (1253.6 eV) and a hemispherical analyzer (Phoibos100, from SPECS) with an energy resolution of 1.2 eV. All spectra were acquired in normal emission, with a photon incident angle of 55° . To minimize possible irradiation damage caused by X-rays, a low excitation power of 100 W (300 W is maximum) was used and the sequence of the measurements was considered.

All samples had a rough size of 1×1 cm. The spatial resolution of the analyzer was approximately 1 mm of diameter. For data evaluation the program Casa XPS was used and the standard elemental sensitivity factors (Handbook of XPS from PHI) were applied.

4.3.8 Contact Angle

Contact angle measurements were performed on a Dataphysics (Filderstadt, Germany) contact angle system (OCA15+) using water and diiodomethane as solvents with a drop volume of $5 \mu\text{l}$.

List of Figures

1	Links: Schematische Darstellung des Dichtstoffsystems, rechts: BSE Querschnittsbild der 'Luftseite' mit abnehmendem Siliciumanteil von (1) zu (2) und (3).	3
2	Left side: schematic description of STPU on substrate, right side: SEM BSE image of the cross section of the 'air side' with decreasing amount of Si from (1) to (2) and (3).	5
1.1	Schematic overview of the project.	14
2.1	Synthesis pathway for STPUs according to Nomura ¹ and Xu. ⁹	16
2.2	Synthesis pathway for STPUs according to Sardon ² and Subramani. ⁵⁻⁷	17
2.3	Isocyanate side reactions according to Dusek. ¹⁷	18
2.4	²⁹ Si NMR spectrum of mixture IV ($w = 1$, pH=1) obtained at 59.59 MHz and 296 K using DEPT sequence recorded by Brunet ²²	19
2.5	Scheme of adhesion models. ³⁵	22
2.6	Mechanical interlocking of an adhesive between two substrates. ²⁷	22
2.7	Contact angle for determination of wetting according to Young. ^{41,42}	24
2.8	Reaction of the silane coupling agent with substrate (left), filler (middle) and polymer (right). ⁴³	24
2.9	Popular silane coupling agents.	25
2.10	Possible reaction of the silane coupling agent with substrate and adhesive. ³³	26
2.11	T-peel test geometry dimensions (mm) with sample in the middle (black). ⁵⁶	29
2.12	Lap shear test setup dimensions with sample (black). ⁵⁷	29
2.13	Schematic of scratch test. ⁶⁰	30
2.14	Pull-off test set up with (a) sample preparation and (b) pull off procedure. ⁶¹	31
2.15	Schematic of tack test according to Hutchinson. ⁵¹	33

2.16	Silanol groups existing on silica surfaces according to Dijkstra: (a) vicinal, (b) geminal and (c) isolated silanols. ⁶⁵	34
3.1	Investigated areas of the samples.	36
3.2	‘Air side’ of sample 2b_0_PVC showing silicon-containing crystallites (BSE image).	39
3.3	Accumulation of silicon on the ‘air and adhesion side’ of sample 2c_10AMMO_Al (SE image) and EDX spectra of the BSE image (‘air side’: left column, ‘adhesion side’: right column).	39
3.4	Decrease of the silicon content at the ‘air side’ of sample 2b_15AMMO_PVC (BSE cross section image).	40
3.5	Silicon (blue) and carbon (red) concentration versus increasing amount of AMMO.	41
3.6	IR spectra of the ‘adhesion side’ of samples 2a_3AMMO_Al, 2a_7AMMO_Al, 2a_10AMMO_Al, 2a_15AMMO_Al having increasing amount of AMMO as adhesion promoter.	42
3.7	IR spectra of the ‘air side’ of samples 2a_3AMMO_Al, 2a_7AMMO_Al, 2a_15AMMO_Al with increasing amount of AMMO as adhesion promoter.	43
3.8	Accumulation of silicon on the ‘air and adhesion side’ of sample 2b_10Alink15_Al, 2b_101189_Al, 2b_101146_Al, 2b_10DAMO-T_Al and EDX spectra of the BSE image (‘air side’: left column, ‘adhesion side’: right column).	44
3.9	Silicon (blue) and carbon (red) concentration versus alkoxysilanes 1189, Alink-15, AMMO, DAMO-D and DAMO-T.	46
3.10	EDX spectra of sample 2a_3.76DAMOT_Al (1a) and 2a_3DAMOT_Al_dc (1b).	47
3.11	IR spectra of the ‘air side’ and ‘adhesion side’ of sample 2a_3.76DAMOT_Al.	48
3.12	IR spectra of the ‘air side’ of samples 2a_3DAMOT_Al (blue) and 2a_3DAMOT_dc (black).	48
3.13	First row: Height AFM images of sample 2a_3DAMO-T_Al (1a), 2a_3DAMOT_dc (1b) and 2a_3AMMO_Al (1c), second row: phase images of sample 2a_3DAMO-T_Al (2a), 2a_3DAMOT_dc (2b) and 2a_3AMMO_Al (2c).	50
3.14	AFM cross section measuring points P1-P5 of sample 2a_3DAMO-T_Al and phase image of P1.	51
3.15	AFM height image (1d) and phase image (2d) of the ‘air side’ of sample 2a_15AMMO_Al.	51
3.16	¹ H array of hydrolysis of AMMO with 1 eq. D ₂ O within 40 minutes.	54

<i>LIST OF FIGURES</i>	97
3.17 Schematic overview of T ⁿ structures. ⁷⁴	55
3.18 ²⁹ Si array of hydrolysis of AMMO with 1 eq. D ₂ O within 40 minutes.	56
3.19 Partial hydrolysis of 1 eq. adhesion promoter with 1 eq. D ₂ O: Methanol CH ₃ OD liberation versus time.	57
3.20 Partial hydrolysis of 1 eq. adhesion promoter with 1 eq. D ₂ O: Increase of the condensation degree versus time.	58
3.21 Decrease of the silicon content at the ‘air side’ of sample 2c_10AMEO_Al (BSE cross section image).	59
3.22 Silicon allocation at the ‘adhesion side’ of sample 2c_10AMEO_Al (BSE cross section image).	60
3.23 Schematic description of sample 2a having a high number of free silanol groups.	64
3.24 Schematic description of samples formulated with high amounts of adhesion promoter.	64
3.25 Surface coating of aluminum and polyethylene with (N,N-dimethyl-3-aminopropyl)trimethoxysilane and AMMO.	71
3.26 Curing boards of steel, aluminum, copper and polyethylene with plane and rough surface.	72
3.27 BSE image of sample Al6 and EDX spectrum of marked area (1), logarithmic scale.	75
3.28 Adhesion of various cured prepolymers on plane and rough surfaces of aluminum, copper, steel and polyethylene (1=no adhesion, 2=some adhesion, 3=strong adhesion).	76
3.29 Adhesion of different cured prepolymers to aluminum, copper and etched copper.	77
3.30 Polymer residues on aluminum (left side) and copper (right side) disks.	78
3.31 Adhesion of cured prepolymers with 3, 10 and 15 wt% DAMO-T to aluminum.	79
3.32 Adhesion of different cured polymers to aluminum, copper and etched copper with same silicon concentration.	80
3.33 Adhesion of GLYMO and GLYMO-amine mixtures to aluminum, copper and etched copper with same silicon concentration.	81
3.34 Adhesion of TEOS and TEOS-amine mixtures to aluminum, copper and etched copper with same silicon concentration.	81
4.1 Tetraalkoxy- and trialkoxysilanes employed as adhesion promoters.	84
4.2 Dialkoxysilanes employed as adhesion promoters.	84
4.3 Amines employed as additives.	85

<i>LIST OF FIGURES</i>	98
4.4 Reaction pathway of 2a	88
4.5 IR progress during the preparation of 2a	88
4.6 STPU 2c' and 2c'' on aluminum substrate.	89
4.7 Pull-off test setup.	90
4.8 Tack test setup.	91

List of Tables

3.1	Sample preparation for SEM measurements, end-capper=adhesion promoter (test series 1).	37
3.2	Sample preparation for SEM measurements, end-capper≠adhesion promoter (test series 2).	37
3.3	Sample preparation for SEM and IR-ATR measurements, end-capper≠adhesion promoter, n(Si)=4.99 mmol (test series 3).	37
3.4	Sample preparation for SEM, IR and AFM measurements, different alkoxy-silanes (test series 4).	38
3.5	Sample preparation for SEM and IR measurements, increasing amount of AMMO (test series 5).	38
3.6	Silane coupling agents employed for hydrolysis.	53
3.7	¹ H and ²⁹ Si NMR shifts of the used methoxysilanes in ppm (D ₂ O, 25°C).	53
3.8	Sample preparation for tack tests, increasing amount of AMMO (test series 1).	61
3.9	Sample preparation for tack tests, different alkoxy-silanes, n(Si)=4.99 mmol (test series 2).	62
3.10	Sample preparation for tack tests, different alkoxy-silanes (test series 3).	62
3.11	Sample preparation for tack tests, 1 wt% of AMMO with different catalysts and VTMO as water scavenger (test series 4).	62
3.12	Manual tack test results, increasing amount of AMMO (test series 1).	63
3.13	Manual tack test in correlation with silicon accumulation detected by SEM-EDX (test series 2).	66
3.14	Manual tack test in correlation with silicon accumulation detected by SEM-EDX (test series 3).	67
3.15	Manual and mechanical tack test results, different curing catalysts (test series 4).	68

3.16	Sample preparation for SEM measurements, surface coating of aluminum and polyethylene.	71
3.17	Sample preparation for roughness test, different alkoxy-silanes on various curing substrates (test series 1).	71
3.18	Sample preparation to detect the influence of different alkoxy-silanes on the adhesion abilities (test series 2).	73
3.19	Sample preparation to detect the influence of different alkoxy-silane-amine mixtures on the adhesion abilities (test series 3).	73
4.1	Isocyanate-terminated Polyurethanes 1a-1d	85
4.2	Silyl-terminated Polyurethanes 2a-2d'''	87
4.3	Tack test scale.	91
4.4	Frequencies for NMR nuclei.	93

Literature

- [1] Nomura, Y.; Sato, A.; Sato, S.; Mori, H.; Endo, T. *Journal of Polymer Science: Part A: Polymer Chemistry* **2007**, *45*, 2689–2704.
- [2] Sardon, H.; Irusta, L.; Fernández-Berridi, M.; Lansalot, M.; Bourgeat-Lami, E. *Polymer* **2010**, *51*, 5051–5057.
- [3] O'Connor, A. E.; Kingston, T. *ASTM Special Technical Publication* **2004**, 143–155.
- [4] Akram, D.; Ahmad, S.; Sharmin, E.; Ahmad, S. *Macromolecular Chemistry and Physics* **2010**, *211*, 412–419.
- [5] Subramani, S.; Lee, J. M.; Lee, J.-Y.; Kim, J. H. *Polymers for Advanced Technologies* **2007**, *18*, 601–609.
- [6] Subramani, S.; Choi, S.-W.; Lee, J.-Y.; Kim, J. H. *Polymer* **2007**, *48*, 4691–4703.
- [7] Subramani, S.; Lee, J.-Y.; Kim, J. H.; Cheong, I. W. *Composites Science and Technology* **2007**, *67*, 1561–1573.
- [8] Vega-Baudrit, J.; Sibaja-Ballesteroa, M.; Vazquez, P.; Torregrosa-Macia, R.; Martin-Martinez, J. M. *International Journal of Adhesion and Adhesives* **2007**, *27*, 469–479.
- [9] Xu, J.; Shi, W.; Pang, W. *Polymer* **2006**, *47*, 457–465.
- [10] Carrard, J.; Cagan, V. Organotin-free adhesive based on moisture-curable, silyl-terminated polymer, FR 2948123 A1. Patent, 2011.
- [11] Ren, Z.; Hou, X. One-component rapidly curing polyurethane sealing adhesive, and its preparation, CN 101818040 A. Patent, 2010.
- [12] Choffat, F. Silane-terminated polyurethane polymers, EP 2221331 A1. Patent, 2010.

- [13] Klapdohr, S.; Walther, B.; Mack, H.; Cai, Z.; Marc, L.; Mezger, J.; Austermann, T.; Flakus, S. Production of silylated polyurethane or polyurea for use in sealants, WO 2010015452 A1. Patent, 2010.
- [14] Seiter, G. Polyurethane Sealant Containing Trialkoxysilane End Groups, 3,627,722. U.S. Patent, 1971.
- [15] Brode, G.; Conte, L. Vulcanizable Silicon Terminated Polyurethane Polymers, 3,632,557. U.S. Patent, 1972.
- [16] Berger, M.; Mayer, W.; Ward, R. Silane-Containing Isocyanate-Terminated Polyurethane Polymers, 4,374,237. U.S Patent, 1983.
- [17] Dusek, K.; Spirkova, M.; Havlicek, I. *Macromolecules* **1990**, *23*, 1774–1781.
- [18] Osterholz, F.; Pohl, E. *Journal of Adhesion Science Technology* **1992**, *6*, 127–149.
- [19] Elschenbroich, C. *Organometallics*, 4th ed.; Teubner, 2003; pp 137–148.
- [20] Surivet, F.; my Lam, T.; Pascault, J.-P.; Pham, Q. T. *Macromolecules* **1992**, *25*, 4309–4320.
- [21] Beari, F.; Brand, M.; Jenkner, P.; Lehnert, R.; Metternich, H. J.; Monkiewicz, J.; Siesle, H. W. *Journal of Organometallic Chemistry* **2001**, *625*, 208.
- [22] Brunet, F. *Journal of Non-Crystalline Solids* **1998**, *231*, 58–77.
- [23] Rankin, S. E.; McCormick, A. V. *Magnetic Resonance in Chemistry* **1999**, *37*, 27–37.
- [24] Salon, M.-C. B.; Abdelmouleh, M.; Boufi, S.; Belgacem, M. N.; Gandini, A. *Journal of Colloid and Interface Science* **2005**, *289*, 249–261.
- [25] Salon, M.-C. B.; Bardet, M.; Belgacem, M. N. *Silicon Chemistry* **2008**, *3*, 335–350.
- [26] Tejedor-Tejedor, M.; Paredes, L.; Anderson, M. *Chemistry of Materials* **1998**, *10*, 3410–3421.
- [27] Awaja, F.; Gilbert, M.; Kellya, G.; Foxa, B.; Pigramb, P. J. *Progress in Polymer* **2009**, *34*, 948–968.
- [28] Gleich, H. Zusammenhang zwischen Oberflächenenergie und Adhäsionsvermögen von Polymerwerkstoffen am Beispiel von PP und PBT und deren Beeinflussung durch die Niederdruck-Plasmatechnologie. Dissertation, Universität Duisburg-Essen, 2004; S.3-22.

- [29] Mühlhan, C. Plasmaaktivierung von Polypropylenoberflächen zur Optimierung von Klebeverbunden mit Cyanacrylat Klebstoffen im Hinblick auf die mechanischen Eigenschaften. Ph.D. thesis, Gerhard-Mercator-Universität-Gesamthochschule Duisburg, 2002.
- [30] Haufe, M. Methoden zur Verbesserung der Adhäsion von Klebstoffen an metallischen Oberflächen. Ph.D. thesis, Universität Bielefeld, 2002.
- [31] Packham, D. *International Journal of Adhesion and Adhesives* **2003**, *23*, 437–448.
- [32] Allen, K. *International Journal of Adhesion and Adhesives* **2003**, *23*, 87–93.
- [33] Habenicht, G. *Kleben Grundlagen, Technologien, Anwendungen*, 6th ed.; Springer, 2009.
- [34] Comyn, J. In *Handbook of Adhesives and Sealants*; Cognard, P., Ed.; Elsevier, 2006; Vol. 2; pp 1–50.
- [35] Butt, M. A.; Chughtaia, A.; Ahmad, J.; Ahmad, R.; Majeed, U.; Khan, I. *Journal of Faculty of Engineering and Technology*, **2007**, 21–45.
- [36] Smith, M. J.; Daib, H.; Ramani, K. *International Journal of Adhesion and Adhesives* **2002**, *22*, 197–2004.
- [37] Basin, V. E. *Progress in Organic Coatings* **1984**, *12*, 213–250.
- [38] Bruyne, N. D. *Flight* **1939**, *28*, 17.
- [39] Derjagin, B. Adhäsion fester Körper. 1973.
- [40] Vojutzkij, S. Autoadhesion and Adhesion of High Polymers. 1963.
- [41] Bischof, C. *Materialwissenschaft und Werkstofftechnik* **1993**, *24*, 33–41.
- [42] Nikolova, D. Charakterisierung und Modifizierung der Grenzflächen im Polymer-Metall-Verbund. Ph.D. thesis, Martin-Luther-Universität Halle-Wittenberg, 2005.
- [43] Wacker, *For Powerful Connections - Organofunctional Silanes*; 2010.
- [44] Plueddemann, E. P. *Silane Coupling Agents*; Plenum Press, 1982.
- [45] Fir,; Orel,; Vuk,; Vilcnik,; Jese,; Francetic, *Langmuir* **2007**, *23*, 5505.
- [46] Leung, Y.; Zhou, P.; Wong, M.; Mitchell, K. *Applied Surface Science* **1992**, *59*, 23.

- [47] Matienzo, L.; Shaffer, D.; Moshier, W.; Davis, G. *Journal of Materials Science* **1986**, *21*, 1601.
- [48] Fang, J.; Flinn, B. J.; Leung, Y. L.; Wong, P. C.; Mitchell, K. A. R. *Journal of Materials Science Letters* **1997**, *16*, 1675–1676.
- [49] Bexell, U.; Olsson, M. *Surface and Interface Analysis* **2001**, *31*, 223–231.
- [50] Yazdani, H.; Morshedian, J.; Khonakdar, H. *Polymer Composites* **2006**, *27*, 491–496.
- [51] Hutchinson, A.; Iglauer, S. *International Journal of Adhesion and Adhesives* **2006**, *26*, 555–566.
- [52] Mittal, K., Pizzi, A., Eds. *Adhesion Promotion Techniques: Technological Applications.*; Dekker, 1999; p 404.
- [53] Koh, W. H. *Journal of Colloid and Interface Science* **1979**, *71*, 613–615.
- [54] Gouvea, D. *Journal of Material Chemistry* **2000**, *10*, 259.
- [55] Teo, M.; Kim, J.; Wong, P.; Mitchell, K. *Applied Surface Science* **2005**, *252*, 1293–1304.
- [56] Broughton, W. R.; Mera, R. D.; Hinopoulos, G. *Creep Testing of Adhesive Joints, T-Peel Test*; 1999.
- [57] Rabilloud, G. In *Handbook of Adhesives and Sealants*; Cognard, P., Ed.; Else, 2006; pp 265–266.
- [58] Li, J.; Beres, W. *Canadian Metallurgical Quarterly* **2007**, *46*, 155–174.
- [59] Bull, S.; Berasetegui, E. *Tribology International* **2006**, *39*, 99–114.
- [60] Bégin, G. *Scratch Adhesion Testing of Bulk Materials*; 2010.
- [61] Kisin, S. Adhesion changes at metalpolymer interfaces: Study of the copper(acrylonitrilebutadienestyrene) system. Ph.D. thesis, Technische Universiteit Eindhoven, 2007.
- [62] Burkstrand, *Journal of Applied Physics* **1981**, *52*, 4795–4800.
- [63] Majumdar, P.; Stafslie, S.; Daniels, J.; Webster, D. *Journal of Coatings Technology and Research* **2007**, *4*, 131–138.

- [64] Zhu, Y.; Yan, L.; Zhang, H.; Lian-Meng, D. *Journal of Applied Polymer Science* **2006**, *100*, 3889.
- [65] Dijkstra, T. W.; Duchateau, R.; van Santen, R. A.; Meetsma, A.; Yap, G. P. A. *Journal of the American Chemical Society* **2002**, *124*, 9856–9864.
- [66] Carteret, C. *The Journal of Physical Chemistry* **2009**, *113*, 133300–133308.
- [67] Vega, A. *Journal of the American Chemical Society* **1988**, *110*, 1049–1054.
- [68] Morrow, B.; Gay, I. *The Journal of Physical Chemistry* **1988**, *92*, 5569–5571.
- [69] Bakaev, V.; Pantano, C. *The Journal of Physical Chemistry* **2009**, *113*, 13894–13898.
- [70] Uehara, N.; Kawata, S.; Shimizu, T. *Analytical Sciences* **2005**, *21*, 1099–1104.
- [71] Kosonen, J.; Ruohonen, J. *International Journal of Polymer Analysis and Characterization* **1998**, *4*, 283–293.
- [72] Kellum, G.; Smith, R. *Analytical Chemistry* **1967**, *39*, 341–345.
- [73] Launer, P. In *Infrared Analysis of Organosilicon Compounds: Spectra-Structure Correlations*; Arkles, B., Ed.; Petrarch Systems: Bristol, 1987; pp 47–53.
- [74] Salon, M.-C. B.; Gerbaud, G.; Abdelmouleh, M.; Bruzzese, C.; Boufi, S.; Belgacem, M. N. *Magnetic Resonance in Chemistry* **2007**, *45*, 473–483.
- [75] Landon, S. J.; N.B.Dawkins.; Waldman, B. *The Journal of the Adhesives and Sealants Council* **1996**, *1*, 21.
- [76] Gardella, A.; Grobe, G. *Analytical Chemistry* **1984**, *56*, 1169–1177.
- [77] Fischer, F. P. G. Untersuchung zur Katalyse der Polykondensation silanterminierter Präpolymere mit zinnfreien Verbindungen. Diploma Thesis, 2009.